Universität Rostock Traditio et Innovatio

Catalysis LIKAT Leibniz-Institut für Katalyse e.V.

Iron and its neighbors, earth-abundant hydrogenation catalysts for the synthesis of heterocycles and ethers

Cumulative Dissertation

to acquire the academic degree
doctor rerum naturalium (Dr. rer. nat.)
of the Faculty of Mathematics and Natural Sciences
at the University of Rostock

Submitted in Rostock, 18.09.23
by Johannes Fessler, born on 30th January 1992, in Münster, Germany

https://doi.org/10.18453/rosdok_id00004603

The present work was accomplished at the Leibniz-Institute for Catalysis e.V. at the chair of Applied Homogeneous Catalysis in the research group of Professor Dr. Matthias Beller during the period from September 2019 to September 2023.

Reviewer 1: Prof. Dr. Matthias Beller
Leibniz-Institut für Katalyse e.V.
Angewandte Homogenkatalyse
Albert-Einstein-Straße 29a
18059 Rostock

Reviewer 2: Prof. Dr. Joachim Mittendorf
Bayer Pharma AG
Medicinal Chemistry
Aprather Weg 18a
42113 Wuppertal

Date of the Submission: 18.09.2023

Date of the Defense: 09.01.2024

Statement of Authorship

I hereby affirm that I have written the present work by myself without outside assistance. No other resources were utilized than stated. All references as well as verbatim extracts were quoted, and all sources of information were specifically acknowledged.

Ich versichere hiermit an Eides statt, dass ich die vorliegende Arbeit selbstständig angefertigt und ohne fremde Hilfe verfasst habe. Dazu habe ich keine außer den von mir angegebenen Hilfsmitteln und Quellen verwendet. Die den benutzten Werken inhaltlich und wörtlich entnommenen Stellen habe ich als solche kenntlich gemacht.

Rostock, 18.09.2023

……
Johannes Fessler

Abstract

This doctoral thesis discusses the topic of earth-abundant metals in hydrogenation catalysis. Hydrogenation (i.e., the addition of hydrogen to an unsaturated substrate) is generally one of the most sustainable and industrially relevant reduction reactions. However, historically the field of homogeneous hydrogenation catalysis was dominated by precious metal catalysts based on rare elements such as ruthenium, rhodium or iridium. Due to the need for “greener” chemical manufacturing, recent scientific endeavors have focused on replacing these expensive and often toxic elements with more abundant, affordable and benign first-row transition metals. Over the course of this thesis, catalysts based on three of these more sustainable elements (namely manganese, iron and cobalt) have been developed and applied in various hydrogenation reactions. Firstly, a new family of manganese PNN-pincer catalysts developed for the hydrogenation of quinolines at ambient temperature is discussed. Secondly, an iron-Tetraphos system is presented that allows direct N-aryl pyrrole synthesis from nitroarenes and 1,4-dicarbonyl compounds in a (transfer) hydrogenation/Paal-Knorr cascade. Lastly, the effect of phosphine oxide promoters on cobalt carbonyl precatalysts is evaluated, leading to improved protocols for the cobalt-catalyzed reductive etherification of aldehydes and the reductive or carbonylative transformation of oxetanes.

Kurzzusammenfassung

Diese Doktorarbeit behandelt das Thema der häufig-vorkommenden Metalle in der Hydrierkatalyse. Hydrierung, also die Addition von Wasserstoff an ein ungesättigtes Substrat, ist eine der ökonomisch und ökologisch wichtigsten Reduktionsreaktionen. Historisch-bedingt dominieren Edelmetallkatalysatoren aus Ruthenium, Rhodium oder Iridium das Feld der homogenen Hydrierkatalyse. Aufgrund der Notwendigkeit einer „grüneren“ chemischen Produktion versucht die wissenschaftliche Forschung daher, diese teuren und oft giftigen Elemente durch besser verfügbare, günstigere und weniger schädlichere 3d-Übergangsmetalle zu ersetzen. Im Rahmen dieser Arbeit wurden daher Hydrierkatalysatoren entwickelt und angewendet, die auf den drei nachhaltigeren Elementen Mangan, Eisen und Cobalt basieren. Zuerst berichten wir über eine neue Gruppe von Mangan-PNN-Pincer Katalysatoren für die Hydrierung von Chinolinderivaten bei Raumtemperatur. Als nächstes wird ein Eisen-Tetraphos-System für die direkte Synthese von N-Arylpyrrolen aus Nitroarenen und 1,4-Dicarbonyl-Verbindungen mithilfe einer Transferhydrierungs-/Paal-Knorr-Kaskade präsentiert. Zuletzt evaluieren wir den positiven Effekt von Phosphinoxid-Promotoren auf Cobaltcarbonyl-Präkatalysatoren in der reduktiven Etherifizierung von Aldehyden und der reduktiven oder carbonylierenden Umwandlung von Oxetanen.

Acknowledgements

At first, I want to thank my supervisor **Prof. Matthias Beller** for accepting me into his exceptional research group. I am grateful for all the advice other the years, for his quick wit and his kindness. Even though his schedule was quite busy, he always managed to make time for me, even on short notice, and listened to any issues I faced. His optimistic and positive outlook on life in any circumstance was truly an inspiration.

The second assessor of this thesis **Prof. Joachim Mittendorf** is thanked for accepting this responsibility as well as for the quick and thorough examination of this dissertation.

I am grateful to **Dr. Kathrin Junge**, leader of the “Sustainable Redox Reactions” subgroup for welcoming me into the fold and for creating such a familiar work atmosphere. Her caring and calm demeanor helped me through the sometimes-challenging times of the PhD. Her support during the preparation of manuscripts, especially her keen eye for detail and design was a great help for me. Furthermore, I want to thank her for her willingness to cover all my (costly) research expenses without hesitation and organizing all the fantastic group events.

I am thankful to my industrial collaborators from Bayer Pharmaceuticals **Dr. Stefan Roggan**, **Dr. Johannes Platzek** and **Dr. Nicolas Guimond** for giving me valuable insights into the field of pharmaceutical process R&D, for the excellent scientific discussions and importantly for generously funding a part of my PhD.

Next, I would like to express my gratitude to my academic collaborators: **Dr. Fábio Delolo** and his supervisors **Prof. Eduardo dos Santos** and **Prof. Elena Gusevskaya** for the joint effort on the cobalt projects; **Dr. Veronica Papa** for her friendly instructions during the beginning of my PhD and the nice work on the manganese topic; recently, **Dr. Edgar Zander** for the pleasant and fruitful collaboration regarding tetraradical-mediated hydrogen activation; **Prof. Haijun Jiao** and **Dr. Zhihong Wei** for their excellent contributions with regards to computational chemistry; as well as, **Dr. Christoph Kubis** and **Phong Dam** for their help with the in-situ spectroscopy.

Furthermore, I want to thank all the other current and former members of the “Sustainable Redox Reactions” group for creating such a pleasant and productive work atmosphere. I would like to specifically mention **Dr. Pavel Ryabchuk** and **Niklas Both** for the helpful scientific discussions; **Dr. Florian Bourriquen** for his excellent editing services and French delicacies; **Dr. Thomas Leischner** for his advice in all matters PhD and countless (more or less) sophisticated conversations; **Dr. David Leonard** for his humor and for introducing me to the science of fermentation; **Dr. Shuxin Mao** for help regarding the layout of this thesis; **Dr. Haifeng Qi** for keeping me company during the late hours in the lab; my supervised students **Andrea Vicenzi** and **Germán Lopez Robledo** for the good work on the currently still ongoing projects; and last but not least our technicians **Helen Hornke** and **Katja Andres** for all their assistance within the lab. Thank you all for the great times in- and outside of work as well as your friendship!

I am thankful to **Prof. Johannes de Vries**, and his group members, **Dr. Brian Spiegelberg**, **Dr. Andrea Dell'Acqua**, **Dr. Soumyadeep Chakrabortty** and **Claas Schünemann** for the sharing of research equipment, the numerous scientific discussions and the technical support.

I want to further acknowledge the whole LIKAT analytical and technical departments for their support: Especially **Dr. Anke Spannenberg**, for her immense help and rigor determining crystal structures by X-ray diffraction; **Dr. Wolfgang Baumann** and **Susann Buchholz** for NMR measurements; as well as **Andreas Koch** for his aid in maintaining the GCs. Additionally, I am indebted to **Andreas Hutter** for all the repairs around the institute and the lab. No matter the device "Hutti will fix it" was the overarching theme: Rotavaps, stir plates, UV-lamps, doors, gas lines, vacuum pumps, clocks etc. Mr. Hutter repaired it all in a heartbeat. I also want to recognize the LIKAT purchasing department, represented by **Torsten Weiss** and **Dr. Torsten Dwars**, for making sure I had a quick and reliable supply of research chemicals delivered to my bench from (sometimes) all over the world.

Again, I want to express my gratitude to all employees of LIKAT and the University of Rostock for their help over the years.

For carefully proofreading this thesis, I would like to thank **David**, **Andrea**, **Florian** and **Thomas** once more.

Finally, I have to thank my parents **Maria** and **Bernhard** for teaching me the immense value of (higher) education and enabling me to follow my scientific passion. Thank you for nurturing my curiosity for the wonders of our natural world and for always supporting me throughout my extensive academic endeavors.

In the end, I am incredibly grateful to my partner **Eva** for sticking by me over all the years, for joining me in Rostock, for all her support especially in the intense phases of my PhD, even when I needed to dedicate the majority of my time to chemistry and I often spent most of my days in the lab instead of with her. Thank you for being so accepting and bringing so much care and happiness into my life!

Table of Contents

List of Abbreviations

Δ*G*	Change in Gibbs free energy
+M-effect	Positive mesomeric effect
Ad	Adamantyl
Ar	Aryl
BASF	Badische Anilin- und Sodafabrik
Bcl-2	B-cell lymphoma 2
Bn	Benzyl
Boc	tertiary butoxycarbonyl
Bu	n-Butyl
Cat/Cat.	Catalyst
Conv.	Conversion
COX-2	Cyclooxygenase-2
Cy	Cyclohexyl
DBU	1,8-Diazabicyclo(5.4.0)undec-7-ene
DFT	Density functional theory
DMC	Dimethyl carbonate
e	Electron
E_a	Energy of activation
Equiv.	Equivalents
Est.	Estimated
Et	Ethyl
Et al.	Et alia (and others)
EU	European union
fac	Facial
FLP	Frustrated Lewis pair
GC	Gas chromatography
Hex	n-Hexyl
^{i}Pr	iso-propyl
IR	Infrared (spectroscopy)
***J*-coupling**	Spin-spin coupling
LED	Light-emitting diode
M	Molarity
Me	Methyl
NAP	2-Naphthylmethyl
NMR	Nuclear magnetic resonance (spectroscopy)
NOESY	Nuclear Overhauser and exchange spectroscopy
OA	Oxidative addition
Oct	n-Octyl
OTf	Triflate (trifluoromethanesulfonate)
Ph	Phenyl
pK_a	Negative logarithmic acid dissociation constant

PMB	*para*-Methoxybenzyl
ppm	Parts per million
Pr	n-Propyl
R	Rest
RE	Reductive elimination
Ref.	Reference
RT	Room temperature (25 °C)
React-IR	*In situ* IR spectroscopy
Syngas	Synthesis gas (mixture of CO and H_2)
^{t}amyl	tertiary amyl (2-methyl-2-butyl)
^{t}Bu	tertiary butyl
TFA	Trifluoroacetic acid
THF	Tetrahydrofuran
THQ	1,2,3,4-Tetrahydroquinoline
TMS	Trimethylsilyl
TOF	Turnover frequency
TON	Turnover number
Vs.	*Versus* (compared with/as opposed to)
Z-Gly-Pro-pNA	Benzyloxycarbonyl-glycyl-L-prolin-4-nitroanilid

1 Introduction

Chemistry lies at the heart of most of the modern manufacturing industries. It enables us to feed (fertilizers, agrochemicals), heal (pharmaceuticals), smell/taste (flavors, fragrances), clean (disinfectants, soaps, detergents), illuminate (LEDs, light bulbs, liquid crystal displays), power (electronics, solar cells, batteries), construct (plastics, polymers, adhesives), color (dyes, coatings) the world we live in and much more. The scientific advancements in chemical research and concurrent increases in production capabilities over the last century have enabled near exponential population growth and have increased the standard of living for billions of people around the world.

1.1 The Need for Green Chemistry

However, on the flipside, many of these positive developments in chemistry and industrial production have had severe side effects. They have taken a large toll on our earth's natural environment and resources. Release and spills of toxic and persistent chemicals such as heavy metals, polycyclic aromatic compounds, chlorofluorocarbons, dioxins, pesticides, and others have led to environmental catastrophes all over the world.[1] Just during the preparation of this doctoral thesis there were numerous disasters, in which toxic or dangerous chemicals were released into the environment, causing tragic loss of life as well as horrific pollution of our ecosystems.[2] In addition to the direct negative impacts on health and the environment, the chemical industry emits a massive amount of greenhouse gases into the atmosphere.[3] This is because many chemical processes are highly energy intensive. As an example 13% of all the energy used in Germany is consumed by the chemical industry, making it the industrial sector with the highest energy demand.[4] A large part of that energy comes from finite fossil fuels (coal, oil and gas), which on top of their detrimental impact on the climate and the depletion of natural resources, leads to the EU's dependance on energy imports. A particularly unfavorable circumstance in a time of international conflicts and unsteady supply chains. To illustrate this point further, in 2021, just BASF Ludwigshafen, the biggest chemical production site in Germany, used up as much natural gas as several entire countries, for example all of Switzerland.[5] Furthermore, fossil fuels serve not only as the main energy source of most of the current chemical manufacturing processes but also as the main building blocks or starting materials of the chemical value chain, further increasing problems associated with their use.[6] In addition, the depletion of natural resources relates not only to fossil fuels, but also to other building blocks required in our current society such as (precious) metals, "rare earths" and other elements whose mining, production or processing is often also highly energy intensive and polluting.[7] It is therefore of paramount importance to ensure that in the future, chemical production becomes more sustainable or so-called "green". Noticing this necessity for a change in chemical manufacturing, with incredible foresight, already in 1998 Paul T. Anastas and John C. Warner formulated the twelve principles of green chemistry that are still very valid today.

The principles (as written in their seminal book *Green Chemistry: Theory and Practice*) are:[8]

1. *Prevention. Preventing waste is better than treating or cleaning up waste after it is created.*
2. *Atom economy. Synthetic methods should try to maximize the incorporation of all materials used in the process into the final product. This means that less waste will be generated as a result.*
3. *Less hazardous chemical syntheses. Synthetic methods should avoid using or generating substances toxic to humans and/or the environment.*
4. *Designing safer chemicals. Chemical products should be designed to achieve their desired function while being as non-toxic as possible.*
5. *Safer solvents and auxiliaries. Auxiliary substances should be avoided wherever possible, and as non-hazardous as possible when they must be used.*
6. *Design for energy efficiency. Energy requirements should be minimized, and processes should be conducted at ambient temperature and pressure whenever possible.*
7. *Use of renewable feedstocks. Whenever it is practical to do so, renewable feedstocks or raw materials are preferable to non-renewable ones.*
8. *Reduce derivatives. Unnecessary generation of derivatives, such as the use of protecting groups, should be minimized or avoided if possible; such steps require additional reagents and may generate additional waste.*
9. *Catalysis. Catalytic reagents that can be used in small quantities to repeat a reaction are superior to stoichiometric reagents (ones that are consumed in a reaction).*
10. *Design for degradation. Chemical products should be designed so that they do not pollute the environment; when their function is complete, they should break down into non-harmful products.*
11. *Real-time analysis for pollution prevention. Analytical methodologies need to be further developed to permit real-time, in-process monitoring and control before hazardous substances form.*
12. *Inherently safer chemistry for accident prevention. Whenever possible, the substances in a process, and the forms of those substances, should be chosen to minimize risks such as explosions, fires, and accidental releases.*

With these guidelines in hand, it is up to society and scientists to apply them more broadly and to further enable industry to be more sustainable by developing greener processes. Chemists in particular are in a unique position to help solve many of the current global challenges such as climate change, environmental pollution and resource depletion since many of these issues are inherently of chemical nature.

1.2 Catalysis – A Brief Introduction

As hinted in the previous chapter, catalysis is an integral part of sustainable chemistry and a crucial tool to overcoming the environmental challenges of today. But why is that and what defines a catalyst?

It had been observed for centuries that certain substances have the ability to speed up chemical processes. In 1835 already, pioneering scientist Jöns Jacob Berzelius gave this phenomenon the name catalysis after the Greek word “καταλύειν” meaning to dissolve or unbind.[9] This was due to the fact that most catalytic reactions known at that time were based on decomposition processes, such as the hydrolytic degradation of starch catalyzed by acids or the platinum-catalyzed oxidation of hydrogen in air.[9] A definition of a catalyst that still holds true today was coined by Wilhelm Ostwald (Nobel prize 1909) in 1895: “*A catalyst is a substance, that increases the rate of a chemical reaction, without being consumed itself and without changing the final position of the thermodynamic equilibrium of that reaction*”.[10] The manner by which a catalyst speeds up a chemical reaction is by offering an alternative reaction pathway, that is lower in activation energy (E_a) than the uncatalyzed reaction (see Figure 1).

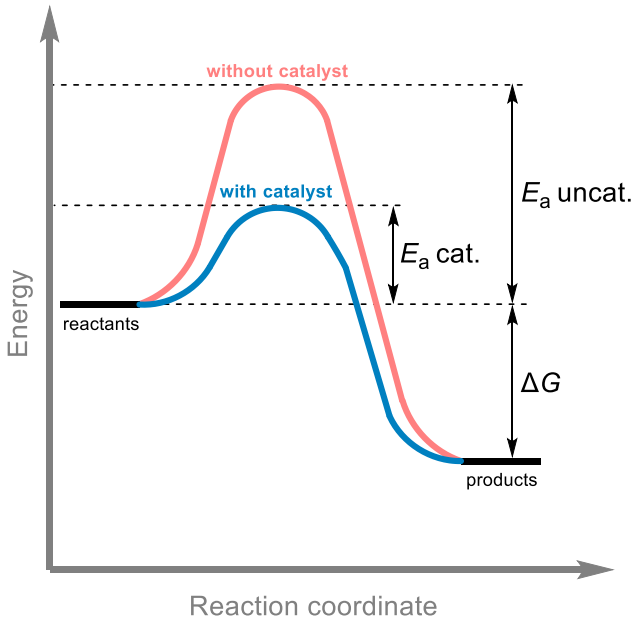

Figure 1. Simplified potential energy diagram of a catalyzed vs. uncatalyzed exergonic reaction.

Typically, this lower energy pathway entails the catalyst binding to the substrate(s) and thus forming an intermediate substrate-catalyst complex, which has a lower energy transition state than the uncatalyzed reaction. According to the Eyring equation, this then enables the reaction to proceed at a higher rate or milder temperature. Finally, the resultingly formed product-catalyst complex dissociates releasing the unchanged catalyst and the product(s). An example of a general catalytic cycle for a monomolecular reaction is shown in Scheme 1.

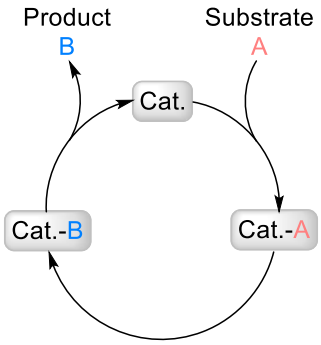

Scheme 1. Exemplary catalytic cycle of a monomolecular reaction.

In theory, a catalyst is not consumed during the catalytic process and therefore could reenter the catalytic cycle an infinite number of times, thus converting (turning over) an unlimited amount of substrate. In practice however, catalysts get deactivated (or "poisoned") over time. Such deactivations can be reversible or irreversible depending on the mechanism of deactivation. Common catalyst poisons include moisture, oxygen or sulfur species. A value that describes the catalyst stability or lifetime is the turnover number (TON) defined as the amount of product formed per amount of catalyst prior to deactivation.[11] TONs can range from single digits to millions for highly efficient molecular catalysts and even several orders of magnitude higher ($>10^{11}$) in the case of enzymes, nature's exceptionally productive catalysts.[12] Catalyst activity is typically expressed by the turnover frequency (TOF), defined as the TON per time.[11] However, since the TOF is strongly dependent on the concentration of reactants and thus can vary over the course of a catalytic experiment, care has to be taken when determining and comparing catalytic activities using this metric.[13] In addition to increasing the rate of chemical reactions, a catalyst can also enable processes that might otherwise have a kinetic barrier too large to be performed under reasonable conditions, thus enabling those reactions to be feasible in the first place. Furthermore, since different catalysts might offer different reaction pathways, by varying the catalyst it is possible to steer the selectivity of a reaction and to even convert the same substrate into multiple different products.[14] In other words, applying catalysis one can increase the selectivity of a given process towards one specific product and thus avoid undesired side-reactions, which in turn leads to reduced waste generation. The incredible potential and impact of catalysis has not been ignored by the academic and industrial communities. Historically, 17 Nobel prizes in chemistry have been awarded to scientists working in and around the field of catalysis. In the developed nations roughly 40% of the nitrogen in our bodies is purported to have been fixated catalytically by the Haber-Bosch process (Nobel prizes 1918 and 1931).[15] It is further estimated that over 90% of all chemical products undergo at least one catalytic step in their lifetime.[11]

1.2.1 Heterogeneous vs. Homogeneous Catalysis

Catalysts can generally be classified by their reactivity (e.g. acid/base, photo, redox, coordination) or by their structure (supramolecular, complex, organic, protein), but the most established classification relates to the physical state of matter (phase) in which the catalysis takes place. In homogenous catalysis catalyst and substrate(s) are present in the same

homogeneous phase (typically liquid solutions), whereas in heterogeneous catalysis catalyst and substrate(s) are contained in different phases (typically solid/liquid or solid/gas) and the catalysis takes place on the catalyst's surface.[14] Both types of catalysis have different benefits and drawbacks that are illustrated in Table 1 below.

Table 1. General comparison of heterogeneous and homogeneous catalysts.[16]

Properties	Heterogeneous Catalyst	Homogeneous Catalyst
Catalyst Preparation	Facile	Facile to highly challenging
Selectivity	Low	High
Reaction Conditions	Harsh	Mild
Activity	Low to variable	High
Tunability/Rational Design	Somewhat	High
Sensitivity	Low	Variable to high
Recyclability	High	Low
Structure	Low-defined	Molecularly-defined
Analytics	Challenging	Facile (mostly)
Mechanistic Studies	Challenging	Feasible
Catalyst Separation	Facile	Challenging
Cost	Low	Medium to high

Since heterogeneous catalysts are easily separated, affordable, robust and often recyclable they are mainly used for bulk chemical processes, where the substrates are cheap and simple molecules that need to be produced in up to multiple million tons per year. Homogeneous catalysts are more commonly used for fine chemical processes because fine chemicals are more complex and consequently more expensive. Therefore, milder and more selective catalysts are often needed, that can be rationally fine-tuned to accommodate the specific needs a process. However, as the following chapters will show, there are also some exceptions to this rule and a few homogeneous catalytic processes are applied on very large scales in industry.

1.3 Homogeneous Catalysis

Homogeneous catalysis can in principle refer to any type of catalysis where reactants and catalyst are present in the same phase.[11] This includes for example simple acid-base catalysis, catalysis with small organic molecules (organocatalysis) and even catalysis conducted with enzymes (biocatalysis).[11] The latter two subfields in particular have seen massive developments in recent years culminating in two Nobel prizes. One was awarded to Frances Arnold in 2018 for developing the directed evolution of enzymes,[17] the other one to Benjamin List and David W. C. MacMillan in 2021 for the development of asymmetric organocatalysis.[18] Traditionally speaking however, homogeneous catalysis refers to catalytic transformations conducted with the aid of a transition metal complex.[11] This will be the focus of the following chapters and this thesis overall.

1.3.1 Homogeneous Transition Metal Catalysis

As indicated by the name, in homogeneous transition metal catalysis the activation of the substrate(s) typically occurs in the coordination sphere of a transition metal complex. The complex consists of a central metal atom or ion, which is coordinated by multiple organic or inorganic ligands. The ligands help to stabilize the central metal atom, solubilize it and can modify the central atoms steric and electronic properties, thereby fine-tuning its reactivity.[11] Furthermore, the ligands can also actively take part in the catalysis, functioning for example as proton or electron shuttles. Additionally, ligands might also just act as labile placeholders that dissociate under catalytic conditions, freeing up a coordination site for the substrate. Since in theory an unlimited variation of metal centers and ligands is possible, homogeneous catalyst's structures and reactivities are highly diverse and functionalizable. Common examples of complexes widely used in homogeneous catalysis are shown in Figure 2.

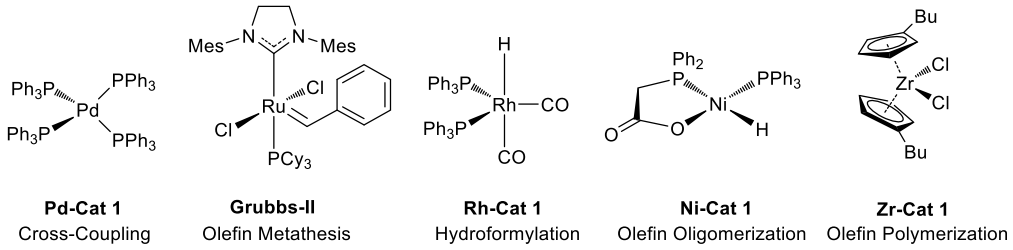

Figure 2. Common industrially applied homogeneous catalysts and their applications.

1.3.2 Homogeneous Hydrogenation Catalysis

Hydrogenation, i.e. the addition of hydrogen to an (unsaturated) substrate is one of the most fundamental reactions in organic chemistry, since organic molecules per definition are rich in C–H bonds. Additionally, hydrogen is one of the cheapest and potentially greenest reducing agents, with incredible importance for a sustainable energy future.[19] The first breakthroughs in the field of hydrogenation were reported in 1897 by Paul Sabatier (Nobel prize 1912) and his coworker Jean-Baptiste Senderens, who discovered that using finely dispersed nickel powder one can hydrogenate small organic molecules that contain multiple bonds.[20] A first example was hydrogenation of the C=C double bond in ethylene resulting in the formation of the saturated product ethane.[20] Over the following years this heterogeneous hydrogenation procedure was extended to many additional substrate classes including carbon dioxide, arenes, nitroarenes, aldehydes, ketones, vegetable oils and others.[20] Early often ill-defined and ineffective "homogeneous" systems for hydrogenations started to be developed several decades later.[21] A quantum leap in homogeneous hydrogenation catalysis however was the discovery of chlorido-tris(triphenylphosphine)-rhodium, now called Wilkinson's catalyst, after one of its inventors Sir Geoffrey Wilkinson (Nobel prize 1973).[22] In 1965, Wilkinson and coworkers observed that this complex is able to efficiently hydrogenate terminal alkenes and alkynes at ambient temperature and pressure.[22] The advent of powerful analytical techniques such as NMR spectroscopy and the increased mechanistic understanding of organometallic reactions consequently ushered in a new era of hydrogenation catalysis (overview of catalysts in Figure 3).[22b, 23] In the following years, Wilkinson's former student, John Osborn, together with his student Richard R. Schrock (Nobel prize 2005) developed an improved family of

cationic bisphosphine-rhodium-diolefin hydrogenation catalysts.[24] Chiral variants of these "Schrock-Osborn" catalysts were applied in pioneering studies on asymmetric hydrogenation in the early 1970s by Knowles (Nobel prize 2001) and others, leading to the development of the first industrial asymmetric hydrogenation process at Monsanto.[25]

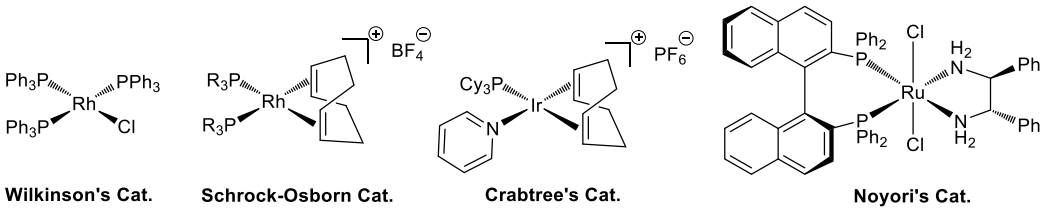

Figure 3. Established homogeneous hydrogenation catalysts developed in the 20th century.

The rhodium-based catalysts however had one significant shortcoming, they exerted only minimal activity towards tri- or tetrasubstituted unfunctionalized alkenes.[24b] This weakness was addressed by Crabtree and coworkers, who replaced the central metal with iridium and switched one phosphine ligand with a more labile nitrogen-based pyridine ligand.[26] Thus in 1977, the Crabtree catalyst was reported, which offered exceptional hydrogenation activity for a broad range of tri- and tetrasubstituted unfunctionalized alkenes.[26] This short historical excerpt on the development of homogeneous alkene hydrogenation is an illustrative example of the power of homogeneous catalysis. From the first breakthrough by Wilkinson, it took only a handful of years until an industrially viable stereoselective process could be developed and just 12 years until a catalyst suitable for even the most challenging substrates was developed by Crabtree.[25, 24b] Roughly a decade after this pioneering work on alkene hydrogenation, Ryōji Noyori (Nobel prize 2001) investigated the (asymmetric) hydrogenation of substrates containing polar double bonds (C=O, C=N) such as ketones and imines.[27] His most effective catalysts were ruthenium complexes supported by a combination of (chiral) bisphosphine and 1,2-diamine ligands (see Figure 3).[28] Noyori realized that under basic conditions catalysts containing at least one protic N–H group directly ligated to the metal showed exceptional improvements in hydrogenation activity.[27] In quantitative terms, a starting TOF of <5 h^{-1} could be increased by more than three orders of magnitude to a TOF of 6700 h^{-1} by introduction of an N–H ligand moiety.[28] This effect of the N–H functionality was studied in detail by Noyori leading to what is now known as the Noyori metal-ligand bifunctional mechanism (Scheme 2).[27, 29]

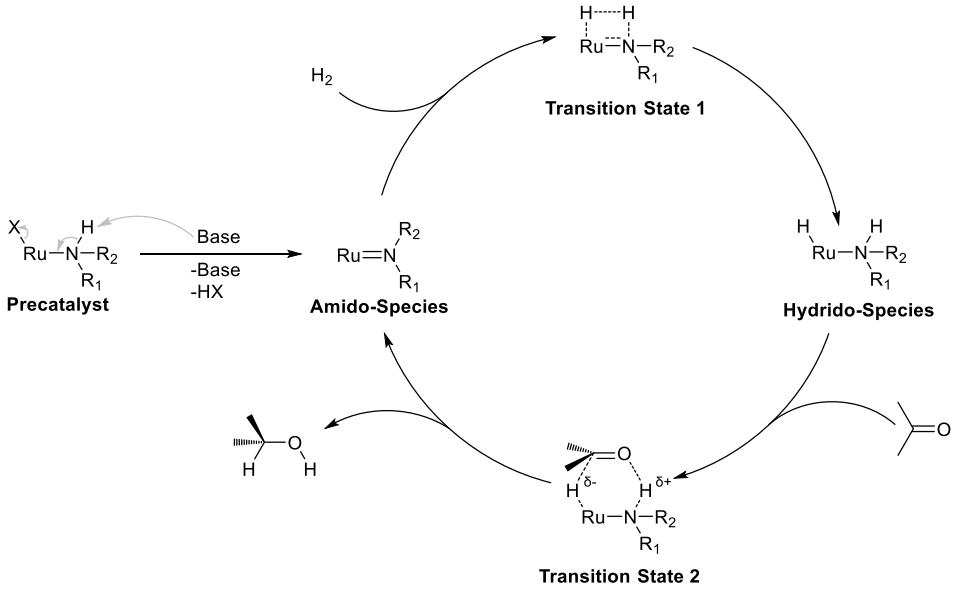

Scheme 2. Noyori mechanism for homogeneous hydrogenation. Spectator ligands omitted for clarity.

According to this mechanism the precatalyst first gets activated by base, which deprotonates the acidic N–H moiety thus forming a Ru-amido species. This species then heterolytically activates hydrogen aided by the build-in amido base leading to a hydrido-species. The protic N–H and the hydridic Ru-hydride of the hydrido-species, then are most likely transferred onto the polar unsaturated substrate in a concerted fashion via a six-membered transition state.[27, 29a] The protic N–H thereby acting as a hydrogen bond donor, thus activating the more electronegative atom of the polar double bond. Notably, herein an outer-sphere hydrogenation mechanism was proposed by Noyori, in which the substrate ketone does not directly coordinate to the catalyst. This was a significant distinction from the previously established inner-sphere hydrogenation mechanisms such as the homolytic oxidative addition pathway known for Rh and Ir catalysts or the heterolytic sigma-bond metathesis type mechanisms (see Scheme 3).[23, 27, 29a]

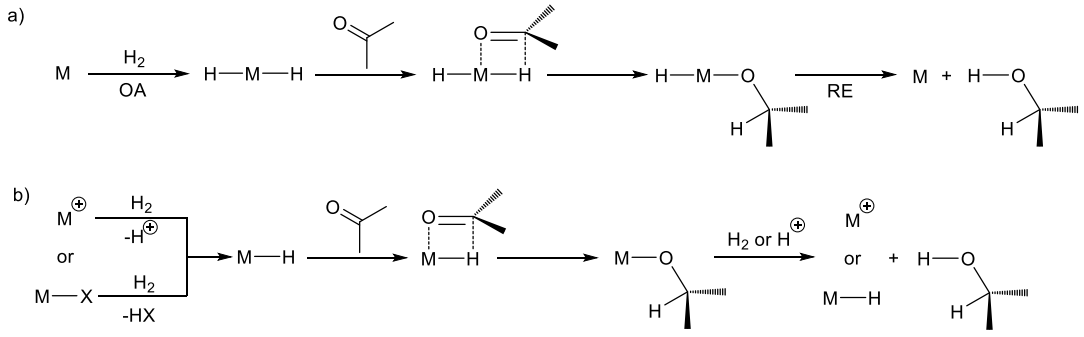

Scheme 3. Traditional pathways for the hydrogenation of polar unsaturated compounds: a) Homolytic dihydride mechanism via oxidative addition (OA) of hydrogen followed by migratory insertion of the substrate into the M–H bond and reductive elimination (RE) releasing product and catalyst; b) Heterolytic monohydride mechanism starting from M–H generation via deprotonation or σ-bond metathesis, then migratory insertion and finally protonolysis or hydrogenolysis.[27]

Since the Noyori type catalysts are also very effective for the reverse reaction (dehydrogenation), they are able to transfer hydrogen from hydrogen sources other than molecular hydrogen such as alcohols or formic acid, thus generating their oxidized counterparts ketones or CO_2 as by-products.[29a] These transfer hydrogenations can be milder, safer and cheaper alternatives to classical hydrogenations. However, due to by-product (i.e. waste) generation from the sacrificial hydrogen donor, they are less atom-economic than traditional hydrogenation. In more recent years, the Noyori-type metal-ligand bifunctional systems were further improved by many academic as well as industrial research groups leading to novel Ru-catalyst with unprecedented reactivity and stability (see Figure 4).[30] These bi- or tridentate PN(P/N) complexes are able to hydrogenate even low-reactive substrates, such as esters and amides, with high activity under comparably mild conditions.[30]

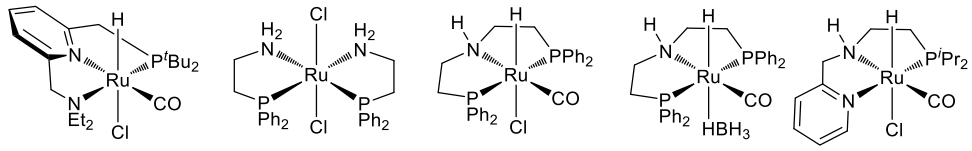

Figure 4. Selected highly active ruthenium-based hydrogenation catalysts.

1.4 Earth-Abundant Hydrogenation Catalysis

As seen in the previous chapters, the field of homogeneous (hydrogenation) catalysis is largely dominated by precious metal catalysts. While they show remarkable stabilities and activities, there are several downsides associated with the use of precious metal-based catalysts such as their low abundance, limited availability, high cost, and often high toxicity.[31] With the increased focus on green chemistry and on more sustainable chemical processes, a shift towards using more abundant and sustainable 3d transition metals (also called base metals) in catalysis has begun in the last decades. A comparison of the three most widely used precious metals in homogeneous hydrogenation catalysis (Ru, Rh, Ir) with three more sustainable base-metal alternatives (Mn, Fe, Co) is found in Table 2.

Table 2. Comparison of common earth-abundant 3d metals and precious metals used in catalysis.

Metal	Est. Abundance in Earth's Crust[32]	World Production [tons/year][33]	Price [€/kg][33]	Allowed Levels in Pharmaceuticals[34]
Mn	0.1%	16,000,000	1.95	250 ppm
Fe	5.6%	1,150,000,000	0.28	1.300 ppm
Co	0.03%	142,000	30.58	5 ppm
Ru	0.0000001%	30	13,789.00	10 ppm
Rh	0.00000002%	30	138,000.00	10 ppm
Ir	0.00000003%	7	160,900.00	10 ppm

Table 2 clearly shows the benefits of applying 3d-transition metals in terms of world-wide abundance, yearly production and consequently price. Measuring a metal's toxicity is more

complex since it relies on several different factors (e.g. ingestion pathway, oxidation state, exposure time).[31b] However a rough estimate can be made by looking at the European Medicines Agency's guidelines for trace elements in pharmaceuticals (Table 2, Column 5).[34] Particularly manganese and iron are permitted at significantly higher concentrations and can thus be deemed less-toxic compared to precious metals.[35] Additionally, all three discussed base-metals (Mn, Fe, Co) are essential elements in human life, playing vital roles in oxygen transport, metabolism, hormone production etc.[31a] However, none of the previously discussed precious metals occur naturally in humans. From a sustainability standpoint it can thus be hypothesized that nature is better adapted to coping with base-metals than with their heavier analogs.[36] Short introductions into historical and more recent developments of homogeneous manganese, iron and cobalt catalysts and their application will follow in the upcoming subchapters.

1.4.1 Manganese (Pincer) Catalysts for Hydrogenation Reactions

As discussed above, switching from precious metals to earth-abundant metals in catalysis is a major goal in sustainable chemistry. One of these metals is manganese, the 3rd most abundant transition metal on earth. Inspired by the remarkable reactivity and stability of the ruthenium (pincer) catalysts discussed in Chapter 1.3, multiple academic groups investigated if manganese-based catalysts supported by a similar ligand system could show comparable reactivity. Thus in 2016 several breakthroughs were made. Initially, Milstein and coworkers reported the first manganese-catalyzed dehydrogenation of alcohols.[37] Just three months later, Beller and coworkers reported Macho-type complexes for the first manganese-catalyzed hydrogenation reactions of nitriles, ketones and aldehydes.[38] Again, three months later, Kempe and coworkers published a triazine-based pincer catalyst for similar transformations, while Beller *et al.* published the first manganese-catalyzed ester hydrogenation.[39] These pioneering Mn-catalysts showed a comparable performance to the precious metal catalysts which they were based on.[40] Thus, an immense interest in manganese catalysis was sparked and dozens of further Mn-catalysts started being developed every year for various hydrogen transfer reactions (see Figure 5 for a selected overview).[40]

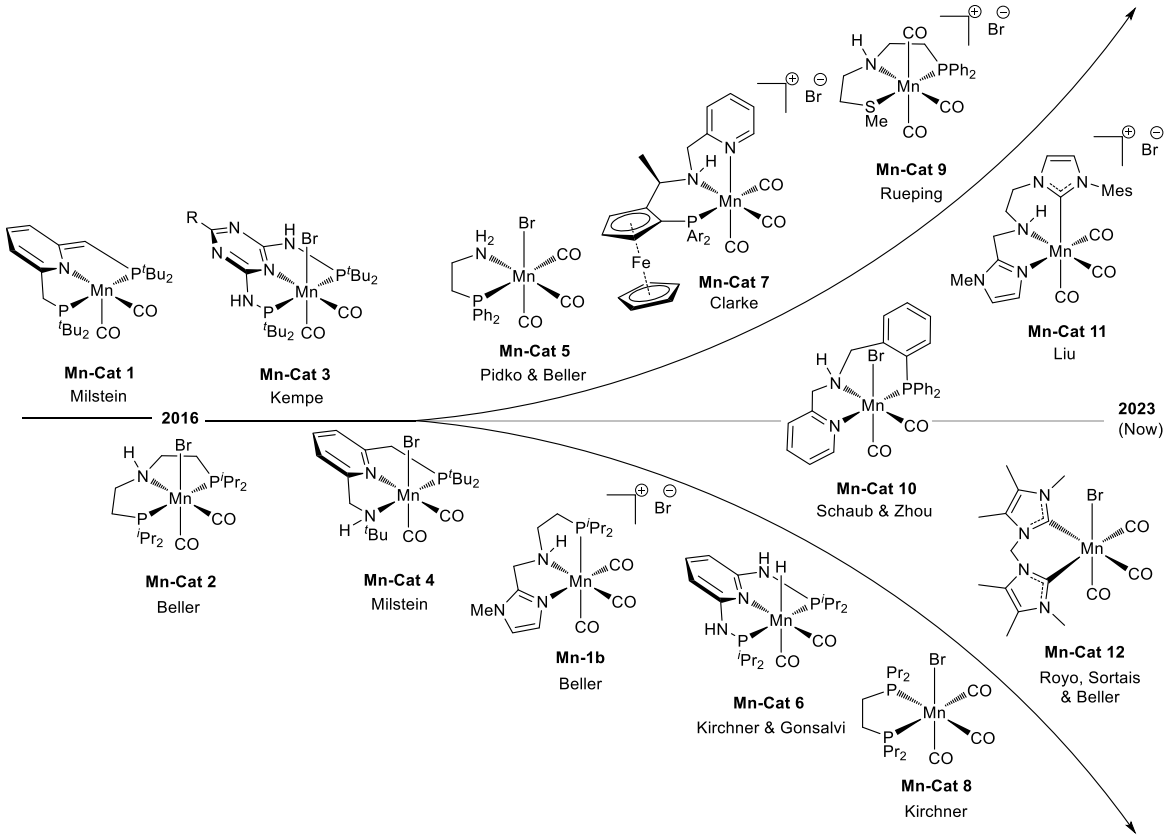

Figure 5. Selected overview of highly active manganese hydrogenation catalysts developed since 2016.[40c]

These transformations include hydrogenations of a plethora of functional groups including aldehydes, ketones, nitriles, esters, amides, imides, imines, CO, CO_2, alkenes, alkynes, heterocycles and more, but also transfer hydrogenations as well as hydrogen borrowing reactions.[40]

1.4.1.1 Manganese-Catalyzed Quinoline Hydrogenation

A particularly interesting substrate class in hydrogenation are quinolines and related N-heterocycles due to the prevalence of their partial-reduction products (tetrahydroquinolines) in bioactive natural products and pharmaceutical ingredients (see Figure 6 for examples).[41]

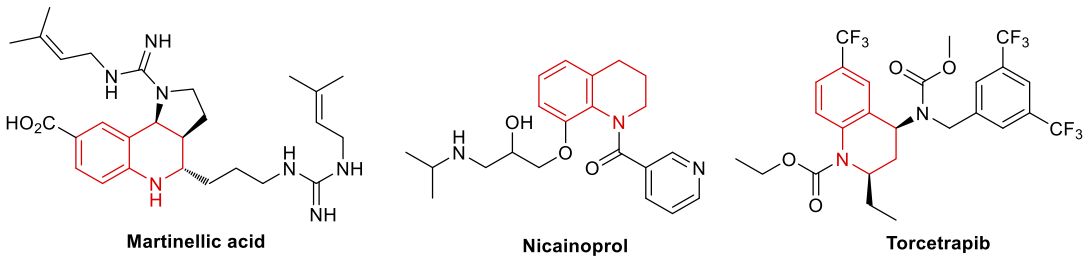

Figure 6. Exemplary bioactive natural products and pharmaceutical ingredients containing the tetrahydroquinoline (THQ) moiety marked in red.

Due to their hard-to-overcome aromaticity and coordinating ability, quinolines are particularly challenging substrates and were typically hydrogenated via heterogeneous or precious metal catalysis, which often required harsh conditions and provided low selectivity.[42] With the advent

of non-precious metal homogeneous catalysis, a handful of milder Mn-based systems were developed very recently (see Scheme 4 for a short overview). In 2019, Liu *et al.* reported the manganese-catalyzed hydrogenation of quinolines using catalyst **Mn-1b**, initially developed by our lab for amide hydrogenation.[43] However, the necessary reaction conditions were relatively harsh. Shortly thereafter our group discovered that simple pincer-ligand-free manganese pentacarbonyl bromide could hydrogenate quinolines under very mild conditions without the requirement of any additives.[44] Similar finding were made by Wang *et al*.[45] In 2021, Liu extended his original methodology to enable asymmetric hydrogenation under slightly less-forcing conditions by using a related chiral catalyst **Mn-Cat 13**.[46]

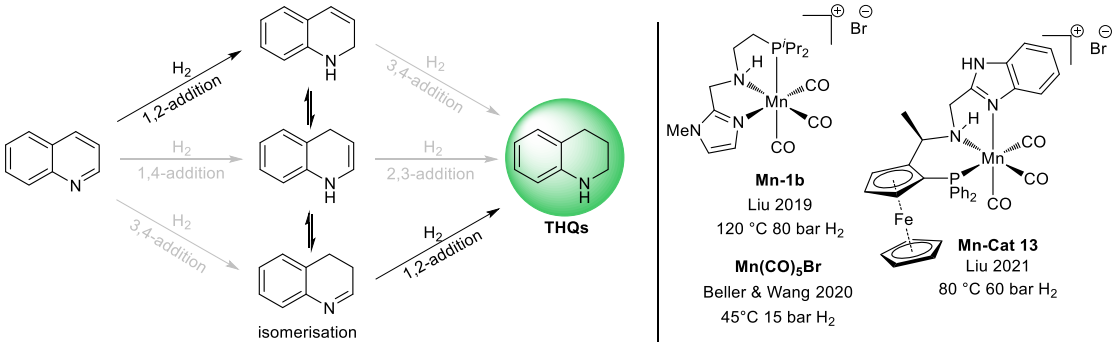

Scheme 4. Pathway of quinoline hydrogenation to tetrahydroquinolines with potential alternative pathways in grey (left) and recently developed Mn-catalyst systems (right).[43-46]

Our investigations into this transformation will be discussed in chapter 2.1.

1.4.2 Sustainable Iron Catalysts for Reduction Reactions

Iron is the 4th most abundant element in the earth's crust and thus offers incredible potential in the fields of sustainable chemistry and catalysis.[47] Whereas heterogeneous iron catalysis was established over a century ago, leading for example to the indispensable Haber-Bosch process for the fixation of nitrogen from the air,[48] defined homogeneous iron systems for hydrogenation were scarce until about the turn of the millennium.[49] One of the first such systems was reported by Bianchini and coworkers in 1992, who discovered that a remarkably stable iron hydride complex supported by the tetradentate Tetraphos ligand (see Figure 7 for overview) was able to selectively hydrogenate terminal alkynes to alkenes under mild conditions.[50] However, not much attention was paid to this breakthrough until Chirik reported that iron complexes supported by redox-non-innocent NNN-pincers catalyze alkene hydrogenation under ambient conditions.[51] Following this, in 2007 Casey and Guan published the first iron-catalyzed ketone hydrogenation using a half-sandwich complex previously prepared by Knölker.[52] These early reports sparked tremendous interest into the field of iron catalysis, leading to the development of many other systems.[49] Prominent further examples are the (transfer) hydrogenation systems of Morris.[53]

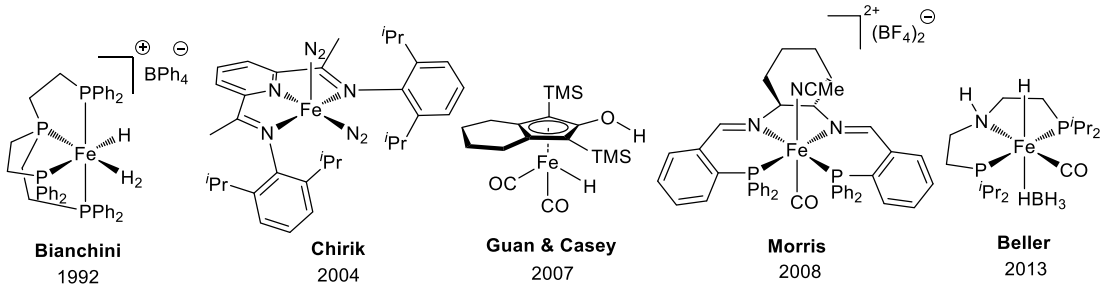

Figure 7. Pioneering molecularly-defined hydrogenation catalysts based on iron.

Additionally, the increased interest in iron catalysis lead Beller and coworkers to reinvestigate Bianchini's complex, finding that iron Tetraphos systems are also potent catalysts for several other hydrogenation reactions such as nitro reduction, CO_2 reduction or reductive anti-Markovnikov epoxide ring-opening.[54] In analogy to the previously discussed Ru-Macho-BH and Mn-Macho pincer systems, another breakthrough in the field of iron catalysis, reported around 2013 independently by Beller and shortly afterwards by Guan and coworkers, was the development of Fe-Macho-BH type catalysts suitable for various highly challenging hydrogenations.[55]

1.4.2.1 Base Metal-Catalyzed Cascade Pyrrole Syntheses

A recent trend in homogeneous catalysis is the application of 3d-metal hydrogen transfer catalysts to the more sustainable synthesis of heterocycles.[56] A particularly interesting heterocyclic moiety are pyrroles, due to their wide array of applications in the life-sciences (pharmaceuticals, agrochemicals, natural products) and other sectors (dyes, materials, etc.).[57]

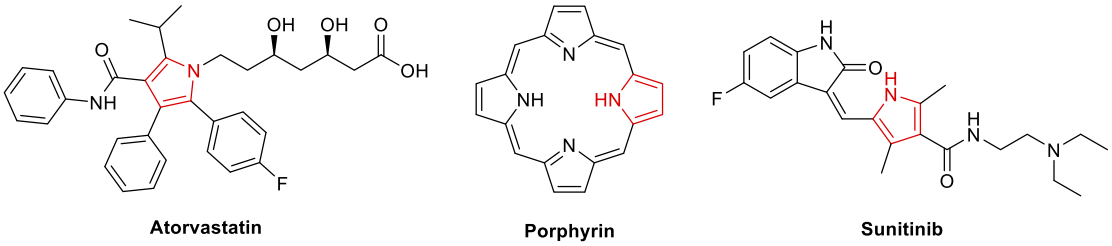

Figure 8. Common pharmaceutically and biologically relevant structures containing pyrroles (red).

Historically, pyrroles were prepared via condensation reactions according to the classical Hantzsch, Knorr or Paal-Knorr protocols (see Scheme 5).[58] Particularly the latter two named reactions are still applied quite regularly today, both in academia and industry, due to their high atom-economy, widely available starting materials and benign byproducts (water).[58]

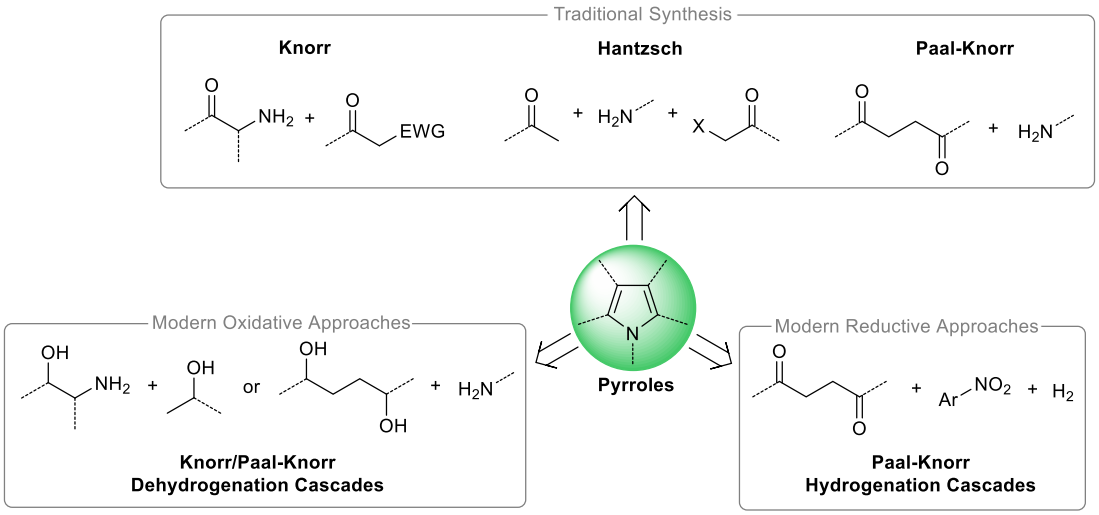

Scheme 5. Traditional pyrrole syntheses and more recent sustainable redox approaches.

Recent green chemistry approaches rely on coupling these classic methods with sustainable redox-processes leading to the development of multicomponent reaction cascades. The main benefit of cascade (a.k.a. tandem or domino) reactions is the decrease in necessary synthetic steps, resulting in additional savings in labor, time, resources and generated waste.[59] Oxidative cascades for pyrrole synthesis typically proceed via base metal-catalyzed dehydrogenation of alcohols followed by cyclization.[60] For N-aryl pyrroles however, several reductive processes starting from 1,4-dicarbonyls and nitroarenes using heterogeneous catalysts have been developed recently.[61] Since nitroarenes are widely available and since nitro reduction is one of the most common industrial methods for amine synthesis (particularly for arylamines), a direct reductive protocol from nitroarenes to N-aryl pyrroles is therefore highly favorable. However, the current heterogeneous methodologies are conducted under harsh conditions unsuitable for producing highly functionalized and thus sensitive drug molecules.[61] Our recent advances on applying milder homogeneous iron catalysts for this transformation will be discussed in Chapter 2.2 below.

1.4.3 Cobalt Carbonyls in Carbonylation and Hydrogenation Catalysis

Homogeneous cobalt catalysis has a long history. The cobalt-catalyzed hydroformylation, also called the “Oxo-process”, was discovered by Otto Roelen in 1938.[62] It is generally considered the oldest and most important homogeneous transition metal-catalyzed chemical process in the world, producing ca. 10 million tons of oxo-products every year.[63] Roelen postulated that this process, which forms a mixture of iso- and n-aldehydes from synthesis gas (CO/H_2) and olefins, is likely catalyzed by a homogeneous organometallic complex.[62] This sensitive and volatile complex $HCo(CO)_4$ was just previously discovered by Hieber in 1932.[64] The generally accepted mechanism for hydroformylation was described by Heck (Nobel prize 2010) and Breslow in 1961 (see Scheme 6).[65]

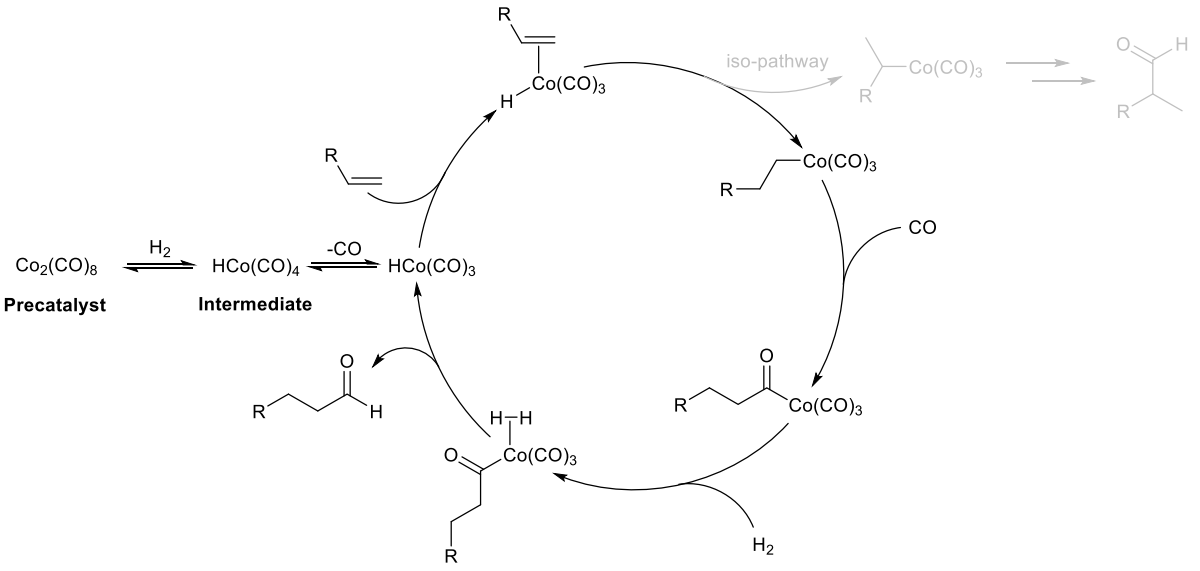

Scheme 6. Generally accepted mechanism for the cobalt-catalyzed hydroformylation of olefins.[63]

While highly selective Rh-based catalysts had started replacing cobalt in several hydroformylation applications in the 1970s, currently due to the volatile and high prices of rhodium, as well as the increased interest in earth-abundant catalysis, cobalt catalysts are still highly relevant, not just in hydroformylation but also in other fields, such as hydrogenation.[66] A particular cobalt-catalyzed hydrogenation reaction investigated in this thesis is the reductive etherification reaction.

1.4.3.1 Reductive Etherification, a Sustainable and Milder Protocol for Ether Synthesis

Ethers are ubiquitous organic chemicals, used as solvents, fragrances, fuel additives, pharmaceuticals, polymers and more.[67] Since the traditional Williamson or acid-catalyzed protocols for ether synthesis require harsh conditions, generate stoichiometric waste or have low selectivity, reductive etherification of aldehydes in the presence of alcohols has arisen as a more selective and sustainable alternative.[68] Classic reductive etherification protocols typically relied on (over)stoichiometric silane or borane reducing agents, resulting in large amounts of waste and thus poor atom-economy.[68]

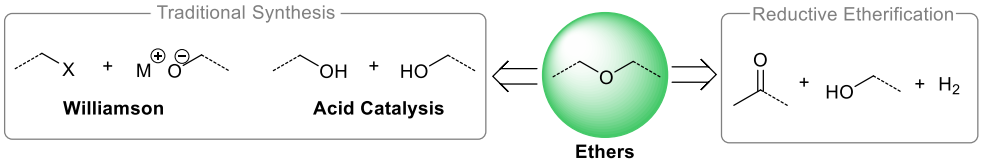

Scheme 7. Traditional pathways vs. more selective and sustainable reductive ether synthesis.

Therefore, modern procedures have focused on molecular hydrogen as a greener and more atom-economical reducing agent. Early variants mainly relied on heterogeneous precious metal hydrogenation catalysts.[69] Yet recently in 2015, Yi and Kalutharage reported a homogeneous ruthenium-catalyzed protocol,[70] whereas in 2017, Soós and coworkers explored metal-free frustrated Lewis pair (FLP) catalysts for the same reaction.[71] In chapter 2.3, our approach to apply the base metal cobalt in combination with a promoter as a catalyst for this transformation will be discussed.

2 Research Summary

2.1 Manganese PNN-Pincer-Catalyzed Hydrogenation of N-Heterocycles at Ambient Temperature

2.1.1 Catalyst Synthesis and Characterization

As discussed in the introduction, manganese catalysts and especially manganese pincer complexes have become a viable alternative to precious metal catalysts in hydrogen transfer reactions. Earlier research by our group on Ru-PN and Ru-PNN pincer catalysts showed improved hydrogenation of nitriles and esters when catalysts contained one electron-rich imidazolyl nitrogen donor moiety on the ligand instead of other nitrogen or phosphorus donors.[72] Additional work on manganese-catalyzed amide hydrogenation supported this trend.[43a] Inspired by these results, we set out to synthesize a small family of imidazolyl-PNN ligands and their corresponding manganese(I) complexes in order to test their reactivity in catalytic hydrogenation reactions (Scheme 8). The ligands could be synthesized in a one-pot reductive amination procedure starting from commercially available methyl imidazolyl aldehyde and a variety of aminophosphines. The phosphorus substituents and bridge length of the aminophosphines were varied to test for steric, electronic, and/or bite-angle effects on catalyst activity and stability. Without the need for further purification, the crude ligands could then be reacted with manganese pentacarbonyl bromide in refluxing tetrahydrofuran to give the corresponding manganese pincer complexes in high yield and just two synthetic steps overall.

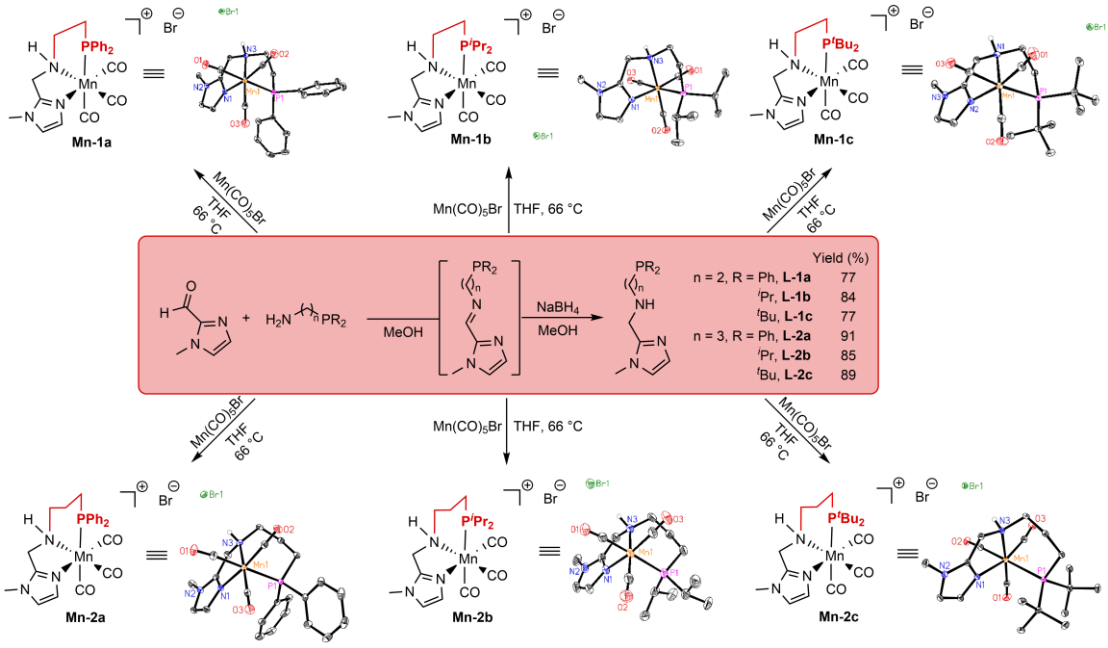

Scheme 8. Synthesis of imidazolyl-PNN pincer ligands (center) and their corresponding manganese complexes.

The obtained complexes were fully characterized by standard analytical techniques including single-crystal X-ray diffraction. This revealed that all six complexes show a slightly distorted octahedral geometry as to be expected for a low-spin d^6 manganese(I) complex. Furthermore,

they are cationic and contain a facially coordinated pincer ligand, the remaining three coordination sites being occupied by carbonyl ligands. The bromide anion, a comparably weakly-binding ligand, is expelled from the coordination sphere and not directly coordinated. The facial geometry of the complex is somewhat unusual since typically one would expect a pincer ligand to bind in a planar meridional fashion. However, in manganese tricarbonyl complexes facial pincer geometry is observed more frequently and can be explained both electronically and sterically.[40c] The strong trans effects of the carbonyl ligands in the manganese pentacarbonyl bromide precursor preferentially labilize two *trans*-binding CO ligands as well as the *trans* bromide, leading to more facile substitution at the facial positions. Additionally, the smaller steric demand of the imidazolyl N-donor ligand, compared to for example a bulky dialkylphosphine moiety, allows the flanking P and N donors to be closer together and thereby *cis* to each other. Exemplary computations on **Mn-1b** and **Mn2-b** also revealed that the effect is not only kinetic in nature but also showed the facial complexes to be ca. 5 kcal/mol more stable than their meridional analogs. ^{1}H NOESY-NMR experiments of **Mn-1b** and **Mn-2b** further revealed that the *fac*-geometry is not only present in the solid state but also maintained in solution by showing a proximity coupling between imidazolyl and alkylphosphine protons. The ligand variations directly translate into geometrical changes in the crystal structures of the six complexes. While changing the PN^{H}-tether length from ethylene, which forms a 5-membered chelate ring, to propylene, giving a 6-membered chelate, an increase of the P–Mn–N^{H} bite angle from around 82° to near 90°, the ideal octahedral angle, is observed (see Table 3).

Table 3 Selected bond angles and distances of manganese PNN-pincer complexes.[43a]

Complex	Tether length	P-Substituent	P–Mn–N^{H} angle	P–Mn bond length
Mn-1a	2 C-atoms	Ph	82.9°	2.33 Å
Mn-1b	2 C-atoms	^{i}Pr	82.2°	2.34 Å
Mn-1c	2 C-atoms	^{t}Bu	82.3°	2.44 Å
Mn-2a	3 C-atoms	Ph	87.7°	2.33 Å
Mn-2b	3 C-atoms	^{i}Pr	88.7°	2.35 Å
Mn-2c	3 C-atoms	^{t}Bu	91.2°	2.46 Å

It should be noted that this change in bite-angle has little to no effect on the P–Mn bond distances, leading one to conclude that the bond strength and consequently the complex stability is not strongly impacted by the variation in bite-angle. Furthermore, while Ph and ^{i}Pr substituted phosphine pincers give close to the expected bond lengths for a Mn–P single bond (sum of covalent radii 2.30 Å),[73] the ^{t}Bu phosphine Mn bond is significantly elongated. This means that the steric bulk of the bis(*tert*-butyl) phosphine variant is likely leading to a weakened Mn–P bond thereby leading to a somewhat destabilized pincer complex. IR stretching vibrations of carbonyl ligands are a good handle for the electron-richness of a metal complex, lower wavenumbers indicating a weakened C≡O triple bond due to increased back-bonding from the metal center to the carbonyl ligand. From IR data one can therefore deduce, that the e-donor capabilities of the phosphine substituents on the manganese center improve in the

order of Ph_2P << $^{i}Pr_2P$ < $^{t}Bu_2P$, which is in accordance with their inductive effects, as well as with previous reports from Liu and seminal reports by Tolman.[74, 43b] Furthermore, the IR stretching vibrations confirm the desired increased σ-donation of the basic imidazole donor compared to weaker arylphosphine or pyridyl donors, in line with studies conducted by Liu on Mn-amide complexes.[43b] Even though the novel complexes contain electron-rich phosphine and nitrogen ligands, they show remarkable stability to air in the solid state, which is nontrivial for low-valent 3d metal catalysts, which generally tend to be more sensitive than their precious metal analogs. This property (the air-stability), aside from their comparable reactivity to precious metals, might be the main reason why low-valent manganese(I) complexes have found so much interest in the catalysis research community since the first breakthrough reports were published in 2016.[38]

2.1.2 Catalytic Testing and Scope

Continuing on from the earlier studies on amide hydrogenation, further screening in our group revealed that the new catalysts are not just active towards amides, but also showed hydrogenation activity for several other substrate classes including aldehydes, ketones, nitriles, and quinolines.[43a] The latter being arguably the most interesting substrates due to their desirable biological properties. As discussed in the introduction, Liu and coworkers had achieved this transformation using specific manganese pincer complexes.[43b, 46] However, they needed drastic reaction conditions of 80-120 °C and 60-80 bar hydrogen pressure.[43b, 46] The simple $Mn(CO)_5Br$-catalyzed protocol simultaneously reported by our group enabled significantly milder conditions, but has some shortcomings regarding substrate scope.[44] Interestingly, initial tests of our small catalyst library revealed that particularly the propylene-bridged **Mn-2b** showed intriguing reactivity for quinoline hydrogenation, which could potentially outperform both systems of Liu *et al.* as well as $Mn(CO)_5Br$ in terms of catalyst activity and applicability. We therefore decided to select **Mn-2b** as our benchmark catalyst as well as quinoline (**1a**) as the benchmark substrate and do a thorough optimization of the reaction conditions to test the limits of this novel catalyst (Highlights in Table 4). Initial solvent and additive screening revealed that alcohols (EtOH, ^{i}PrOH, ^{t}amylOH) and alkoxide bases resulted in the highest catalytic activity in combination with **Mn-2b**. Therefore, we settled on ^{i}PrOH as solvent and solid KO^{t}Bu base as additive for the further screening. Starting from relatively harsh conditions of 140 °C, 40 bar H_2 and 5 mol% catalyst, which gave decent conversion and yields (Entries 1 and 2), we went to consecutively milder conditions. Since ^{i}PrOH could also act as a hydrogen donor in transfer hydrogenative fashion, a control reaction without hydrogen gas was conducted (Entry 3). However, a massive reduction in both conversion and yield was observed, pointing towards transfer hydrogenation being only a minor pathway. Stepwise decreases in temperature from 140 to 100, 80 and then 60 °C, as well as simultaneous reduction in catalyst loading indicated that the catalyst **Mn-2b** shows excellent performance under more favorable conditions, giving full conversion and quantitative yields in all three cases (Entries 4-6). Further reducing the reaction temperature (from 60 °C to RT) and/or hydrogen pressure (from 40 bar to 20 bar) showed a negative effect, giving decreased but still acceptable yields of 61 to 76% (Entries 7 and 9). A control reaction further revealed that in the absence of base no reduction takes place (Entry 8). This is in line with

previous reports on manganese pincers and conforms to Noyori's metal-ligand bifunctional mechanism, which is likely at work here.[40c] At this point, we decided to reevaluate the solvent and base additive again since the conditions were now significantly different to the original screening conditions and maybe new effects would arise at milder conditions. As expected, the screening revealed that at room temperature and only 20 bar of hydrogen tertiary amyl alcohol (^{t}amylOH) was superior to ^{i}PrOH. In addition, a marked improvement in reactivity was observed when the base additive (KO^{t}Bu) was predissolved in THF before addition to the reaction mixture (Entry 10), leading to unprecedented full conversion and near quantitative yield of the corresponding 1,2,3,4-tetrahydroquinoline (**2a**) at ambient temperature. We believe a likely explanation for the enhanced reactivity is the improved mixing of catalyst and base during the precatalyst activation, which leads to a higher concentration of the active catalyst species in solution. Further reductions in hydrogen pressure or catalyst loading coincided with slight decreases in both conversion and yield (Entries 11 and 12). Notably, catalyst **Mn-2b** even showed hydrogenation activity under both ambient temperature as well as pressure (1 bar H_2). While the yield is only poor (25%), these conditions represent, to the best of our knowledge, the mildest ever achieved with a homogeneous earth-abundant catalyst for this type of reaction. Moreover, this exemplifies a significant improvement of the previously developed catalysts in and outside of our own group, including $Mn(CO)_5Br$.

Table 4 Optimization of conditions for the manganese-catalyzed quinoline hydrogenation.

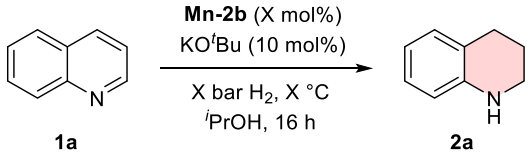

1a **2a**

Entry	H_2 [bar]	T [°C]	Mn-2b [mol%]	Conv. 1a[a]	Yield 2a[a]
1[b]	40	140	5.0	79%	77%
2	40	140	5.0	85%	84%
3	-	140	2.5	13%	11%
4	40	100	2.5	>99%	99%
5	40	80	2.5	>99%	99%
6	40	60	2.5	>99%	99%
7	20	60	2.5	78%	76%
8[c]	20	60	2.5	0%	0%
9	20	RT	2.5	61%	61%
10[b,d]	20	RT	2.5	>99%	97%
11[b,d]	20	RT	2.0	85%	83%
12[b,d]	10	RT	2.5	93%	85%
13[b,d]	1	RT	2.5	30%	25%
14[e]	1	45	2.0 ($Mn(CO)_5Br$)	25%	10%

Reaction conditions: **1a** (0.5 mmol), KO^{t}Bu (10 mol%), ^{i}PrOH (2 mL), 16 h. [a] Determined by GC using hexadecane as internal standard. [b] ^{t}amylOH (2 mL). [c] without KO^{t}Bu. [d] using KO^{t}Bu in THF (1 M). [e] see Ref. 44.

Having found optimal conditions for our benchmark substrate quinoline (see Entry 10), we investigated if **Mn-2b** not only possesses improved catalytic activity but also an improved general applicability in comparison to previous systems. Therefore, a scope of quinolines and related N-heteroarenes was prepared and directly compared to the simple but effective $Mn(CO)_5Br$ system (Scheme 9). Initially, we put our focus on steric and electronic variations of the quinoline core. Substrates containing electron-donating as well as electron-withdrawing functional groups were converted well (see Examples **2c-2k**). Furthermore, substituents with increasing steric demand were tolerated at various positions on the heterocyclic ring. A notable example is substrate **1c**, which contains an aryl group in the 3-position and thus gave poor yields with $Mn(CO)_5Br$ even under more drastic conditions, but with our novel catalyst system it provided a good isolated yield of 72%. Substituents on the 8-position (**1f**, **1h**, **1i**) had also been particularly challenging previously, but novel **Mn-2b** converted these compounds very efficiently.

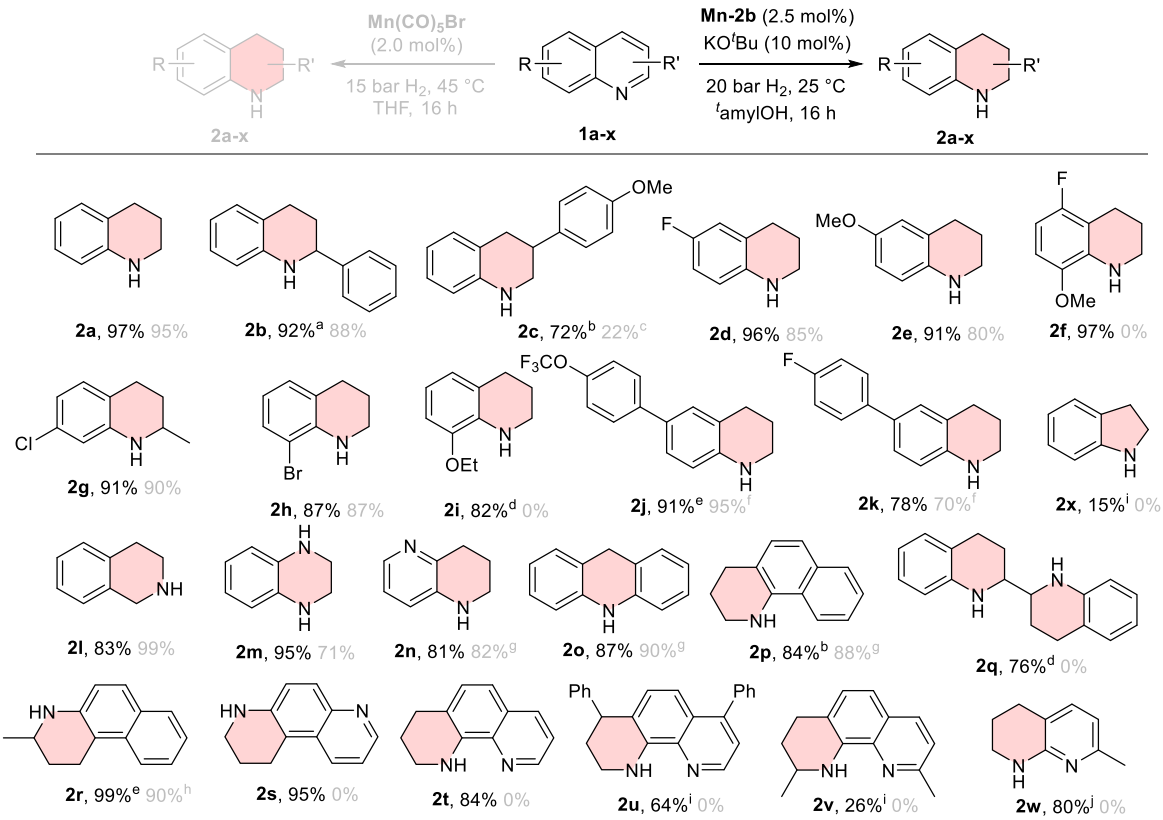

Scheme 9. Hydrogenation scope of quinolines and related N-heterocycles: Direct comparison of **Mn-2b** with $Mn(CO)_5Br$ (grey).[44] [a] 50 bar H_2, 100 °C. [b] 80 °C. [c] 20 bar H_2, 80 °C, 4 mol% $Mn(CO)_5Br$. [d] 40 bar H_2, 80 °C. [e] 60 °C. [f] 20 bar H_2, 60 °C, 4 mol% $Mn(CO)_5Br$. [g] 20 bar H_2, 80 °C. [h] 20 bar H_2, 60 °C. [i] 50 bar H_2, 150 °C. [j] Combined yield.

Next, related heterocycles such as isoquinoline (**1l**), quinoxaline, (**1m**) 1,5-naphthyridine (**1n**), and acridine (**1o**), were all reacted at room temperature giving very good to excellent yields. Benzo[*h*]quinolines (**1p**, **1r**) were also suitable substrates. However, using both $Mn(CO)_5Br$ and **Mn-2b** slightly harsher conditions (60-80 °C) were necessary. A huge improvement in reactivity was observed for substrates containing multiple basic nitrogen atoms, that could potentially inhibit a catalyst by coordinating to the metal center in bidentate fashion. While

$Mn(CO)_5Br$ showed no conversion for any of these substrates (**1q**, **1s**-**2w**), our newly developed pincer catalyst system was able to hydrogenate the majority of them quite effectively. Even 2,2'-biquinoline (**1q**) and strongly-coordinating phenanthroline (**1t**) could be converted. Interestingly, while in the former substrate both heteroarene rings were fully hydrogenated, in the latter phenanthroline (and its derivates) only one N-containing ring was hydrogenated. This gives rise to intriguing unsymmetrical bidentate NN^H-ligand motives. A possible explanation for the different reactivity in the case of phenanthroline is that after the hydrogenation of the first ring, the newly formed amine donor stays directly attached to the remaining heteroaromatic system. The resulting strong +M-effect of the amine then leads to a decreased electrophilicity of the remaining quinolyl moiety, impeding further nucleophilic metal hydride attack. Another prominent substrate is 1,8-naphthyridine (**1w**) since its hydrogenation is an important step in the synthesis of several pharmaceutical candidates.[75] While **Mn-2b** gave full conversion and a good combined isolated yield of 80% at ambient temperature, simple $Mn(CO)_5Br$ was again totally inactive towards this substrate. Lastly, it is worth noting that even the challenging electron-rich heteroaromatic indole (**2x**) showed some conversion to the corresponding dihydro-indole when applying our new catalyst at elevated temperatures. To summarize **Mn-2b** displayed remarkable hydrogenation activity under mild conditions as well as a significantly improved substrate scope. In fact, 9 out of the 24 substrates tested in this study gave no reduction at all when using $Mn(CO)_5Br$. For ordinary substrates $Mn(CO)_5Br$ might remain the catalyst of choice due to its simplicity, commercial availability, and affordability. However, when keeping in mind that pharmaceutical building blocks are often highly complex, multi-functionalized molecules, it is evident that the newly developed pincer system is a valuable improvement to the state of the art, due to its mildness and generality.

2.1.3 Mechanistic Investigations

To get further insights into the catalytic mechanism and some reasoning as to why **Mn-2b** shows such improved hydrogenation activity in comparison to e.g. **Mn-1b**, mechanistic studies using analytical, as well as computational methods, were conducted. Extensive mechanistic studies on **Mn-1b** had been conducted earlier by Liu *et al.* in their seminal 2019 report.[43b] To confirm that **Mn-2b** also functions via Noyori's metal-ligand bifunctional mechanism, we started our investigation by treating **Mn-2b** with base to deprotonate its acidic N–H in the pincer backbone (see Scheme 10).

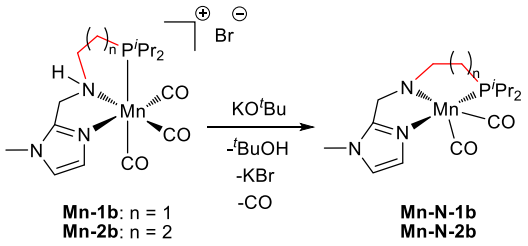

Scheme 10. Activation of precatalysts **Mn-1b**/**Mn-2b** forming amide species **Mn-N-1b**/**Mn-N-2b**.

Doing so, we were able to isolate the corresponding manganese amide species **Mn-N-2b** as a highly sensitive deep red-purple solid. Unfortunately, we were unable to obtain crystals suitable for X-ray diffraction analysis. Therefore, **Mn-N-2b** was analysed extensively by NMR

and IR. The amido species' ^{31}P NMR resonance at 84.9 ppm is significantly shifted to lower field in comparison to the resonance of the parent complex **Mn-2b** at 39.5 ppm. Additionally, its ^{1}H NMR spectrum appears considerably simpler than before, indicating an increase of symmetry in **Mn-N-2b**, likely due to the formation of a trigonal-bipyramidal complex structure with a now meridionally coordinated PNN pincer ligand (as depicted in Scheme 10). This assignment is further corroborated by ^{1}H NOESY experiments, which no longer show promixity of the ^{i}Pr$_2$P and methyl-imidazolyl moeties. Characterization by IR showed two characteristic CO vibrational bands at 1896 and 1818 cm^{-1} for both **Mn-N-2b** as well as **Mn-N-1b**, indicating no significant difference in electronics of the ethylene vs. propylene bridged amide complexes. Reactivity differences are therefore probably induced by different (e.g. steric) features. To test if **Mn-N-2b** is prone to ligand exchange or substrate coordination, NMR experiments were conducted in which substrate was dosed to a solution of amido complex. However no interaction could be observed in ^{1}H or ^{31}P NMR. Identical observations were made for **Mn-N-1b**. This points towards H_2 activation being the directly consecutive step following catalyst activation by base. This "hydrogen-first" mechanism is common for this type of pincer complexes, which typically function via an outer-sphere bifunctional hydrogenation mechanism.[29a] Furthermore, no sign of hemilability of neither the imidazole-N nor the diisopropylphosphine-P donor was detected for the amido species. Next, we set our eyes on studying the proposed manganese hydride species. Initially, we tried generating the manganese hydride by treating **Mn-N-2b** with 1 bar of H_2 in benzene in the absence of substrate (Scheme 11). After this failed to produce any measurable hydridic species, we decided to switch the solvent to more polar THF and increase the hydrogen pressure to 20 bar.

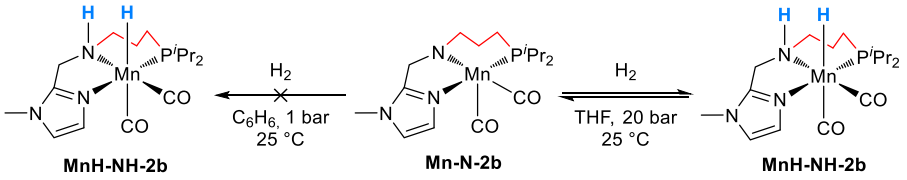

Scheme 11. Test reactions to generate manganese hydride **MnH-NH-2b** from **Mn-N-2b**.

Indeed, after 20 h we were then able to observe a broad doublet at -9.1 ppm in the ^{1}H NMR indicative of a manganese hydride (see Figure 9). The peak splitting can be attributed to a ^{1}H-^{31}P ^{2}J coupling from the hydride ligand to the phosphine ligand. The coupling constant of 53 Hz suggests a *cis* H–Mn–P configuration in line with the expected structure **MnH-NH-2b** shown in Scheme 11. The hydride species was very sensitive and all attempts to isolate it failed. Very likely this species is only stable under an atmosphere of H_2.

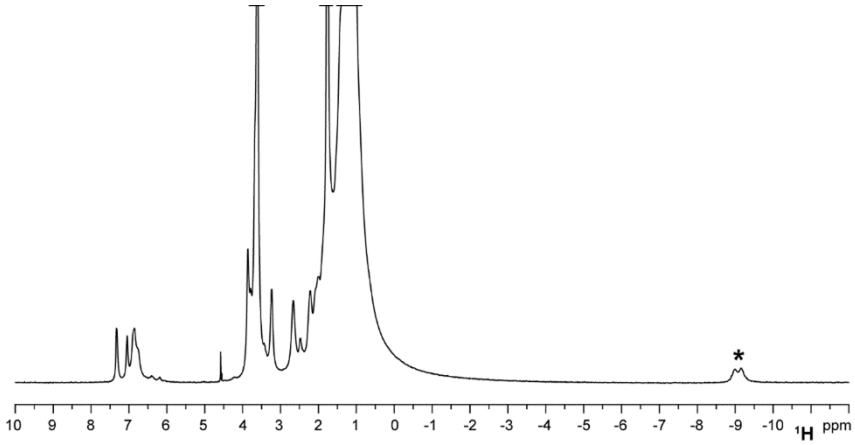

Figure 9. ^{1}H NMR of *in situ* generated **Mn-N-2b** after treatment with 20 bar hydrogen for 20 h. (*) hydride signal of proposed active hydride complex **MnH-NH-2b**.[76]

Due to the sensitivity observed for both **Mn-N-2b** and tentative **MnH-NH-2b** we decided to further analyse the catalyst activation via React-IR *in situ* studies. Therefore, we titrated a suspension of **Mn-2b** in THF with a solution of KO^{t}Bu, while monitoring the reaction by IR, specifically focussing on changes in the characteristic carbonyl region (Figure 10). After addition of 1 equivalent of KO^{t}Bu the three distinctive carbonyl peaks of **Mn-2b** immediately dissappeared and two new peaks (1867, 1781 cm^{-1}) at significantly smaller wavenumbers appeared. This indicates loss of one carbonyl ligand with the concomitant formation of a significantly more electron-rich, previously unknown species. We assigned this species tentatively as alcoholate species **MnO^{t}Bu-NH-2b**, which likely forms initially and is in agreement with previous mechanistic studies on basic Mn-pincer activation.[77] Upon adding further equivalents of base (2, 3, and 4 equiv.) a new set of signals slowly appeared at 1815 and 1894 cm^{-1}. These are in accordance with the already isolated amido species **Mn-N-2b** discussed above.

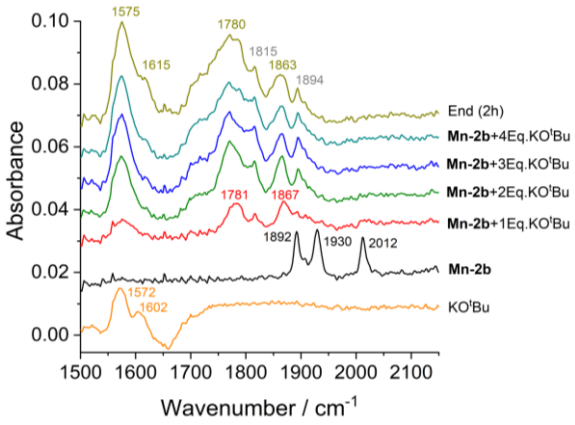

Figure 10. React-IR spectra during basic catalyst activation of **Mn-2b**.[76]

When such a mixture of **MnO^{t}Bu-NH-2b** and **Mn-N-2b** was placed under a hydrogen atmosphere (20 bar), we were unable to detect any new set of carbonyl peaks ascribable to **MnH-NH-2b** by React-IR over the course of 4 h. Potential explanations for this could be a spectral overlap of the hydride species with the alkoxide/amido species, the slow formation of

the hydride species at room temperature, or the large amount of background “noise” in the IR setup. Now, having a rough idea in mind of the sequence of events taking place during the catalyst activation, computational experiments were conducted in collaboration with the group of Prof. Haijun Jiao to check if our observations are in line with theoretical expectations.

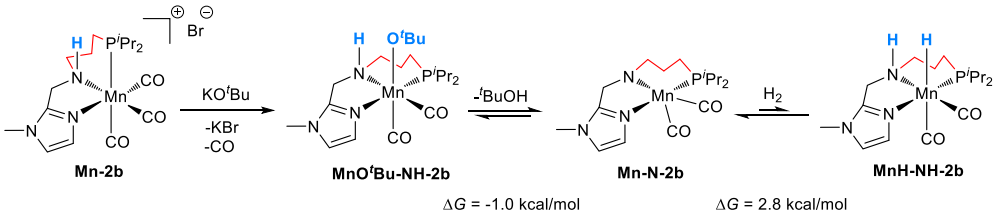

Scheme 12. Proposed catalyst activation pathway and DFT computed Gibbs free energies.

Initial calculations focussed on the energies for the elimination of *tert*-butyl alcohol from **MnO^{t}Bu-NH-2b** to form amide species **Mn-N-2b** and the following reaction of the latter with hydrogen gas to form hydride species **MnH-NH-2b** (Scheme 12). The computed Gibbs free energy for alcohol elimination was very slightly exergonic by -1.0 kcal/mol, while the computed energy for the addition of hydrogen to **Mn-N-2b** was slightly endergonic by 2.8 kcal/mol. The overall small energy differences between the three species support the possibilty of an equilibrium with co-existence of all three species in the catalytic reaction. The endergonicity of the hydrogen activation step explains the difficulties observed experimentally when investigating the hydride species **MnH-NH-2b**. Since hydrogen elimination from **MnH-NH-2b** is exergonic, the equilibrium is likely shifted towards the amido species, which is in accordance with the previous spectroscopic results.

Additionally, we wanted to investigate if computation could give some insight as to why **Mn-2b** has such improved catalytic activity compared to **Mn-1b**. DFT calculations revealed hydrogen activation by the amido species to be the rate determining step of the quinoline hydrogenation reaction. While the energetic barrier for H_2 activation was calculated to be 23.6 kcal/mol for **Mn-N-1b**, it was calculated as 21.1 kcal/mol for **Mn-N-2b**. This 2.5 kcal/mol lower energy barrier may explain the increased catalytic activity of **Mn-N-2b**, especially at lower temperature. Furthermore, it was shown that hydrogen transfer from the corresponding manganese hydrides to quinoline also has a lower energetic barrier for **MnH-NH-2b** (15.9 kcal/mol) compared to **MnH-NH-1b** (18.4 kcal/mol), see Scheme 13. Once more indicating, that **Mn-2b** derived propylene-bridged pincers form active species with a higher kinetic activity.

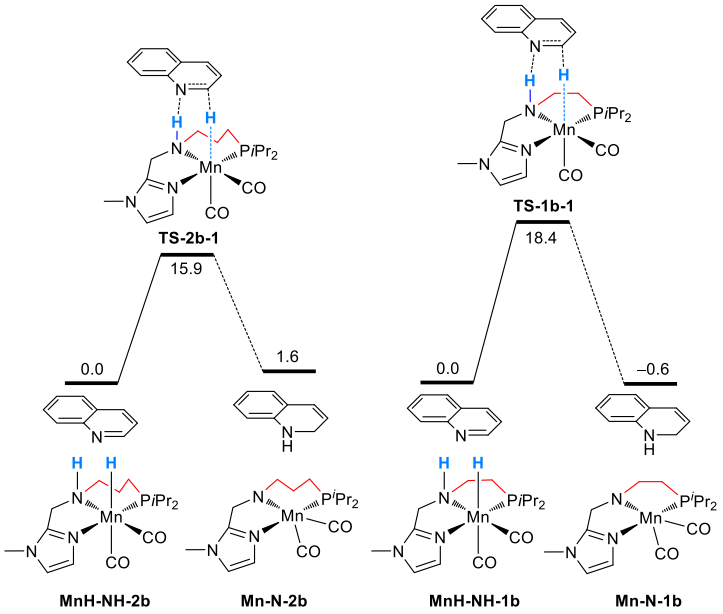

Scheme 13. DFT calculated energy barriers (kcal/mol) for the hydrogen transfer from **MnH-NH-2b**/**MnH-NH-1b** to the quinoline substrate.

2.2 Mild Iron-Catalyzed Reductive Cascade Synthesis of Pyrroles from Nitroarenes

2.2.1 Catalyst Screening and Optimization

As discussed in the introduction, pyrroles are indispensable building blocks in our modern fine chemical and pharmaceutical industries. Inspired by the earlier work on heterogeneous cobalt- and iron-catalyzed cascade pyrrole syntheses from nitroarenes, we identified several shortcomings of the previous methods such as the need for harsh reaction conditions (100-120 °C) and in several cases the need for basic additives (Et_3N, DBU).[61] These issues disagree with the green chemistry principles discussed in the introduction, which recommend running reactions at ambient temperature without any additives.[8] To address these drawbacks, we therefore decided for the first time to test homogeneous iron catalysts for this type of reaction due to their favorable abundance, low toxicity as well as their likelihood of exhibiting improved reactivity. Such iron catalysts would need to be tolerant of acid and water, as well as chemoselective for nitro reduction over carbonyl reduction. Finding a homogeneous 3d metal catalyst that fulfills all these requirements is far from trivial, since 3d metal complexes are generally less stable than their corresponding 4d or 5d counterparts.[78] In line with our expertise in the field of iron catalysis we decided to try the reliable iron Tetraphos system, which had previously shown very favorable reactivity for nitroarene transfer hydrogenation with formic acid under mild conditions.[54c] Interestingly, formic acid could play a dual role as both the reductant as well as the Brønsted acid catalyst for the following Paal-Knorr reaction in our desired cascade. We therefore started a screening using simple nitrobenzene (**3a**) and hexane-2,5-dione (**4a**) as benchmark substrates (Table 5). We were pleasantly surprised to find that applying the identical conditions used for nitroarene transfer hydrogenation (EtOH solvent, 40 °C, 2h) lead to full conversion of the nitrobenzene starting material and 99% GC yield of the corresponding phenyl dimethyl pyrrole (**5a**) (Entry 1). Highlighting the remarkable chemoselectivity, no reduction of hexane-2,5-dione was observed. Furthermore, reducing the temperature to room temperature was also possible when running the reaction for slightly longer time (5 h, Entry 5). At this point control reactions were conducted, proving that without iron source, ligand or formic acid, no reaction took place (Entries 2-4). Since solvents have a big impact on the reactivity as well as the sustainability of a process, being the main cause of waste and energy-usage, a solvent screening was conducted next (Entries 9-13).[79] Under these conditions, none of the tested solvents performed better than EtOH, which is already quite a sustainable solvent due to its biorenewability and biodegradability.[80] Pursuing our investigations with EtOH, we then investigated alternative iron sources (Entries 6-8). Replacing iron tetrafluoroborate with iron triflate also lead to near quantitative yield, while using the commercially available molecularly defined complex **Fe-1** gave drastically reduced yields of 24%. Likely its unusual tetraphenylborate anion is responsible for this drop in yield, because simply switching to the tetrafluoroborate anion in the related complex **Fe-2** again lead to very good yields. Nevertheless, since the *in situ* prepared catalyst showed superior performance, it was applied for further studies. Notably, also hydrogen gas could be used as a reductant in this iron-catalyzed cascade reaction (Entries 14-16). Particularly good performance was observed when using a slightly modified Ph-Tetraphos ligand. To the best of our knowledge,

this represents the first time that such an iron cascade protocol could directly apply molecular hydrogen. However, the direct hydrogenation conditions needed to be more drastic (20 bar, 100-120 °C, TFA additive) and therefore the focus was put on the significantly milder transfer hydrogenation protocol.

Table 5. Optimization of the iron-catalyzed reductive cascade pyrrole synthesis.

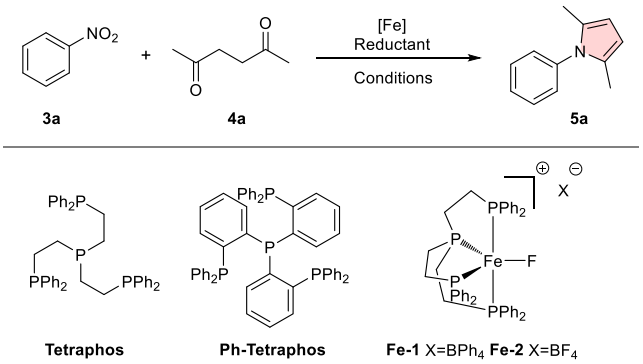

Entry	Metal salt	Ligand	Solvent	Reductant	Yield 5a[a]
1[b]	$Fe(BF_4)_2{\cdot}6H_2O$	Tetraphos	EtOH	HCO_2H	99%
2	$Fe(BF_4)_2{\cdot}6H_2O$	-	EtOH	HCO_2H	0%
3	-	Tetraphos	EtOH	HCO_2H	0%
4	$Fe(BF_4)_2{\cdot}6H_2O$	Tetraphos	EtOH	-	0%
5	$Fe(BF_4)_2{\cdot}6H_2O$	Tetraphos	EtOH	HCO_2H	97%
6	$Fe(OTf)_2$	Tetraphos	EtOH	HCO_2H	99%
7	**Fe-1**, [Fe(Tetraphos)F][BPh_4]		EtOH	HCO_2H	24%
8	**Fe-2**, [Fe(Tetraphos)F][BF_4]		EtOH	HCO_2H	87%
9	$Fe(BF_4)_2{\cdot}6H_2O$	Tetraphos	iPrOH	HCO_2H	89%
10	$Fe(BF_4)_2{\cdot}6H_2O$	Tetraphos	THF	HCO_2H	40%
11	$Fe(BF_4)_2{\cdot}6H_2O$	Tetraphos	Dioxane	HCO_2H	25%
12	$Fe(BF_4)_2{\cdot}6H_2O$	Tetraphos	DMC	HCO_2H	47%
13	$Fe(BF_4)_2{\cdot}6H_2O$	Tetraphos	H_2O	HCO_2H	0%
14[c]	$Fe(BF_4)_2{\cdot}6H_2O$	Tetraphos	THF	H_2	16%
15[c]	$Fe(BF_4)_2{\cdot}6H_2O$	Ph-Tetraphos	THF	H_2	96%
16[d]	$Fe(BF_4)_2{\cdot}6H_2O$	Ph-Tetraphos	THF	H_2	99%

Reaction conditions: **3a** (0.5 mmol), **4a** (1.2 equiv.), $Fe(BF_4)_2{\cdot}6H_2O$ (5 mol%), Tetraphos (5 mol%), 4.5 equiv. HCO_2H, EtOH (2 mL), 25 °C, 5 h. [a] Determined by GC using hexadecane as internal standard. [b] 40 °C, 2 h. [c] $Fe(BF_4)_2{\cdot}6H_2O$ (2 mol%), Ph-Tetraphos (2 mol%), 20 µL TFA, 20 bar H_2, THF (1.5 mL), 120 °C, 2 h. [d] $Fe(BF_4)_2{\cdot}6H_2O$ (2 mol%), Ph-Tetraphos (2 mol%), 20 µL TFA, 20 bar H_2, THF (1.5 mL), 100 °C, 6 h.

To summarize, as initially proposed, by changing from heterogeneous cobalt and iron catalysts to a homogeneous iron catalyst, it was possible to perform the same type of transfer hydrogenation reaction under significantly milder conditions. Due to the high catalytic activity of the iron Tetraphos catalyst, a remarkable reduction of reaction temperature from 100-120 °C to ambient temperature, as well as a reduction of reaction time by >50% was possible, while at the same time avoiding any use of additives.[61]

2.2.2 Scope of the Iron-Catalyzed Reductive Paal-Knorr Cascade

To investigate if the previous improvements would also translate into a more general applicability of this catalyst system, an extensive substrate scope was prepared (Schemes 14 and 15). Because pyrroles are important building blocks in the pharmaceutical and agrochemical industries, special attention was put on including diverse functional groups commonly present in bioactive agents. Beginning with the simple benchmark substrates, phenyl dimethyl pyrrole **5a** was isolated in excellent yield (91%). To gauge the influence of steric bulk on the catalytic performance, bulky 2-isopropyl nitrobenzene **3b** was tested next, giving a good isolated yield of 72%. Aryl halides are ubiquitous both as intermediates as well as final products in the fine chemical industries. An undesired side reaction commonly encountered with precious metal catalysis is reductive dehalogenation.[81] Pleasingly, applying our mild iron based protocol, aryl fluorides **3c**, chlorides **3d**, bromides **3e** and even iodides **3f** were all converted well without any sign of dehalogenation. Additionally, trifluoromethyl-containing nitroarene **3g** gave a good isolated yield, proving that electron-poor substrates are well-tolerated. Neither alkene hydrogenation, nor alkene polymerization was observed when transforming 4-nitrostyrene to its corresponding pyrrole **5h**, highlighting again the remarkable chemoselectivity of this system. Substrates containing electron-donating groups including ether **3j**, thioether **3i** and phenol **3k** also showed good reactivity. The latter two substrates are particularly challenging since sulfur-containing **3i** is known to inhibit precious metal catalysts,[82] while **3k** is rather acidic ($pK_a(H_2O)$ =7.15), which could cause problems when applying catalysts that are only active under neutral or basic conditions.[83] Still, our acid-tolerant iron catalyst gave good to excellent yields in both cases. Due to their use in cross-coupling reactions and pharmaceuticals, organoboron compounds are widely employed in industry and academia. Such compounds can be sensitive to protodeboronation under harsh aqueous conditions.[84] Interestingly, when applying our mild protocol, boronic acid **3m** and corresponding boronate **3l** were smoothly converted to the corresponding pyrroles, without any signs of protodeboronation. Excellent chemoselectivities were also observed with carbonyl group containing ketone **3n**, ester **3o** and amide **3p**. Notably, primary amides such as **3p** are rarely part of catalytic substrate scopes due to their coordinating ability as well as their two protic hydrogens. Importantly, no pyrrole formation was observed on the amide nitrogen of **3p**. At this point we investigated the effect of varying the 1,4-dicarbonyl precursor, since most of the previous reports on this type of cascade reaction had shown little diversity in this respect.[61] Thus, we were able to synthesize 2,3,4,5-unsubsituted **5q**, 2-alkyl 1,5-diaryl pyrrole **5r**, challenging 1,2,5-triaryl **5s** and even the fully substituted **5t** in very good yields using our novel methodology. Particularly the yield of **5s**, which was transformed using our more forcing hydrogenation conditions, is remarkable since previous methods only provided minimal amounts of product for this challenging example.[61]

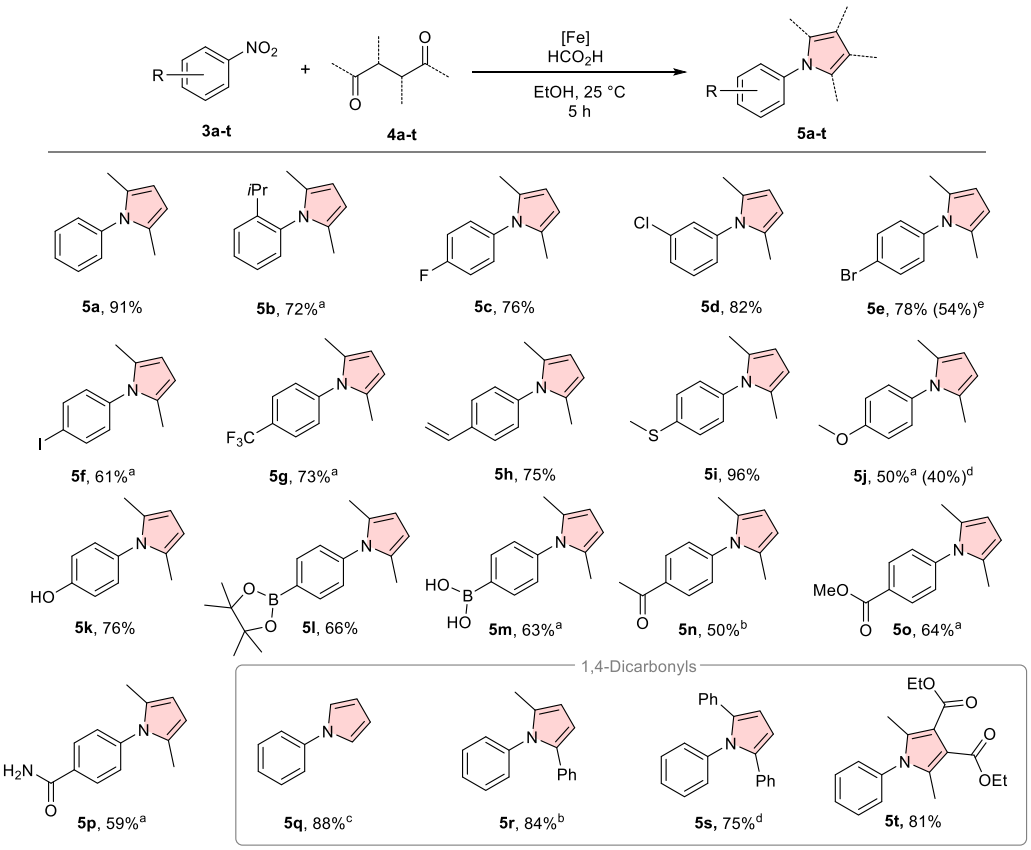

Scheme 14. Scope of nitroarenes for the iron-catalyzed cascade pyrrole synthesis. Reaction conditions: **3** (0.5 mmol), **4a** (1.2 equiv.), $Fe(BF_4)_2 \cdot 6H_2O$ (5 mol%), Tetraphos (5 mol%), 4.5 equiv. HCO_2H, EtOH (2 mL), 25 °C, 5 h. [a] 24 h. [b] 40 °C, 24 h. [c] 24 h, from 2,5-dimethoxytetrahydrofuran, after 5 h addition of 1.5 mL aq. 50% HCO_2H. [d] $Fe(BF_4)_2 \cdot 6H_2O$ (2 mol%), Ph-Tetraphos (2 mol%), 20 µL TFA, 20 bar H_2, THF (1.5 mL), 120 °C, 20 h. [e] $Fe(BF_4)_2 \cdot 6H_2O$ (3 mol%), Ph-Tetraphos (3 mol%), 20 µL TFA, 20 bar H_2, THF (1.5 mL), 120 °C, 20 h.

Because bioactive agents often contain multiple heterocyclic groups beside pyrroles, next we looked into how well the catalyst could tolerate heterocyclic substrates. Basic heterocycles that could potentially coordinate and thus inhibit a catalyst posed no obstacle for our iron system, as demonstrated by pyridine **6a**, quinoline **6b** and benzimidazole **6d**. 5-Nitrobenzofuran **6c** gave a good isolated yield of 74%, too. Surprisingly, unprotected indole **6e** showed low conversion and yield. Since related indazole **6g** however gave very good conversion and yield, we hypothesized that the electron-richness of the indole core is leading to a reduced electrophilicity of the corresponding nitro group and thus likely to blame for the decreased reduction reactivity. In line with our hypothesis, when the indole nitrogen was Boc-protected in example **6f** to reduce some of the electron-richness of the indole, the yield increased significantly. Similarly reduced reactivites were observed for electron-rich benzodioxole **6h** and morpholine-substituted **6j**. In the latter case however, merely increasing the reaction temperature to 40 °C already significantly alleviated these issues. Highlighting again the remarkable chemoselectivity, phthalimide derivate **6i**, while giving only moderate yields, also exhibited no overreduction.

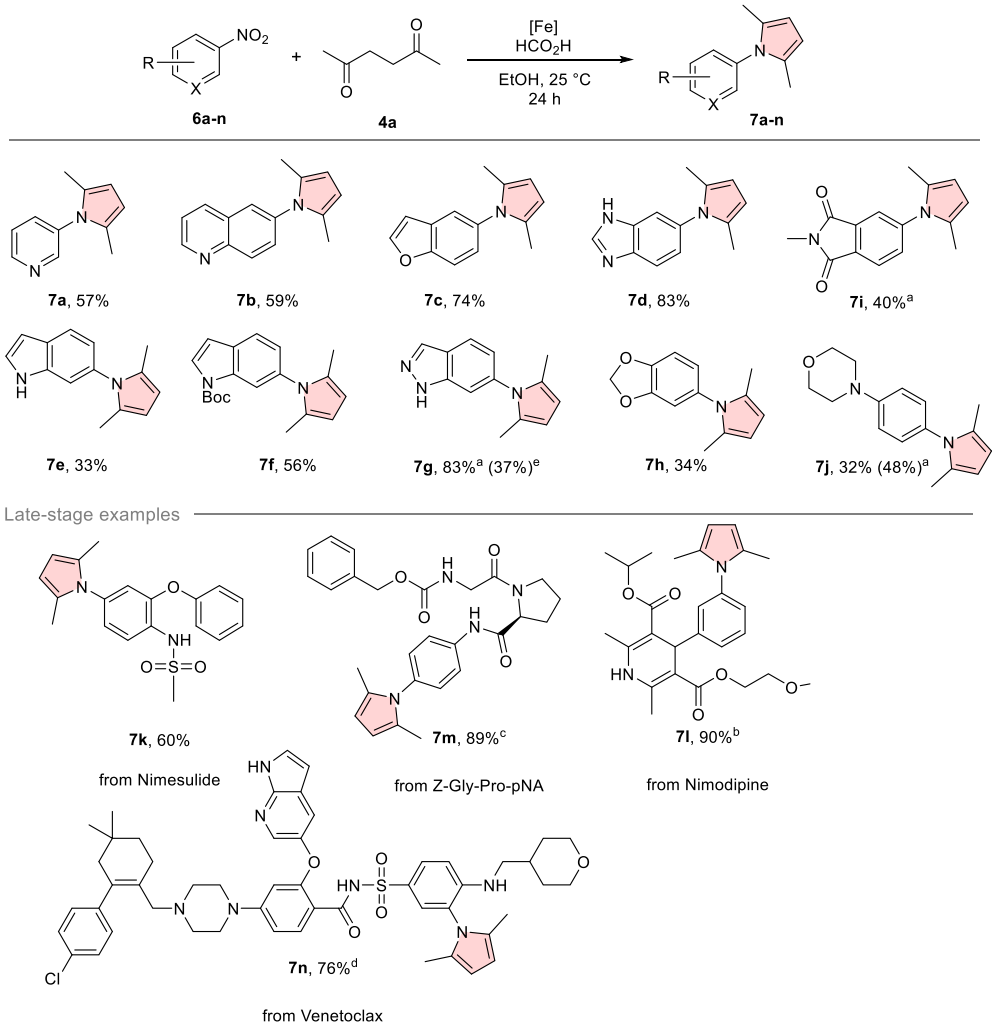

Scheme 15. Scope of nitroheteroarenes and late-stage examples for the iron-catalyzed cascade pyrrole synthesis. Reaction conditions: **3** (0.5 mmol), **4a** (1.2 equiv.), $Fe(BF_4)_2 \cdot 6H_2O$ (5 mol%), Tetraphos (5 mol%), 4.5 equiv. HCO_2H, EtOH (2 mL), 25 °C, 24 h. [a] 40 °C [b] 0.25 mmol scale, 5h. [c] 0.25 mmol scale. [d] 0.25 mmol scale, solvent (EtOH/toluene, 1:1, 2 mL). [e] $Fe(BF_4)_2 \cdot 6H_2O$ (2 mol%), Ph-Tetraphos (2 mol%), 20 µL TFA, 20 bar H_2, THF (1.5 mL), 120 °C, 20 h.

At this point, we switched from evaluating functional group tolerance individually to directly applying multifunctionalized drug(-like) molecules to our methodology. The first active pharmaceutical ingredient tested was Nimesulide **6k**, a COX-2 inhibitor, which gave a decent isolated yield of 60%. Next, Nimodipine (**6l**), a common calcium channel blocker, was transformed to **7l** in excellent yield. Likewise, dipeptidic endopeptidase probe Z-Gly-Pro-pNA gave a very high yield of its corresponding pyrrole **7m**. Remarkably, the cascade methodology could even be applied to the highly-complex Bcl-2 inhibitor Venetoclax, affording the pyrrol-modified product **7n** in 76% yield. Both Venetoclax ($pK_a(H_2O)$ =3.4) and Nimesulide (pK_a(MeOH) =6.5) contain quite acidic sulfonamide groups, but again our catalyst system tolerated these groups very well.[85] These four successful late-stage modifications of complex molecules clearly underline the outstanding chemoselectivity and robustness of our novel protocol.

2.2.3 One-Pot Synthesis of the Bioactive Agent BM-635

In the end, it was important to show that the newly-developed methodology can not only be applied to the modification of existing bioactive agents but also to the rapid *de novo* synthesis thereof. We thus selected **BM-635**, an antitubercular agent with a central pyrrole unit as a synthetic target.[86] Traditionally this compound would be synthesized in a three step sequence starting from fluoronitrobenzene **3c**, which is first hydrogenated to the corresponding aniline **8** (see Scheme 16).[86b, 86c, 87] Then follows the Paal-Knorr cyclization giving trisubstituted pyrrole **9** and finally a Mannich reaction affords the desired tetrasubstituted pyrrole scaffold of **BM-635**.[86]

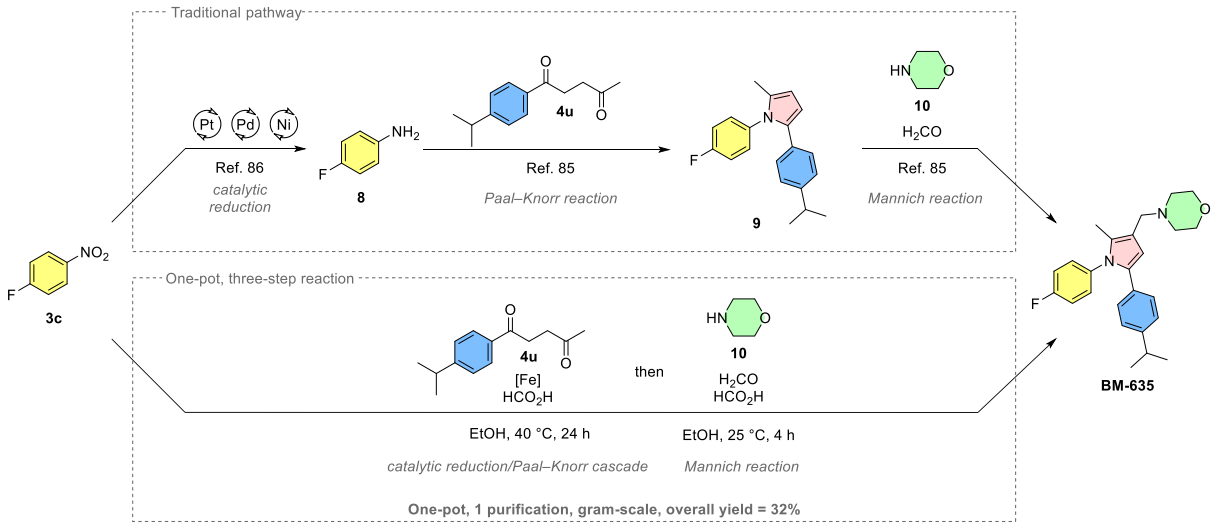

Scheme 16. Synthetic application of the Fe-catalyzed reduction cascade to the synthesis of the bioactive agent **BM-635**: traditional synthesis (top), one-pot gram-scale synthesis (bottom).

Because the ultimate Mannich reaction is performed under acidic conditions, like our cascade protocol, we assumed that it might be possible to perform the whole three step sequence in a one-pot cascade fashion, thereby even further reducing the stepcount and purification steps. Consequently, we set up a cascade reaction starting from fluoronitrobenzene **3c** and diketone **4u**, introducing morpholine and formaldehyde as soon as **3c** was fully consumed. Thus, we were able to synthesize **BM-635** in one-pot fashion giving 32% overall yield of the bioactive agent. Statistically this repesents a remarkable average yield of 68% per synthetic step. The scaled-up procedure was also successful on gram-scale, yielding 1.27 g of the target compound **BM-635** in a single batch. This synthetic application of our multicomponent protocol highlights the power of cascade reactions in rapidly constructing molecular complexity from simple starting materials.

2.3 Cobalt-Catalyzed Reductive Etherification and Oxetane Transformation

2.3.1 Screening of Phosphine Oxides and Reaction Optimization

As discussed in the introduction, catalytic reductive etherification of aldehydes with alcohols has been established as a more selective method for the synthesis of unsymmetrical ethers over the years. Interestingly, already in 1976 Fleming and Bolker found that simple cobalt carbonyl can reduce both *in situ* formed, as well as isolated acetals, efficiently to the corresponding ethers under syngas conditions.[88] However, this protocol was only applied to a handful of substrates and needed very harsh conditions, particularly a pressure of 165 bar CO/H_2 (syngas), which is hard to achieve for most laboratories.[88] Thus, the synthetic method never gained significant popularity and was somewhat forgotten. Recent research in our group on cobalt carbonyl-catalyzed alkene hydroformylation revealed a remarkable promoting effect of phosphine oxides on the catalytic activity, thus allowing hydroformylation at significantly lower temperature and pressure.[89] Consequently, we contemplated investigating if such an effect could also be observed for a different reaction catalyzed by the same cobalt catalyst. With the recently increased focus on sustainable processes in mind, we therefore evaluated if the procedure of Fleming and Bolker could be conducted under significantly milder conditions when applying phosphine oxide promoters. Thus, we tested a variety of phosphine oxide promoters in combination with cobalt carbonyl under significantly milder reaction conditions of 100 °C and only 40 bar syngas (CO/H_2, 1:1) (Table 6). Benzaldehyde was chosen as the benchmark substrate and methanol as the alcohol coupling partner. To have a point of reference, the reaction was initially conducted in the absence of promoter giving a poor yield of 27% of the methyl benzyl ether product **13aa** (Entry 1). Adding only 4 mol% of the common triphenylphosphine oxide **P1** nearly doubled the product yield (51%, Entry 2). Next, different trialkylphosphine-derived promoters were tested showing even higher yields (Entries 3-7). This is remarkable, since in previous carbonylation reactions triarylphosphine oxide additives gave the best yields. In this case however, tributylphosphine oxide **P3** showed the highest yield of 62% (Entry 4). Unsymmetrically substituted (Entries 8-13), as well as potentially bidentate phosphine oxides (Entry 14), were also tested. Although they did not outperform tributylphosphine oxide **P3**, it can generally be said that all phosphine oxides tested in this study showed some promotional effect and thus improvement in yield. Interestingly, when unoxidized tributylphosphine was tested, a near complete shutdown in reactivity was observed (Entry 15). It is therefore unlikely that the parent phosphines are responsible for the observed promoting effect, nor that phosphine oxides are reduced back to their corresponding phosphines under catalytic conditions. Having found a suitable and cheap promoter in **P3**, further screening of reaction parameters was conducted, which lead to the optimized loading of catalyst (2 mol%), promoter (6 mol%), and alcohol (2 equiv.), (partial) pressure (40 bar, 1:1 CO/H_2), temperature (120 °C) and solvent (toluene or neat alcohol).

Table 6. Evaluation of phosphine oxides in the cobalt-catalyzed reductive etherification.

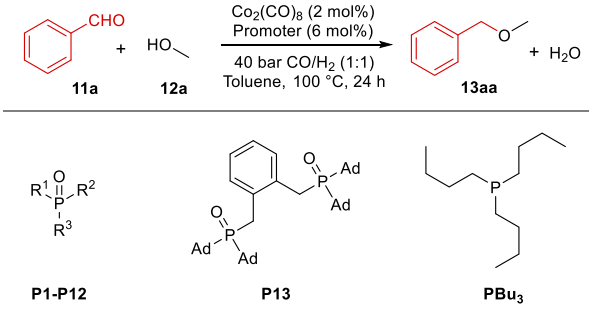

Entry	Promoter/Ligand	Yield 13aa[a]
1	-	27%
2	**P1**, R^1=R^2=R^3=Ph	51%
3	**P2**, R^1=R^2=R^3=Me	57%
4	**P3**, R^1=R^2=R^3=Bu	62%
5	**P4** R^1=R^2=R^3=Oct	59%
6	**P5**, R^1=R^2=R^3=Cy	56%
7	**P6**, R^1=R^2=R^3=Ad	56%
8	**P7**, R^1=Bu, R^2=R^3=Ad	54%
9	**P8**, R^1=Hex, R^2=R^3=Ad	54%
10	**P9**, R^1=Benzoyl, R^2=R^3=Ad	38%
11	**P10**, R^1=2-Naphthoyl, R^2=R^3=Ad	36%
12	**P11**, R^1=2-Furoyl, R^2=R^3=Ad	47%
13	**P12**, R^1=2-Furoyl, R^2=R^3=Cy	47%
14	**P13**	54%
15	**PBu_3**	2%

Reaction conditions: **11a** (0.5 mmol), **12a** (1.2 equiv.), $Co_2(CO)_8$ (2 mol%), promoter (4 mol%), 40 bar H_2/CO (1:1), toluene (1 mL), 100 °C, 24 h. [a] Determined by GC using isooctane or hexadecane as internal standard.

2.3.2 Scope of the Cobalt-Catalyzed Phosphine Oxide Promoted Reductive Etherification

To test the generality and versatility of the improved synthetic protocol, a substrate scope was prepared (Scheme 17). Initially, aromatic aldehydes were tested. Starting from the benchmark substrate benzaldehyde, a very promising isolated yield of 82% of the corresponding ether **13aa** was obtained. Furthermore, this process was successfully scaled up to multigram scale giving 7.5 g of benzyl methyl ether in a slightly reduced but still good yield of 71%. Additional substituents were then evaluated including electron-donating groups such as *ortho*/*para*-methoxy (**13fa** and **13ea**) or 3,4-methylenedioxy (**13ga**), which were tolerated well. Likewise, electron-withdrawing groups were permitted as exemplified by halogen-containing substrates **11h**, **11i**, **11j** and **11k** or ester **11l**, which gave near quantitative yield of the corresponding ether **13la**. Remarkable functional group tolerance was shown when converting sensitive substrates such as pinacol boronate **11m** or oxygen- and sulfur-containing heteroaromatics **11o** and **11p**. Even though the latter **11p** contains a potentially coordinating sulfur atom, no catalyst-poisoning was observed. Furthermore, dialdehyde **11n** was a suitable substrate,

yielding diether **13na** in a double reductive etherification protocol in 81%. Unfortunately, alkyl aldehyde **11q** showed no product formation. The sole isolated product in this case was the corresponding dimethyl acetal. This hints at mesomeric stabilization being essential for the reaction to proceed efficiently. While this limits the synthetic applicability of our protocol somewhat, it should be noted that using this protocol three widely applied ether protecting groups could be introduced very efficiently, namely benzyl (Bn), *para*-methoxybenzyl (PMB) and 2-naphthylmethyl (NAP). Thus, this methodology could still be of significant use to the synthetic chemistry community.

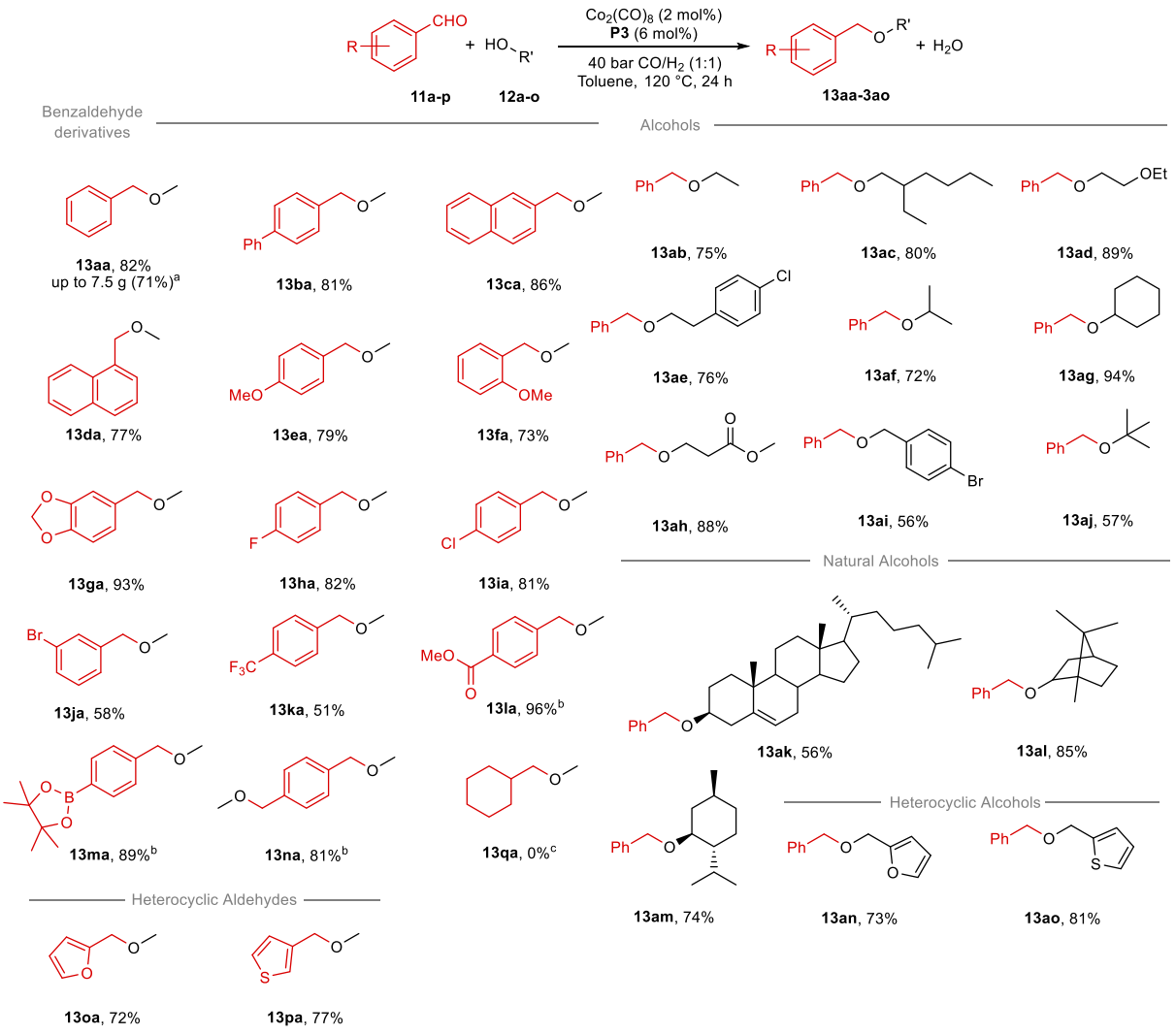

Scheme 17. Scope of the cobalt-catalyzed reductive etherification. [a] Multigram scale. [b] Neat MeOH. [c] (Dimethoxymethyl)cyclohexane is the sole isolated product.

Subsequently, we evaluated the reaction performance of various alcohol coupling partners. Starting from simple primary alcohols such as ethanol **13ab**, Guerbet alcohol **13ac**, or 2-ethoxyethanol **13ad**, good to very good yields of the corresponding ethers were obtained. The same was observed for alcohols containing ester (**13ah**) or (hetero)arene moieties (**13ae**, **13ai**, **13an**, **13ao**). Switching to more bulky secondary alcohols did not significantly hinder reactivity, as exemplified by products derived from simple isopropanol **13af** or cyclohexanol **13ag**, as well as the complex natural alcohols menthol **13am**, cholesterol **13ak** and borneol

13al. Interestingly, the trisubstituted alkene functionality of cholesterol is left intact using this methodology. Lastly, even poorly nucleophilic tertiary alcohol *tert*-butanol could be etherified in fair yield (**13aj**), which is considered challenging using traditional methods.

2.3.3 Control Reactions and Mechanistic Insights

At this point, several control reactions were devised to gain a deeper understanding of the catalytic mechanism (Scheme 18). First, the role of syngas was evaluated by performing reactions only in the presence of either hydrogen or carbon monoxide. In neither case was product formation observed. Especially under solely hydrogen atmosphere, formation of black cobalt (nano)particles was detected, while under merely CO atmosphere the reaction mixture remained homogeneous, but no reduction was observed. Thus, hydrogen is likely needed as the reductant, while CO gas is probably necessary to stabilize the active cobalt carbonyl hydride species. This is in line with previous mechanistic studies by Fleming and Bolker which revealed that stoichiometric $HCo(CO)_4$, the proposed active species, can reduce aromatic acetals to their corresponding ethers.[88]

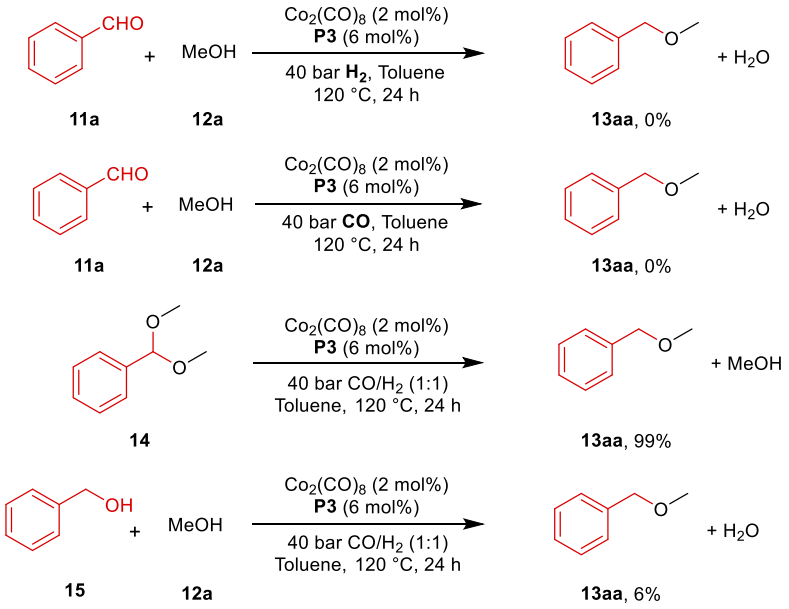

Scheme 18. Control reactions into the role of syngas (CO/H_2) and possible acetal intermediacy.

A first hint that acetals might also be intermediates in our phosphine oxide promoted protocol was the isolation of an acetal in the case of the non-reduced aliphatic substrate **11q**. Additionally, acetal traces were found in the scale-up experiment of **11a**. A kinetic study however revealed no significant build-up of acetal species, probably because they are quickly converted further. To investigate this point more, we directly treated aromatic acetal **14** with our comparably mild conditions and were delighted to find near quantitative yield of the corresponding ether (Scheme 18). Additionally, when benzyl alcohol (**15**) and methanol were treated under the same conditions, only minimal ether formation was observed. Consequently, the reaction likely proceeds through (hemi)acetal hydrogenation and not an aldehyde hydrogenation/etherification sequence. This is also in line with the generally low hydrogenation activity of $HCo(CO)_4$ towards aldehydes when applied in hydroformylation. A more probable

explanation is that highly acidic $HCo(CO)_4$ catalyzes the formation of (hemi)acetals from aldehydes and alcohols, then protonates the intermediate (hemi)acetal, leading to the formation of highly reactive oxocarbenium ions that are finally reduced by the cobalt carbonyl hydride to give the ether products (see Scheme 19).

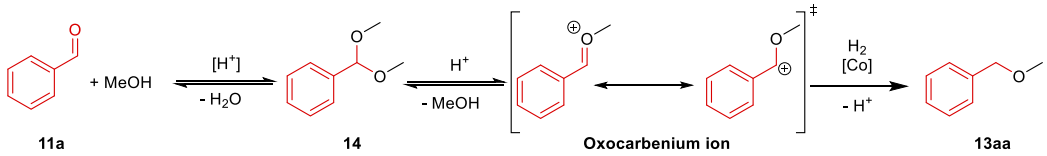

Scheme 19. Proposed reaction sequence of the reductive etherification.

With regards to the role of the promoter, previous kinetic studies on phosphine oxide promoted hydroformylation showed that in the presence of a promoter the induction period was reduced from several hours to just minutes. Furthermore, Darensbourg *et. al.* already showed in the 1980s that tributyl phosphine oxide specifically is able to labilize CO ligands and instantly disproportionate dicobalt octacarbonyl to form deep-blue $[(Bu_3PO)_4Co][Co(CO)_4]_2$.[90] The same deep-blue species was observed in our experiments. The anion of this salt $[Co(CO)_4]^-$ represents the deprotonated equivalent of the assumed active species $HCo(CO)_4$, which is known to only form slowly from dicobalt octacarbonyl under non-forcing conditions.[63] To check if this valence disproportionation of dicobalt octacarbonyl is responsible for the improved catalytic activity we selected a Co^{2+} ($Co(OTf)_2$) and Co^{1-} ($K[Co(CO)_4]$) source and tested their reactivity. Interestingly, while both salts individually showed only minimal product formation, the combination of Co^{2+}/Co^{1-} salts in a 1:2 ratio, the same stoichiometry as in the previously observed $[(Bu_3PO)_4Co][Co(CO)_4]_2$ species, showed excellent activity even in the absence of phosphine oxide. This proves that the effect of phosphine oxide is truly just promoting in nature by improving the activation of the precatalyst via disproportionation.[63]

2.3.4 Application of the Cobalt Phosphine Oxide System to Oxetanes: Carbonylative Ring Expansion vs. Hydrogenative Ring Opening

As a follow-up study, we investigated if yet another cobalt-catalyzed reaction could be promoted by phosphine oxides. Since the catalytic system had performed so favourably in alkene hydroformylation and reductive etherification, we wondered if carbonylation of oxetanes to form γ-lactones would also be feasible under our mild conditions. This reaction had first been reported in 1989 by Alper and coworkers, using a $Co_2(CO)_8/Ru_3(CO)_{12}$ catalyst mixture under relatively harsh conditions (10 mol% cat. loading each, 60 bar CO, 165-190 °C, 48 h).[91] Recently however, increased interest into milder and more economical catalytic systems for this transformation has arisen.[92] Therefore, we evaluated our previously developed system in the carbonylation of benchmark substrate 3,3-dimethyloxetane **16a**, which readily gave 68% GC yield of the desired product at significantly milder conditions (see Scheme 20).

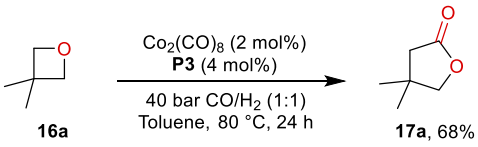

Scheme 20. Benchmark substrate in the phosphine oxide promoted carbonylation of oxetanes. Reaction conditions: **16a** (1.0 mmol), $Co_2(CO)_8$ (2 mol%), **P3** (4 mol%), 40 bar H_2/CO (1:1), toluene (2 mL), 80 °C, 24 h. Yield determined by GC using isooctane as internal standard.

Even more pronounced than for reductive etherification, in the absence of promoter little to no carbonylation of oxetane could be observed. Additionally, even though formally only a molecule of CO is inserted into oxetane to give the γ-lactone product, as before, if only CO gas was employed instead of syngas, no conversion of starting material was detected. This again points towards cobalt carbonyl hydrides as the active species, whose acidity is probably necessary for oxetane activation. This is in line with the current literature on Lewis acid assisted oxetane carbonylation.[92a] With minor adjustments of the reaction conditions, including a solvent switch from toluene to greener dimethylcarbonate (DMC) and a promoter switch from Bu_3PO (**P3**) to Cy_3PO (**P5**), we were able to improve the product yield even further (for details see original manuscript below). We then applied the optimized conditions to a handful of substrates and found an interesting substrate dependent reactivity trend. While 2,4-unsubstituted oxetanes gave the desired γ-lactone products in moderate to good isolated yields, substrates with arene substituents in the 2-position gave hydrogenatively ring-opened alcohols as products (see Scheme 21).

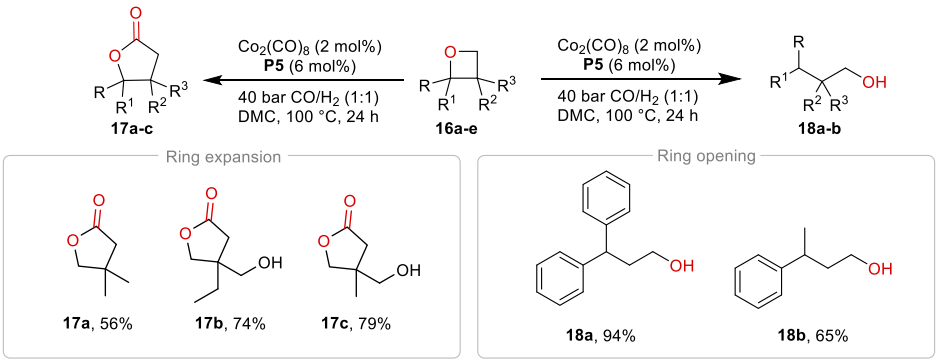

Scheme 21. Cobalt-catalyzed ring expansion vs. hydrogenative ring opening of oxetanes. Reaction conditions: **16** (1.0 mmol), $Co_2(CO)_8$ (2 mol%), **P5** (6 mol%), 40 bar H_2/CO (1:1), DMC (2 mL), 100 °C, 24 h.

The divergent chemoselectivity can be explained by the different stabilities of the formed cations when the oxetane is protonated by the acidic $HCo(CO)_4$ (Scheme 22). While in the unsubstituted case the formed unstabilized oxonium ion **A** is likely ring-opened via nucleophilic attack of the tetracarbonylcobaltate anion, forming a neutral cobalt hydroxyalkyl species **B**. This species **B** then inserts CO to form cobalt hydroxyacyl species **C**, that finally recyclizes giving the carbonylated C-1 extended product (**17**) and the regenerated $HCo(CO)_4$ catalyst. In the case of the 2-aryl substituted oxetane however the oxonium ion **A** likely rearranges to the resonance-stabilized ring-opened carbocation **D**, which is then trapped by a second molecule of $HCo(CO)_4$ (or $HCo(CO)_3$) giving the hydrogenated alcohol product **18**. This type of

hydrogenative quenching of a mesomerically stabilized carbocation is reminiscent of the proposed reductive etherification pathway discussed above.

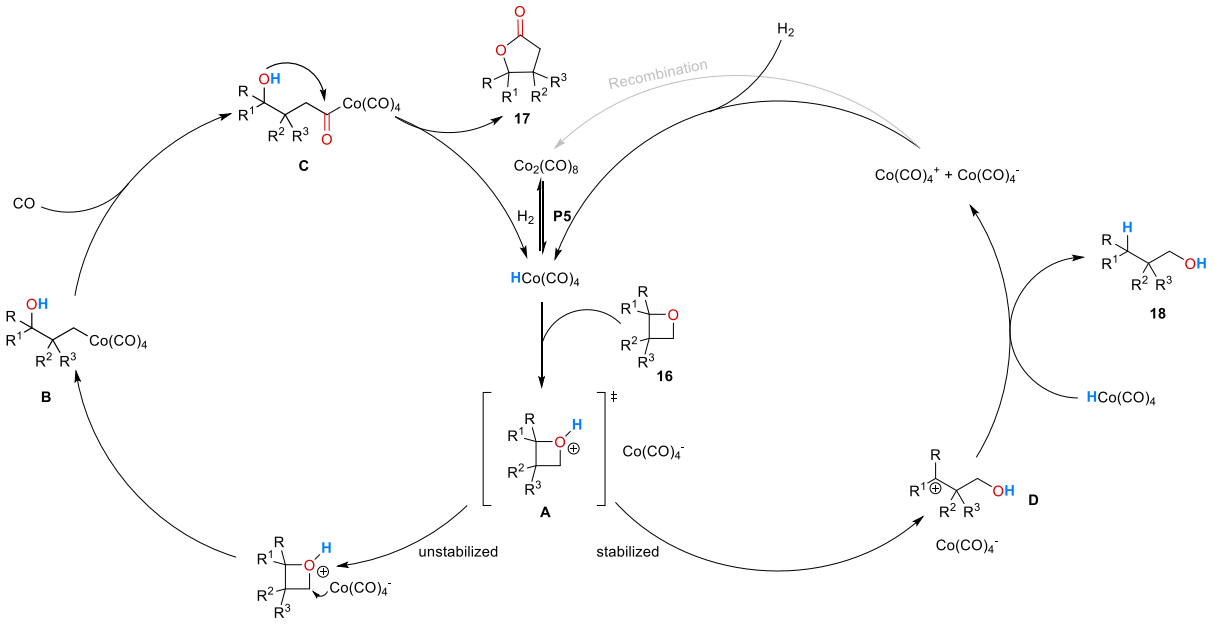

Scheme 22. Proposed catalytic cycles for the cobalt-catalyzed conversion of oxetanes with syngas: carbonylative ring expansion (left) vs. hydrogenative ring opening (right).

3 Conclusion and Outlook

The goal of this thesis was the development and application of homogeneous earth-abundant catalysts for more sustainable (transfer) hydrogenation reactions, with a particular focus on the common 3d transition metals manganese, iron and cobalt.

In the case of manganese, a novel family of PNN-pincer catalysts was synthesized, fully characterized and successfully applied to the challenging hydrogenation of quinolines and related N-heterocycles. Extensive mechanistic investigations were conducted, providing significant insights into the catalytic metal ligand bifunctional mechanism and reasoning for the improved performance of the system. Importantly, the conditions applied in our system are the mildest reported for a manganese catalyst to date! Furthermore, the substrate scope could be significantly extended, now including even particularly challenging heterocyclic substrates as well as industrially relevant building blocks.

On the subject of iron catalysis, we developed a reductive cascade synthesis of pyrroles from nitroarenes, proving that a homogeneous iron system can be remarkably tolerant of acids and water, while also providing a higher chemoselectivity than heterogeneous catalysts. Our system could use both molecular hydrogen and formic acid as green reducing agents and ethanol as a green solvent. Especially under transfer hydrogenation conditions, strikingly mild conditions were achieved and there was no need for basic additives as compared to previous protocols. Late-stage modifications of several multi-functionalized pharmaceutical agents as well as a one-pot gram-scale synthesis of the bioactive agent BM-635 further underlined the incredible potential of our system.

With regards to cobalt, the reductive etherification of aldehydes with alcohols was achieved under significantly milder conditions (from 165 bar to 40 bar). This was enabled by activating the precatalyst dicobalt octacarbonyl with a substoichiometric amount of phosphine oxide promoter. Mechanistic control reactions proved the important role of the syngas reducing agent in stabilizing the active catalyst species and provided insights into a potential reaction pathway. The methodology was further extended to oxetanes, which showed an interesting divergence in chemoselectivity depending on the substrate structure, leading to either carbonylative ring expansion or reductive ring opening.

We have thus demonstrated the potential of three earth-abundant catalyst systems in sustainable (transfer) hydrogenation reactions. Particularly the work on manganese and iron agrees very well with the green chemistry principles, since both systems use benign reagents and ambient temperatures. Further work on the iron system will be conducted with regards to the milder direct use of molecular hydrogen as a reducing agent. In case of the cobalt system, it would be favorable to fully replace toxic syngas by pure hydrogen in the future, potentially by replacing CO with a π-accepting ligand that can stabilize the active cobalt species in a similar manner.

In conclusion, while there is still a long way to go to fully replace precious metal catalysis in the chemical industry, we have shown that replacement of precious metal catalysts is generally possible for several relevant chemical transformations. By optimizing the catalyst structure and the catalytic conditions, it is even possible to obtain active complexes that have similar or even improved performance compared to precious metal catalysts. We are hopeful that in the future this positive trend in the field will continue and we will see more and more sustainable chemical processes inspired by green chemistry.

4 References

[1] J.-C. Kitzler, https://www.br.de/nachricht/40-jahre-seveso-100.html, **2016**, (accessed 09.09.2023).

[2] a) G. Fox, https://www.independent.co.uk/news/world/middle-east/beirut-explosion-lebanon-harbour-port-a9653696.html, **2020**, (accessed 09.09.2023); b) A. Scheuermann, https://www.chemietechnik.de/sicherheit-umwelt/explosion-im-chempark-leverkusen-zweites-todesopfer-gefunden-117.html, **2021**, (accessed 09.09.2023); c) J. Al Tahat, H. Ghaboun, C. Alkhaldi, C. Faraj, M. Salem, https://edition.cnn.com/2022/06/27/middleeast/jordan-toxic-gas-leak-aqaba-port-intl/index.html, **2022**, (accessed 09.09.2023); d) T. Perkins, https://www.theguardian.com/us-news/2023/feb/11/ohio-train-derailment-wake-up-call, **2023**, (accessed 09.09.2023).

[3] Environmental Protection Agency, https://www.epa.gov/trinationalanalysis/greenhouse-gas-reporting-chemical-manufacturing-sector#:~:text=The%20chemical%20manufacturing%20sector%20reported,an%208%25%20increase%20since%202012, **2023**, (accessed 09.09.2023).

[4] Umweltbundesamt, https://www.umweltbundesamt.de/daten/umwelt-wirtschaft/industrie/branchenabhaengiger-energieverbrauch-des#der-energiebedarf-deutschlands, **2022**, (accessed 09.09.2023).

[5] R. Höltschi, https://www.nzz.ch/wirtschaft/chemiekonzern-basf-das-gas-wird-teuer-doch-die-geschaefte-bluehen-noch-ld.1695326, **2022**, (accessed 09.09.2023).

[6] L. Wollensack, K. Budzinski, J. Backmann, *Curr. Opin. Green Sustain. Chem.* **2022**, *33*, 100586.

[7] B. B. Mencho, *Heliyon* **2022**, *8*, e11882.

[8] P. T. Anastas, J. C. Warner, *Green Chemistry: Theory and Practice*, Oxford University Press, New York, **1998**.

[9] B. Lindström, L. J. Pettersson, *CATTECH* **2003**, *7*, 130-138.

[10] E. Hintsches, *MaxPlanckForschung* **2002**, *4*, 44–50.

[11] M. Röper, *Chem. Unserer Zeit* **2006**, *40*, 126-135.

[12] a) R. Tanaka, M. Yamashita, K. Nozaki, *J. Am. Chem. Soc.* **2009**, *131*, 14168-14169; b) A. S. Bommarius, *Chem. Ing. Tech.* **2023**, *95*, 491-497.

[13] S. Kozuch, J. M. L. Martin, *ACS Catal.* **2012**, *2*, 2787-2794.

[14] R. H. Crabtree, in *The Organometallic Chemistry of the Transition Metals*, **2014**, pp. 224-258.

[15] T. E. Crews, M. B. Peoples, *Agric. Ecosyst. Environ.* **2004**, *102*, 279-297.

[16] T. Vielhaber, PhD Thesis thesis, Johannes Kepler University Linz (Linz), **2023**.

[17] A. Fernholm, https://www.nobelprize.org/prizes/chemistry/2018/popular-information/, **2018**, (accessed 28.08.2023).

[18] A. Fernholm, https://www.nobelprize.org/prizes/chemistry/2021/popular-information/, **2021**, (accessed 28.08.2023).

[19] Y. Dou, L. Sun, J. Ren, L. Dong, in *Hydrogen Economy* (Eds.: A. Scipioni, A. Manzardo, J. Ren), Academic Press, **2017**, pp. 277-305.

[20] a) H. B. Kagan, *Angew. Chem. Int. Ed.* **2012**, *51*, 7376-7382; b) I. Fechete, *C. R. Chim.* **2016**, *19*, 1374-1381.

[21] a) M. Calvin, M. Polanyi, *Trans. Faraday Soc.* **1938**, *34*, 1181-1191; b) M. Calvin, *J. Am. Chem. Soc.* **1939**, *61*, 2230-2234; c) C. W. Bird, *Chem. Rev.* **1962**, *62*, 283-302; d) M. Masuo, K. Jung-Wong, *Bull. Chem. Soc. Jpn.* **1963**, *36*, 763-769.

[22] a) J. A. Osborn, G. Wilkinson, J. F. Young, *Chem. Comm.* **1965**, 17-17; b) J. F. Young, J. A. Osborn, F. H. Jardine, G. Wilkinson, *Chem. Comm.* **1965**, 131-132; c) J. A. Osborn, F. H. Jardine, J. F. Young, G. Wilkinson, *J. Chem Soc. A* **1966**, 1711-1732; d) J. A. Osborn, G. Wilkinson, J. J. Mrowca, in *Inorg. Synth.*, **1967**, pp. 67-71.

[23] J. Halpern, *Inorg. Chim. Acta* **1981**, *50*, 11-19.

[24] a) J. R. Shapley, R. R. Schrock, J. A. Osborn, *J. Am. Chem. Soc.* **1969**, *91*, 2816-2817; b) G. Helmchen, *Chem. Eur. J.* **2023**, e202301488.

[25] W. S. Knowles, *Acc. Chem. Res.* **1983**, *16*, 106-112.

[26] a) R. H. Crabtree, H. Felkin, G. E. Morris, *J. Organomet. Chem.* **1977**, *141*, 205-215; b) R. Crabtree, *Acc. Chem. Res.* **1979**, *12*, 331-337.

[27] R. Noyori, T. Ohkuma, *Angew. Chem. Int. Ed.* **2001**, *40*, 40-73.

[28] T. Ohkuma, H. Ooka, S. Hashiguchi, T. Ikariya, R. Noyori, *J. Am. Chem. Soc.* **1995**, *117*, 2675-2676.

[29] a) R. Noyori, M. Yamakawa, S. Hashiguchi, *J. Org. Chem.* **2001**, *66*, 7931-7944; b) P. A. Dub, J. C. Gordon, *ACS Catal.* **2017**, *7*, 6635-6655; c) P. A. Dub, J. C. Gordon, *Nat. Rev. Chem.* **2018**, *2*, 396-408.

[30] a) J. Zhang, G. Leitus, Y. Ben-David, D. Milstein, *Angew. Chem. Int. Ed.* **2006**, *45*, 1113-1115; b) L. A. Saudan, C. M. Saudan, C. Debieux, P. Wyss, *Angew. Chem. Int. Ed.* **2007**, *46*, 7473-7476; c) E. Balaraman, B. Gnanaprakasam, L. J. W. Shimon, D. Milstein, *J. Am. Chem. Soc.* **2010**, *132*, 16756-16758; d) J. M. John, S. H. Bergens, *Angew. Chem. Int. Ed.* **2011**, *50*, 10377-10380; e) W. Kuriyama, T. Matsumoto, O. Ogata, Y. Ino, K. Aoki, S. Tanaka, K. Ishida, T. Kobayashi, N. Sayo, T. Saito, *Org. Process. Res. Dev.* **2012**, *16*, 166-171; f) D. Spasyuk, S. Smith, D. G. Gusev, *Angew. Chem. Int. Ed.* **2012**, *51*, 2772-2775; g) J. Pritchard, G. A. Filonenko, R. van Putten, E. J. M. Hensen, E. A. Pidko, *Chem. Soc. Rev.* **2015**, *44*, 3808-3833.

[31] a) P. Chirik, R. Morris, *Acc. Chem. Res.* **2015**, *48*, 2495-2495; b) K. S. Egorova, V. P. Ananikov, *Organometallics* **2017**, *36*, 4071-4090.

[32] W. M. Haynes, *CRC Handbook of Chemistry and Physics*, CRC Press, Boca Raton, **2016**.

[33] a) United States Geological Survey, https://pubs.usgs.gov/periodicals/mcs2022/, **2022**, (accessed 04.09.2023); b) United States Geological Survey, https://www.usgs.gov/centers/national-minerals-information-center/platinum-group-metals-statistics-and-information, **2023**, (accessed 04.09.2023).

[34] a) European Medicines Agency, https://www.biospectra.us/images/whitepapers/elemental/EMA_CHMP_SWP_4446_2000_Feb-2008-guidline-for-metal-catalysts-and-reagents.pdf, **2008**, (accessed 04.09.2023); b) European Medicines Agency, https://www.ema.europa.eu/en/documents/scientific-guideline/international-conference-harmonisation-technical-requirements-registration-pharmaceuticals-human-use_en-32.pdf, **2018**, (accessed 04.09.2023).

[35] P. J. Chirik, K. M. Engle, E. M. Simmons, S. R. Wisniewski, *Org. Process. Res. Dev.* **2023**, *27*, 1160-1184.

[36] R. M. Bullock, J. G. Chen, L. Gagliardi, P. J. Chirik, O. K. Farha, C. H. Hendon, C. W. Jones, J. A. Keith, J. Klosin, S. D. Minteer, R. H. Morris, A. T. Radosevich, T. B. Rauchfuss, N. A. Strotman, A. Vojvodic, T. R. Ward, J. Y. Yang, Y. Surendranath, *Science* **2020**, *369*, eabc3183.

[37] A. Mukherjee, A. Nerush, G. Leitus, L. J. W. Shimon, Y. Ben David, N. A. Espinosa Jalapa, D. Milstein, *J. Am. Chem. Soc.* **2016**, *138*, 4298-4301.

[38] S. Elangovan, C. Topf, S. Fischer, H. Jiao, A. Spannenberg, W. Baumann, R. Ludwig, K. Junge, M. Beller, *J. Am. Chem. Soc.* **2016**, *138*, 8809-8814.

[39] a) S. Elangovan, M. Garbe, H. Jiao, A. Spannenberg, K. Junge, M. Beller, *Angew. Chem. Int. Ed.* **2016**, *55*, 15364-15368; b) F. Kallmeier, T. Irrgang, T. Dietel, R. Kempe, *Angew. Chem. Int. Ed.* **2016**, *55*, 11806-11809.

[40] a) M. Garbe, K. Junge, M. Beller, *Eur. J. Org. Chem.* **2017**, *2017*, 4344-4362; b) F. Kallmeier, R. Kempe, *Angew. Chem. Int. Ed.* **2018**, *57*, 46-60; c) K. Das, S. Waiba, A. Jana, B. Maji, *Chem. Soc. Rev.* **2022**, *51*, 4386-4464.

[41] A. N. Kim, A. Ngamnithiporn, E. Du, B. M. Stoltz, *Chem. Rev.* **2023**, *123*, 9447-9496.

[42] a) R. H. Fish, A. D. Thormodsen, G. A. Cremer, *J. Am. Chem. Soc.* **1982**, *104*, 5234-5237; b) V. Sridharan, P. A. Suryavanshi, J. C. Menéndez, *Chem. Rev.* **2011**, *111*, 7157-7259.

[43] a) V. Papa, J. R. Cabrero-Antonino, E. Alberico, A. Spanneberg, K. Junge, H. Junge, M. Beller, *Chem. Sci.* **2017**, *8*, 3576-3585; b) Y. Wang, L. Zhu, Z. Shao, G. Li, Y. Lan, Q. Liu, *J. Am. Chem. Soc.* **2019**, *141*, 17337-17349.

[44] V. Papa, Y. Cao, A. Spannenberg, K. Junge, M. Beller, *Nat. Catal.* **2020**, *3*, 135-142.

[45] Z. Wang, L. Chen, G. Mao, C. Wang, *Chin. Chem. Lett.* **2020**, *31*, 1890-1894.

[46] C. Liu, M. Wang, S. Liu, Y. Wang, Y. Peng, Y. Lan, Q. Liu, *Angew. Chem. Int. Ed.* **2021**, *60*, 5108-5113.

[47] P. A. Frey, G. H. Reed, *ACS Chem. Biol.* **2012**, *7*, 1477-1481.

[48] a) Badische Anilin- & Soda-Fabrik, *Verfahren zur synthetischen Darstellung von Ammoniak aus den Elementen*, DE235421C, **1908**; b) J. W. Erisman, M. A. Sutton, J. Galloway, Z. Klimont, W. Winiwarter, *Nat. Geosci.* **2008**, *1*, 636-639.

[49] a) C. Bolm, J. Legros, J. Le Paih, L. Zani, *Chem. Rev.* **2004**, *104*, 6217-6254; b) I. Bauer, H.-J. Knölker, *Chem. Rev.* **2015**, *115*, 3170-3387; c) A. Guðmundsson, J.-E. Bäckvall, *Molecules* **2020**, *25*, 1349.

[50] a) C. Bianchini, M. Peruzzini, F. Zanobini, *J. Organomet. Chem.* **1988**, *354*, C19-C22; b) C. Bianchini, A. Meli, M. Peruzzini, P. Frediani, C. Bohanna, M. A. Esteruelas, L. A. Oro, *Organometallics* **1992**, *11*, 138-145; c) C. Bianchini, E. Farnetti, M. Graziani, M. Peruzzini, A. Polo, *Organometallics* **1993**, *12*, 3753-3761.

[51] S. C. Bart, E. Lobkovsky, P. J. Chirik, *J. Am. Chem. Soc.* **2004**, *126*, 13794-13807.

[52] a) H.-J. Knölker, E. Baum, H. Goesmann, R. Klauss, *Angew. Chem. Int. Ed.* **1999**, *38*, 2064-2066; b) C. P. Casey, H. Guan, *J. Am. Chem. Soc.* **2007**, *129*, 5816-5817.

[53] C. Sui-Seng, F. Freutel, A. J. Lough, R. H. Morris, *Angew. Chem. Int. Ed.* **2008**, *47*, 940-943.

[54] a) C. Federsel, A. Boddien, R. Jackstell, R. Jennerjahn, P. J. Dyson, R. Scopelliti, G. Laurenczy, M. Beller, *Angew. Chem. Int. Ed.* **2010**, *49*, 9777-9780; b) A. Boddien, D. Mellmann, F. Gärtner, R. Jackstell, H. Junge, P. J. Dyson, G. Laurenczy, R. Ludwig, M. Beller, *Science* **2011**, *333*, 1733-1736; c) G. Wienhöfer, I. Sorribes, A. Boddien, F. Westerhaus, K. Junge, H. Junge, R. Llusar, M. Beller, *J. Am. Chem. Soc.* **2011**, *133*, 12875-12879; d) G. Wienhöfer, F. A. Westerhaus, R. V. Jagadeesh, K. Junge, H. Junge, M. Beller, *Chem. Comm.* **2012**, *48*, 4827-4829; e) C. Ziebart, C. Federsel, P. Anbarasan, R. Jackstell, W. Baumann, A. Spannenberg, M. Beller, *J. Am. Chem. Soc.* **2012**, *134*, 20701-20704; f) G. Wienhöfer, M. Baseda-Krüger, C. Ziebart, F. A. Westerhaus, W. Baumann, R. Jackstell, K. Junge, M. Beller, *Chem. Comm.* **2013**, *49*, 9089-9091; g) G. Wienhöfer, F. A. Westerhaus, K. Junge, M. Beller, *J. Organomet. Chem.* **2013**, *744*, 156-159; h) G. Wienhöfer, F. A. Westerhaus, K. Junge, R. Ludwig, M. Beller, *Chem. Eur. J.* **2013**, *19*, 7701-7707; i) W. Liu, W. Li, A. Spannenberg, K. Junge, M. Beller, *Nat. Catal.* **2019**, *2*, 523-528.

[55] a) E. Alberico, P. Sponholz, C. Cordes, M. Nielsen, H.-J. Drexler, W. Baumann, H. Junge, M. Beller, *Angew. Chem. Int. Ed.* **2013**, *52*, 14162-14166; b) S. Chakraborty, H. Dai, P. Bhattacharya, N. T. Fairweather, M. S. Gibson, J. A. Krause, H. Guan, *J. Am. Chem. Soc.* **2014**, *136*, 7869-7872; c) S. Werkmeister, K. Junge, B. Wendt, E. Alberico, H. Jiao, W. Baumann, H. Junge, F. Gallou, M. Beller, *Angew. Chem. Int. Ed.* **2014**, *53*, 8722-8726.

[56] R. H. Crabtree, *Chem. Rev.* **2017**, *117*, 9228-9246.

[57] V. Bhardwaj, D. Gumber, V. Abbot, S. Dhiman, P. Sharma, *RSC Adv.* **2015**, *5*, 15233-15266.

[58] a) L. Knorr, *Chem. Ber.* **1884**, *17*, 2863-2870; b) C. Paal, *Chem. Ber.* **1884**, *17*, 2756-2767; c) A. Hantzsch, *Chem. Ber.* **1890**, *23*, 1474-1476; d) B. Borah, K. D. Dwivedi, L. R. Chowhan, *RSC Adv.* **2021**, *11*, 13585-13601.

[59] a) L. F. Tietze, U. Beifuss, *Angew. Chem. Int. Ed.* **1993**, *32*, 131-163; b) L. F. Tietze, *Chem. Rev.* **1996**, *96*, 115-136; c) K. C. Nicolaou, D. J. Edmonds, P. G. Bulger, *Angew. Chem. Int. Ed.* **2006**, *45*, 7134-7186; d) J. Zhou, *Chem. Asian J.* **2010**, *5*, 422-434; e) R. Ardkhean, D. F. J. Caputo, S. M. Morrow, H. Shi, Y. Xiong, E. A. Anderson, *Chem. Soc. Rev.* **2016**, *45*, 1557-1569.

[60] a) F. Kallmeier, B. Dudziec, T. Irrgang, R. Kempe, *Angew. Chem. Int. Ed.* **2017**, *56*, 7261-7265; b) N. Hofmann, K. C. Hultzsch, *Eur. J. Org. Chem.* **2021**, *2021*, 6206-6223; c) M. Maji, D. Panja, I. Borthakur, S. Kundu, *Org. Chem. Front.* **2021**, *8*, 2673-2709.

[61] a) Z. Gong, Y. Lei, P. Zhou, Z. Zhang, *New J. Chem.* **2017**, *41*, 10613-10618; b) P. Ryabchuk, T. Leischner, C. Kreyenschulte, A. Spannenberg, K. Junge, M. Beller, *Angew. Chem. Int. Ed.* **2020**, *59*, 18679-18685; c) Y. Lin, F. Wang, E. Ren, F. Zhu, Q. Zhang, G.-P. Lu, *J. Catal.* **2022**, *416*, 39-46.

[62] B. Cornils, W. A. Herrmann, M. Rasch, *Angew. Chem. Int. Ed.* **1994**, *33*, 2144-2163.

[63] F. Hebrard, P. Kalck, *Chem. Rev.* **2009**, *109*, 4272-4282.

[64] W. Hieber, F. Mühlbauer, E. A. Ehmann, *Ber. Dtsch. Chem. Ges.* **1932**, *65*, 1090-1101.

[65] R. F. Heck, D. S. Breslow, *J. Am. Chem. Soc.* **1961**, *83*, 4023-4027.

[66] C. S. MacNeil, L. N. Mendelsohn, H. Zhong, T. P. Pabst, P. J. Chirik, *Angew. Chem.* **2020**, *132*, 8997-9001.

[67] a) R. Frlan, D. Kikelj, *Synthesis* **2006**, *2006*, 2271-2285; b) U. Mondal, G. D. Yadav, *J. CO2 Util.* **2019**, *32*, 299-320.

[68] a) E. Fuhrmann, J. Talbiersky, *Org. Process. Res. Dev.* **2005**, *9*, 206-211; b) A. Pelosi, D. Lanari, A. Temperini, M. Curini, O. Rosati, *Adv. Synth. Catal.* **2019**, *361*, 4527-4539; c) A. Prajapati, M. Kumar, R. Thakuria, A. K. Basak, *Tetrahedron Lett.* **2019**, *60*, 150955; d) J. E. Rorrer, A. T. Bell, F. D. Toste, *ChemSusChem* **2019**, *12*, 2835-2858.

[69] L. J. Gooßen, C. Linder, *Synlett* **2006**, *2006*, 3489-3491.

[70] N. Kalutharage, C. S. Yi, *Org. Lett.* **2015**, *17*, 1778-1781.

[71] M. Bakos, Á. Gyömöre, A. Domján, T. Soós, *Angew. Chem. Int. Ed.* **2017**, *56*, 5217-5221.

[72] a) K. Junge, B. Wendt, F. A. Westerhaus, A. Spannenberg, H. Jiao, M. Beller, *Chem. Eur. J.* **2012**, *18*, 9011-9018; b) S. Werkmeister, K. Junge, B. Wendt, A. Spannenberg, H. Jiao, C. Bornschein, M. Beller, *Chem. Eur. J.* **2014**, *20*, 4227-4231; c) R. Adam, E. Alberico, W. Baumann, H.-J. Drexler, R. Jackstell, H. Junge, M. Beller, *Chem. Eur. J.* **2016**, *22*, 4991-5002.

[73] P. Pyykkö, M. Atsumi, *Chem. Eur. J.* **2009**, *15*, 12770-12779.

[74] C. A. Tolman, *Chem. Rev.* **1977**, *77*, 313-348.

[75] a) W. H. Miller, P. J. Manley, R. D. Cousins, K. F. Erhard, D. A. Heerding, C. Kwon, S. T. Ross, J. M. Samanen, D. T. Takata, I. N. Uzinskas, C. C. K. Yuan, R. C. Haltiwanger, C. J. Gress, M. W. Lark, S.-M. Hwang, I. E. James, D. J. Rieman, R. N. Willette, T.-L. Yue, L. M. Azzarano, K. L. Salyers, B. R. Smith, K. W. Ward, K. O. Johanson, W. F. Huffman, *Bioorganic Med. Chem. Lett.* **2003**, *13*, 1483-1486; b) N. A. Anderson, I. B. Campbell, B. J. Fallon, S. M. Lynn, S. J. F. Macdonald, J. M. Pritchard, P. A. Procopiou, S. L. Sollis, L. R. Thorp, *Org. Biomol. Chem.* **2016**, *14*, 5992-6009; c) P. A. Procopiou, N. A. Anderson, J. Barrett, T. N. Barrett, M. H. J. Crawford, B. J. Fallon, A. P. Hancock, J. Le, S. Lemma, R. P. Marshall, J. Morrell, J. M. Pritchard, J. E. Rowedder, P. Saklatvala, R. J. Slack, S. L. Sollis, C. J. Suckling, L. R. Thorp, G. Vitulli, S. J. F. Macdonald, *J. Med. Chem.* **2018**, *61*, 8417-8443.

[76] V. Papa, J. Fessler, F. Zaccaria, J. Hervochon, P. Dam, C. Kubis, A. Spannenberg, Z. Wei, H. Jiao, C. Zuccaccia, A. Macchioni, K. Junge, M. Beller, *Chem. Eur. J.* **2023**, *29*, e202202774.

[77] a) S. Fu, Z. Shao, Y. Wang, Q. Liu, *J. Am. Chem. Soc.* **2017**, *139*, 11941-11948; b) Z. Shao, Y. Wang, Y. Liu, Q. Wang, X. Fu, Q. Liu, *Org. Chem. Front.* **2018**, *5*, 1248-1256.

[78] A. Fürstner, *ACS Cent. Sci.* **2016**, *2*, 778-789.

[79] a) K. Alfonsi, J. Colberg, P. J. Dunn, T. Fevig, S. Jennings, T. A. Johnson, H. P. Kleine, C. Knight, M. A. Nagy, D. A. Perry, M. Stefaniak, *Green Chem.* **2008**, *10*, 31-36; b) R. K. Henderson, C. Jiménez-González, D. J. C. Constable, S. R. Alston, G. G. A. Inglis, G. Fisher, J. Sherwood, S. P. Binks, A. D. Curzons, *Green Chem.* **2011**, *13*, 854-862; c) D. Prat, O. Pardigon, H.-W. Flemming, S. Letestu, V. Ducandas, P. Isnard, E. Guntrum, T. Senac, S. Ruisseau, P. Cruciani, P. Hosek, *Org. Process. Res. Dev.* **2013**, *17*, 1517-1525.

[80] a) D. Jaiswal, A. P. De Souza, S. Larsen, D. S. LeBauer, F. E. Miguez, G. Sparovek, G. Bollero, M. S. Buckeridge, S. P. Long, *Nat. Clim. Change* **2017**, *7*, 788-792; b) L. M.

Rossi, J. M. R. Gallo, L. H. C. Mattoso, M. S. Buckeridge, P. Licence, D. T. Allen, *ACS Sustainable Chem. Eng.* **2021**, *9*, 4293-4295.

[81] F. Alonso, I. P. Beletskaya, M. Yus, *Chem. Rev.* **2002**, *102*, 4009-4092.

[82] a) T. Kondo, T.-a. Mitsudo, *Chem. Rev.* **2000**, *100*, 3205-3220; b) J. K. Dunleavy, *Platinum Metals Rev.* **2006**, *50*, 110; c) A. Kolpin, G. Jones, S. Jones, W. Zheng, J. Cookson, A. P. E. York, P. J. Collier, S. C. E. Tsang, *ACS Catal.* **2017**, *7*, 592-605; d) R. Xiong, W. Ren, Z. Wang, M. Zhang, *ChemCatChem* **2021**, *13*, 548-552.

[83] G. Kortüm, W. Vogel, *Dissociation Constants of Organic Acids in Aqueous Solution*, Butterworths, London, **1961**.

[84] a) H. G. Kuivila, K. V. Nahabedian, *J. Am. Chem. Soc.* **1961**, *83*, 2159-2163; b) P. A. Cox, A. G. Leach, A. D. Campbell, G. C. Lloyd-Jones, *J. Am. Chem. Soc.* **2016**, *138*, 9145-9157.

[85] a) P. R. B. Fallavena, E. E. S. Schapoval, *Int. J. Pharm.* **1997**, *158*, 109-112; b) European Medicines Agency, https://www.ema.europa.eu/en/documents/assessment-report/venclyxto-epar-public-assessment-report_en.pdf, **2016**, (accessed 09.09.2023).

[86] a) M. Biava, G. C. Porretta, G. Poce, A. De Logu, M. Saddi, R. Meleddu, F. Manetti, E. De Rossi, M. Botta, *J. Med. Chem.* **2008**, *51*, 3644-3648; b) G. Poce, R. H. Bates, S. Alfonso, M. Cocozza, G. C. Porretta, L. Ballell, J. Rullas, F. Ortega, A. De Logu, E. Agus, V. La Rosa, M. R. Pasca, E. De Rossi, B. Wae, S. G. Franzblau, F. Manetti, M. Botta, M. Biava, *PLOS ONE* **2013**, *8*, e56980; c) G. Poce, S. Consalvi, M. Cocozza, R. Fernandez-Menendez, R. H. Bates, F. Ortega Muro, D. Barros Aguirre, L. Ballell, M. Biava, *Eur. J. Pharm. Sci.* **2017**, *99*, 17-23.

[87] a) C. Lu, Q. Zhu, X. Zhang, H. Ji, Y. Zhou, H. Wang, Q. Liu, J. Nie, W. Han, X. Li, *ACS Sustainable Chem. Eng.* **2019**, *7*, 8542-8553; b) X. Deng, B. Qin, R. Liu, X. Qin, W. Dai, G. Wu, N. Guan, D. Ma, L. Li, *J. Am. Chem. Soc.* **2021**, *143*, 20898-20906; c) L. Huang, F. Tang, F. Hao, H. Zhao, W. Liu, Y. Lv, P. Liu, W. Xiong, H. Luo, *ACS Sustainable Chem. Eng.* **2022**, *10*, 2947-2959.

[88] B. I. Fleming, H. I. Bolker, *Can. J. Chem.* **1976**, *54*, 685-694.

[89] F. G. Delolo, J. Yang, H. Neumann, E. N. dos Santos, E. V. Gusevskaya, M. Beller, *ACS Sustainable Chem. Eng.* **2021**, *9*, 5148-5154.

[90] a) D. J. Darensbourg, N. Walker, M. Y. Darensbourg, *J. Am. Chem. Soc.* **1980**, *102*, 1213-1214; b) D. J. Darensbourg, M. Y. Darensbourg, N. Walker, *Inorg. Chem.* **1981**, *20*, 1918-1921.

[91] M. D. Wang, S. Calet, H. Alper, *J. Org. Chem.* **1989**, *54*, 20-21.

[92] a) J. Jiang, S. Yoon, *J. Mater. Chem. A* **2019**, *7*, 6120-6125; b) Y. Tang, C. Shen, Q. Yao, X. Tian, B. Wang, K. Dong, *ChemCatChem* **2020**, *12*, 5898-5902.

5 Selected Publications

5.1 Efficient Hydrogenation of N-Heterocycles Catalyzed by NNP-Manganese(I) Pincer Complexes at Ambient Temperature

V. Papa[+], J. Fessler[+], F. Zaccaria, J. Hervochon, P. Dam, C. Kubis, A. Spannenberg, Z. Wei, H. Jiao, C. Zuccaccia, K. Junge, A. Macchioni, M. Beller, *Chem. Eur. J.* **2023**, *29*, e202202774.

DOI: https://doi.org/10.1002/chem.202202774

Electronic supporting information is available online.

For this manuscript, I synthesized and fully characterized the novel ligands and complexes. I took part in the optimization of the reaction, performed most of the substrate scope and isolated the products. I conducted mechanistic NMR and IR experiments together with our collaborators. In addition, I cowrote the draft of the paper and the supporting information. I then finalized the draft and performed all the revisions after editing and peer review. My overall contribution to this work accounts for approximately 40%.

[+] Authors contributed equally.

Signature of the student (Johannes Fessler)	Signature of the supervisor (Prof. Matthias Beller)

Chemistry–A European Journal | Research Article
doi.org/10.1002/chem.202202774
Chemistry Europe
European Chemical Societies Publishing

www.chemeurj.org

VIP Efficient Hydrogenation of N-Heterocycles Catalyzed by NNP–Manganese(I) Pincer Complexes at Ambient Temperature

Veronica Papa[+],[a, b] Johannes Fessler[+],[a] Francesco Zaccaria,[c] Julien Hervochon,[a] Phong Dam,[a] Christoph Kubis,[a] Anke Spannenberg,[a] Zhihong Wei,[a, d] Haijun Jiao,*[a] Cristiano Zuccaccia,[c] Alceo Macchioni,*[c] Kathrin Junge,*[a] and Matthias Beller*[a]

Abstract: Manganese-catalyzed hydrogenation reactions have aroused widespread interest in recent years. Among the catalytic systems described, especially PNP- and NNP–Mn pincer catalysts have been reported for the hydrogenation of aldehydes, ketones, nitriles, aldimines and esters. Furthermore, NNP–Mn pincer compounds are efficient catalysts for the hydrogenolysis of less reactive amides, ureas, carbonates, and carbamates. Herein, the synthesis and application of specific imidazolylaminophosphine ligands and the corresponding Mn pincer complexes are described. These new catalysts have been characterized and studied by a combination of experimental and theoretical investigations, and their catalytic activities have been tested in several hydrogenation reactions with good to excellent performance. Especially, the reduction of N-heterocycles can be performed under very mild conditions.

Introduction

Pincer ligands and their metal complexes have become powerful tools in organometallic and organic chemistry, with many applications in homogeneous catalysis.[1,2,3] The architecture of a pincer ligand can modulate the reactivity of a coordinated metal center, by modifying its electronic and steric properties and conferring improved stability to the resulting catalysts. Additionally, the N-containing pincer ligands are often involved in the elementary steps of a catalytic cycle through reversible bond activation (bifunctional catalysis).[4] These properties lead to improved reactivities, and thus, several redox transformations could be achieved under milder conditions.[5]

Some of the most common classes of pincer ligands are based on the 2,6-lutidine skeleton[6] ($PN^{Py}P$) or a central aliphatic NH group ($PN^{H}P$).[7] An important feature in the design of these pincer ligands are the "arms" flanking the pyridine or NH groups where different donor sets can be introduced to create a symmetrically or asymmetrically substituted ligand. The latter (non-symmetrical) pincer complexes are less studied, even though they offer a higher number of potential combinations for catalyst design.[8]

It has been shown that the replacement of one phosphino group with either an (di)alkylamino ($NN^{Py}P$) or pyridino group ($N^{Py}N^{Py}P$, $N^{Py}N^{H}P$) improved the catalytic performance in many reductions.[9,10] As an example, the dehydrogenative coupling of alcohols and amines to form amides catalyzed by ruthenium-NNP^{tBu} pincer complexes proceeds with enhanced activity,[10] ascribed to the potentially hemilabile nature[11] of the ligated amino group.

In recent years, considerable efforts have been dedicated to the development of first-row transition metal-based catalysts due to their lower cost, often reduced toxicity, and improved sustainability.[12] In this context, particularly Mn-based catalysts are of continuing interest to the scientific community. Indeed, several Mn PNP pincer complexes were reported to catalyze the hydrogenation of aldehydes,[13] imines,[14,15] ketones,[13,16] carbon monoxide,[17] indoles,[18] nitriles,[13] as well as the isomerization of allylic/homo-allylic alcohols to ketones.[19] Interestingly, the reduction of esters to alcohols can be performed at milder

[a] Dr. V. Papa,[+] J. Fessler,[+] Dr. J. Hervochon, P. Dam, Dr. C. Kubis, Dr. A. Spannenberg, Dr. Z. Wei, Dr. H. Jiao, Dr. K. Junge, Prof. M. Beller
Leibniz-Institut für Katalyse e. V.
Albert-Einstein-Straße 29A, 18059 Rostock (Germany)
E-mail: haijun.jiao@catalysis.de
kathrin.junge@catalysis.de
matthias.beller@catalysis.de

[b] Dr. V. Papa[+]
Istituto italiano di tecnologia
Via Morego 30, 16163 Genova (Italy)

[c] Dr. F. Zaccaria, Prof. C. Zuccaccia, Prof. A. Macchioni
Dipartimento di Chimica, Biologia e Biotecnologie and CIRCC
Università degli Studi di Perugia
06123 Perugia (Italy)
E-mail: alceo.macchioni@unipg.it

[d] Dr. Z. Wei
Institute of Molecular Science
Key Laboratory of Materials for Energy Conversion and Storage of Shanxi Province
Shanxi University
030006 Taiyuan (P. R. China)

[+] These authors contributed equally to this manuscript.

Supporting information for this article is available on the WWW under https://doi.org/10.1002/chem.202202774

Chemistry–A European Journal | Research Article doi.org/10.1002/chem.202202774 | Chemistry Europe European Chemical Societies Publishing

conditions when using an NNP-based Mn complex instead of PNP-Mn pincer complexes.[20] Furthermore, the manganese-catalyzed hydrogenation of amides, urea derivatives, carbamates, and noncyclic carbonates was exclusively accomplished using NNP ligands.[9,10,21] Research on replacing one or multiple N and P donors of the Mn-pincer ligands with sulfur or carbene based donors has also received significant attention.[22] In 2017, some of us described the catalytic hydrogenolysis of amides to amines and alcohols in the presence of complex **Mn-1 b** (Figure 1).[9] Furthermore, in 2019 this complex has been reported as a performant catalyst for the reduction of N-heterocycles by Liu and co-workers.[23] Parallel to this work, we reported that the simple manganese carbonyl complex $Mn(CO)_5Br$ allows for the chemoselective hydrogenation of N-heterocycles, especially quinolines, under very mild reaction conditions without the presence of any sophisticated ligands (Figure 1).[24] Despite all these advances, there is still room for improvement and related mechanistic studies on PNP/NNP-manganese systems remain scarce, especially for the relationship between ligand structure and catalytic reactivity.[14,15]

Inspired by our previous works on the synthesis of bi-[25] and tridentate[26] imidazolyl phosphine ligands and their successful application in Ru-catalyzed hydrogenations, in this work we report the synthesis of $N^{Im}N^{H}P$-type pincer ligands and the corresponding family of Mn-pincer complexes (Figure 1 and Scheme 1). In more detail, ligands with different substituents on the phosphino groups and either a two- or three-carbon methylene chain connecting the central aliphatic nitrogen and the phosphorus donor have been prepared.

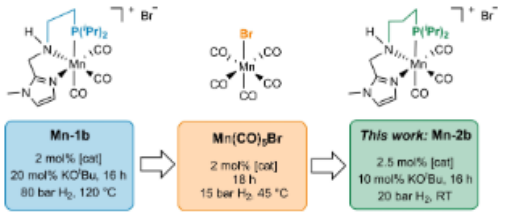

Figure 1. Reported Mn-based catalytic systems for the hydrogenation of N-heterocycles.

Results and Discussion

Synthesis and characterization of the $N^{Im}N^{H}P$-Mn(I) complexes

By combining commercially available 1-methyl-2-imidazole carboxaldehyde and either an ethyl or propyl aminophosphine, the $N^{Im}N^{H}P$ pincer ligands were synthesized in a one-pot, two-step procedure (Scheme 1) without the need for further purification. Subsequently, the complexes were prepared through addition of the NNP pincer ligand to a solution of the manganese precursor $Mn(CO)_5Br$ in tetrahydrofuran (THF) and stirring overnight at reflux. To the best of our knowledge, these complexes, except **Mn-1 a** and **Mn-1 b**, have not been described before.[22] The Mn(I)-complexes were fully characterized by nuclear magnetic resonance (NMR), infrared (IR) spectroscopy, high resolution mass spectrometry (HR-MS), elementary analysis

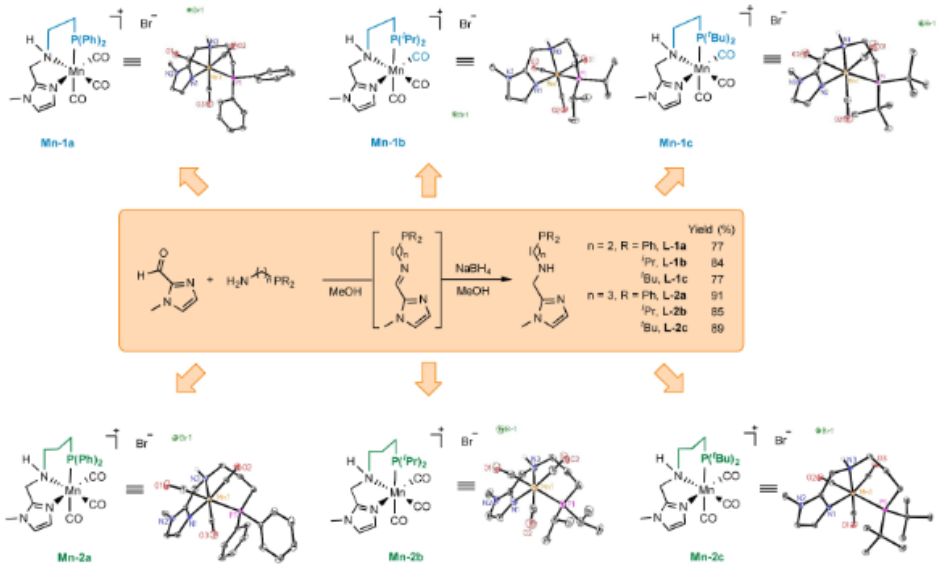

Scheme 1. Preparation of $N^{Im}N^{H}P$–Mn(I) pincer complexes; molecular structures drawn with thermal ellipsoids at the 30% probability level. C-bonded hydrogen atoms and solvent molecules omitted for clarity.[27]

Chemistry–A European Journal | Research Article doi.org/10.1002/chem.202202774 | Chemistry Europe European Chemical Societies Publishing

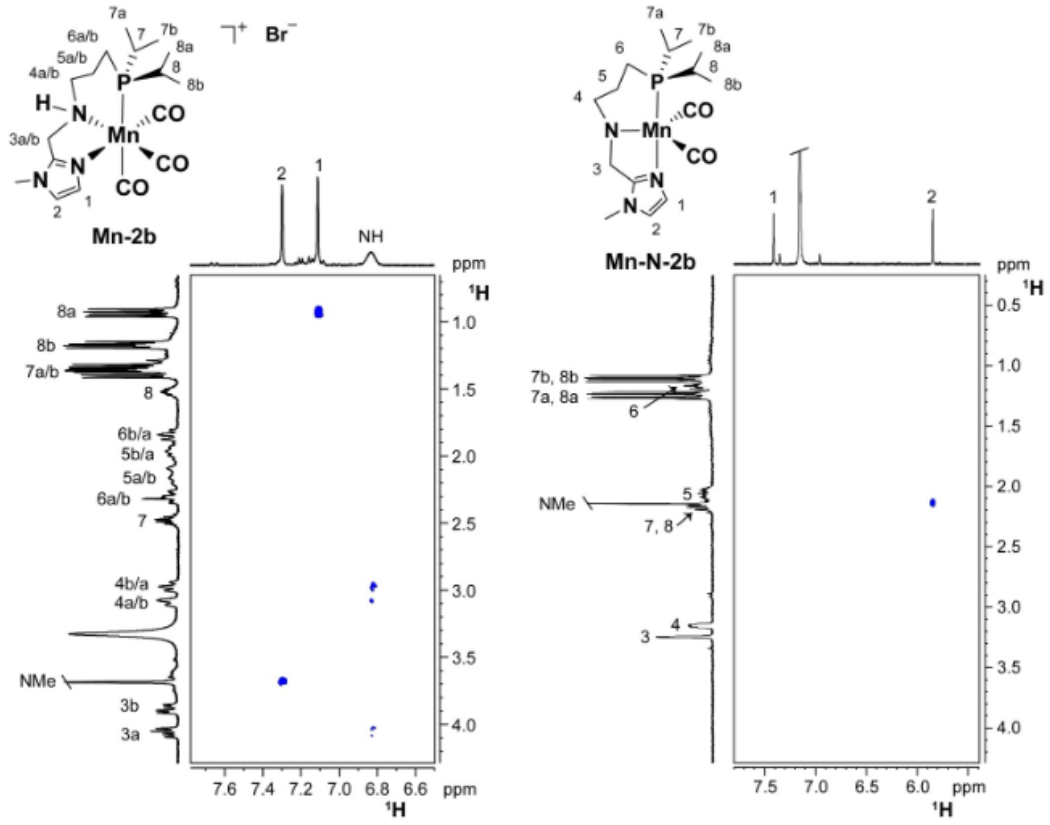

Figure 2. Sections of ^{1}H NOESY NMR spectra of **Mn-2b** (left; methanol-d_4, 298 K) and **Mn-N-2b** (right; benzene-d_6, 298 K).

and the molecular structures were resolved by X-ray diffraction analysis.

The manganese complexes share similar structural features: They all exhibit a distorted octahedral geometry in which the $N^{Im}N^{H}P$ ligand adopts a facial coordination, thus acting as an unsymmetrical tripodal rather than meridional pincer ligand. Consequently, in all complexes the three CO ligands also coordinate in a facial fashion. Indeed, the most important NMR feature of complex **Mn-2b** is the presence of a NOE contact between H8a (on one ^{i}Pr group) and the aromatic proton H1 (on the imidazolyl group) (Figure 2). This is direct evidence supporting the presence of the *fac*-**Mn-2b** isomer in solution; similar spectral features were observed for **Mn-1b**. Computationally, the facial structure of **Mn-1b** and **Mn-2b** is more stable than the meridional isomer by 6.4 and 4.7 kcal/mol, respectively, indicating that the formation of **Mn-1b** and **Mn-2b** is controlled thermodynamically rather than kinetically.

Notably, this new family of $N^{Im}N^{H}P$ Mn(I) pincer complexes is quite stable in the solid state and does not decompose when handled in air.

Catalytic application in hydrogenation reactions

The catalytic hydrogenation potential of the new class of Mn complexes was explored in preliminary tests with several model compounds (Scheme 2). In general, the complexes **Mn-1b** and **Mn-2b** showed the best results. In detail, complexes bearing an ethyl bridged PR_2 linker in the pincer scaffold (**Mn-1**) were more efficient in the C=O bond hydrogenation, while the complexes with a three-carbon methylene chain in the ligand structure (**Mn-2**) were better suited towards the reduction of the various C=N bonds.

In 2017, our group presented **Mn-1b** as the first homogeneous Mn-based catalyst for the hydrogenolysis of amides to amines and alcohols under mild conditions.[9] Furthermore, this complex was active in the homogeneous hydrogenation of cyclic carbonates[28] and carbon monoxide to methanol.[31] Remarkably, in 2019 the Liu group analyzed in detail the hydrogenation of N-heterocycles catalyzed by **Mn-1b** through experimental and computational studies. Albeit they reported a noteworthy catalytic performance of **Mn-1b** with a broad applicability, the catalytic conditions are more drastic (80 bar of

Chemistry–A European Journal | Research Article doi.org/10.1002/chem.202202774 | Chemistry Europe European Chemical Societies Publishing

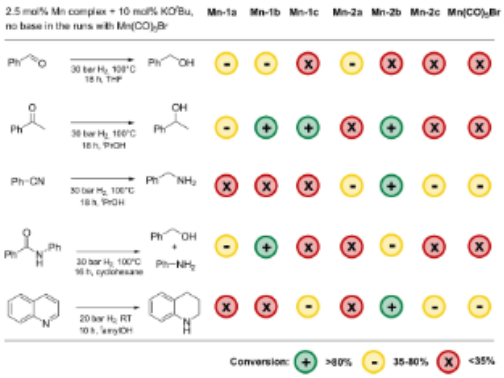

Scheme 2. Catalytic applications of the NNP–Mn complexes in different hydrogenation reactions.

Table 1. Hydrogenation of quinoline **1a** to 1,2,3,4-tetrahydroquinoline **2a**: Optimization of catalytic conditions.[a]

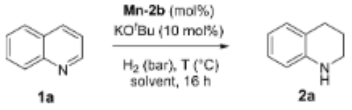

1a 2a

Entry	H_2 [bar]	T [°C]	Mn-2b [mol%]	Conv. [%][b]	2a Yield [%][b]
1[c]	40	140	5	79	77
2	40	140	5	85	84
3	–	140	2.5	13	11
4	40	100	2.5	>99	99
5	40	80	2.5	>99	99
6	40	60	2.5	>99	99
7	20	60	2.5	78	76
8[d]	20	60	2.5	–	–
9	20	RT	2.5	61	61
10[e,c]	20	RT	2.5	>99	97
11[e,c]	20	RT	2	85	83
12[e,c]	10	RT	2.5	93	85
13[e,c]	1	RT	2.5	30	25
14[f]	1	45	$Mn(CO)_5Br$ (2 mol%)	25	10

[a] Standard reaction conditions: quinoline **1a** (64.58 mg, 0.5 mmol), KO'Bu (10 mol%), 'PrOH (2 mL), 16 h. [b] Conversion of **1a** and yield of **2a** were calculated by GC using hexadecane as internal standard. [c] 'amylOH (2 mL). [d] without KO'Bu. [e] using 10 mol% of KO'Bu in THF [1 M]. [f] See Reference [23].

H_2, 120 °C, 20 mol% of KO'Bu, 2 mol% **Mn-1b**) and not accessible to all laboratories. In parallel, our group reported the hydrogenation of a broad number of *N*-heteroarenes catalyzed by the well-known manganese pentacarbonyl bromide.[23] We proved that the ligand-free precursor, in absence of any additives and under very mild conditions (15 bar of H_2, 40 °C, 2 mol% $Mn(CO)_5Br$), is able to form Lewis and Brønsted acid species in situ that act as co-catalysts and significantly improve the catalytic performance of $Mn(CO)_5Br$. In our initial catalytic survey, we realized that complex **Mn-2b** bearing a propyl bridge in the pincer backbone provided a similar or in some cases improved reactivity compared to manganese pentacarbonyl bromide (Scheme 2).

Therefore, we explored **Mn-2b** for this class of compounds in more detail. Initially, the NNP–Mn complex was tested in the benchmark hydrogenation of quinoline (**1a**) using 5 mol% catalyst under 40 bar of H_2 and 140 °C, in presence of a slight excess of base (10 mol%) and 'amyl alcohol as solvent. Under these conditions complex **Mn-2b** affords 1,2,3,4-tetrahydroquinoline (**2a**) in 77% yields (Table 1, entry 1). After a screening of solvents (See Supporting Information S4), 'PrOH was identified as a suitable solvent for this transformation (Table 1, entry 2). To ensure that transfer hydrogenation mechanisms aren't involved in the catalytic reaction, the reduction was carried out in absence of hydrogen (Table 1, entry 3) with poor conversion and yield of the final product **2a**.

Next, the variation of pressure, temperature, catalyst loading and base concentration was performed (Table 1, entries 4–7). It was found that **Mn-2b** was efficient also under much milder conditions (40 bar of H_2, 60 °C, 10 mol% KO'Bu). Even with reduced catalyst loading of 2.5 mol% (Table 1, entry 6) the product **2a** was obtained in 99% yield. However a further reduction of the hydrogen pressure was detrimental (Table 1, entries 7). Notably, no reaction took place in the absence of base as predictable in a system with non-innocent pincer ligands (Table 1, entry 8). During the screening of bases (see Supporting Information), we realized the beneficial effect of using a stock solution of KO'Bu (1 M in THF) rather than the neat solid base, improving greatly the catalytic performance of the system (Table 1, entries 9 and 10). Indeed, the catalytic performance did not decrease when the temperature was reduced to room temperature at 20 bar of H_2, 2.5 mol% of **Mn-2b** and 10 mol% of KO'Bu in THF. Diminishing the catalyst loading from 2.5 to 2 mol% implicated a marginal drop of conversion and yield (Table 1, entry 11). The like was observed upon lowering of the hydrogen pressure to 10 bar (Table 1, entry 12). Remarkably, the complex **Mn-2b** was still working for the hydrogenation of quinoline at room temperature and 1 bar of H_2 producing 1,2,3,4-tetrahydroquinoline **2a** in 25% yield (Table 1, entry 13). To the best of our knowledge such mild conditions were never reached for a homogeneous non-noble metal catalyst in this type of reduction including our own previously developed system.[23] Albeit the reaction conditions applied with bromopentacarbonylmanganese(I) in the homogeneous hydrogenation of *N*-heteroarenes were already mild (Table 1, entry 14), additional improvements have been achieved using complex **Mn-2b.**

At this stage, the following reaction conditions (20 bar of H_2, room temperature, 2.5 mol% of complex **Mn-2b** and 10 mol% of KO'Bu in THF [1 M]) were applied to study the general applicability of the novel complex (Table 2). Here, the hydrogenation of a wide range of quinolines was tested, comparing the results with the previous data obtained applying $MnCO_5Br$ as catalyst.[23] Also, for complex **Mn-2b**, we observed a high tolerance of several electron-donating and electron-withdrawing substituents. There was no strong influence of the position and type of substituent (**1a–k**) in both mono- and multiple-substituted quinolines on the catalytic activity of **Mn-2b**.

Chemistry–A European Journal | Research Article doi.org/10.1002/chem.202202774 | Chemistry Europe European Chemical Societies Publishing

Table 2. Hydrogenation of quinolines **1a–k** to 1,2,3,4-tetrahydroquinolines **2a–k**.

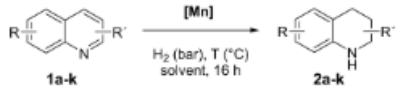

Entry	Quinoline **1**		**Mn-2b**[a] Conv. (%),[k] **2** Yield (%)[k]	$Mn(CO)_5Br$[b]
1		**1a**	>99, **2a** 97	>99, **2a** >99[k]
2	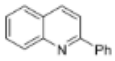	**1b**	>99, **2b** (92)[c,d]	>99, **2b** 88[k]
3	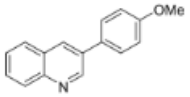	**1c**	85, **2c** (72)[e]	25, **2c** 20[h,k]
4	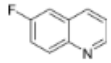	**1d**	>99, **2d** 96	>99, **2d** 85[k]
5	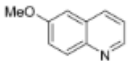	**1e**	>99, **2e** 91	89, **2e** 80[k]
6	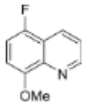	**1f**	>99, **2f** (97)	–[j]
7	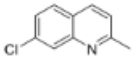	**1g**	>99, **2g** 91	>99, **2g** 90[k]
8		**1h**	>99, **2h** 87	>99, **2h** 87[k]
9		**1i**	>99, **2i** 82[f]	–[j]
10	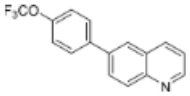	**1j**	>99, **2j** 91[g]	96, **2j** 95[h,k]
11	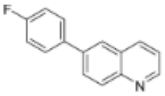	**1k**	82, **2k** (78)	76, **2k** 70[h,k]

[a] Standard reaction conditions: **Mn-2b** (2.5 mol%), quinoline **1** (0.5 mmol), KO^tBu (10 mol%), ^{t}amylOH (2 mL), 20 bar of H_2, RT, 16 h. [b] Standard reaction conditions: $Mn(CO)_5Br$ (2 mol%), quinoline **1** (0.5 mmol), THF (2 mL), 15 bar of H_2, 45 °C, 16 h. [c] Conversion of starting material and yield of **2** was calculated by GC using hexadecane as internal standard. Yield of isolated product given in round brackets. [d] 50 bar of H_2 and 100 °C. [e] 80 °C. [f] 40 bar of H_2 and 80 °C. [g] 60 °C. [h] 20 bar of H_2 and 80 °C, 4 mol% $Mn(CO)_5Br$. [i] 20 bar of H_2 and 60 °C, 2–4 mol% $Mn(CO)_5Br$. [j] No conversion of the starting material was detected. [k] See Reference [23].

Moreover, the complex was performant also for the reduction of derivatives with aryl groups in the 3-position (**1c**) while $Mn(CO)_5Br$ showed lower catalytic activity for this class of substrates. Remarkably, complex **Mn-2b** was able to hydrogenate quinolines bearing multiple substituents in the 5- and 8-positions under these mild reaction conditions (**1f**, **1h**, **1i**). Often, quinolines substituted in these positions are reluctant towards the reduction of the N-ring. In the case of electron-donating moieties such as methoxy and ethoxy groups (**1f**, **1i**) in the 8-position; **Mn-2b** is the first example of homogeneous Mn-based catalyst able to hydrogenate this type of quinolines.

Quinoline derivatives featuring 4-fluoro- or 4-trifluoromethoxyphenyl (**1j**, **1k**) in the 6-position were also transformed to the corresponding 1,2,3,4-tetrahydroquinoline congeners (**2j**, **2k**) in good to excellent yields at 20 bar H_2 and 60 °C.

Besides quinolines, this mild hydrogenation methodology could be extended to the hydrogenation of other important *N*-heteroarenes (Table 3), increasing the value of this protocol from the organic synthesis viewpoint. Thus, several heterocycles such as isoquinoline (**1l**) and quinoxaline (**1m**) were hydrogenated with full conversion and very good to excellent yield under the optimized reaction conditions. Noteworthy, the catalytic protocol based on **Mn-2b** gave often better yields than the $Mn(CO)_5Br$ protocol when applied to N-heterocycles other than quinolines. The conditions required for the reduction of 1,5-naphthyridine (**1n**) and acridine (**1o**) as well as benzo[h]quinolines (**1p**) are milder using **Mn-2b** instead of $Mn(CO)_5Br$. In several cases, the catalyst **Mn-2b** was even performant for N-polycyclic compounds not accessible to the carbonyl complex $Mn(CO)_5Br$ (**1q**, **1s-v**).

Indeed, the hydrogenation of 2,2′-biquinoline (**1q**) has been performed applying the complex **Mn-2b** at slightly higher temperature (80 °C), obtaining a 76% of yield. Furthermore, 1,10-phenanthroline (**1t**), a more challenging substrate often used as a strong bidentate ligand, was converted to 1,2,3,4-tetrahydro-1,10-phenanthroline (**2t**) in 84% yield. The reaction of bulkier substrates 4,7-diphenyl- and 2,9-dimethyl-1,10-phenanthroline (**1u**, **1v**) also proceeded smoothly. Undoubtedly, the selective hydrogenation on only one heterocyclic moiety of phenanthroline is a difficult transformation. It was rarely reported with catalysts based on non-noble metals[29] and to the best of our knowledge this reduction has never been achieved under such mild conditions using molecular hydrogen. These methodologies can open the door to the potential application of this type of earth-abundant metal pincer complexes in the synthesis of non-symmetrical N,N-ligands. Pleasingly, other polycyclic N-heterocycles (**1r**, **1s**) were also suitable substrates for this transformation. A reaction of particular interest to the pharmaceutical industry is the hydrogenation of 2-methyl-1,8-naphthyridine (**1w**).[30] While $Mn(CO)_5Br$ again showed no conversion of the starting material at ambient temperature, catalyst **Mn-2b** gave full conversion and a combined isolated yield of 80%. Finally, even indole (**1x**) could be converted to the corresponding indoline applying this protocol, however relatively low conversion and yield were observed at elevated temperatures. Notably, indoles are known to be reluctant towards hydrogenation due to their electron-richness and strong aromaticity.[17]

Chemistry–A European Journal | Research Article doi.org/10.1002/chem.202202774 | Chemistry Europe European Chemical Societies Publishing

Table 3. Hydrogenation of various *N*-heteroarenes **1l–x** to the corresponding products **2l–x**.

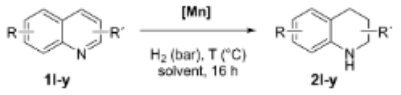

Entry	Quinoline **1**		Mn-2b[a] Conv. (%),[c] **2** Yield (%)[c]	$Mn(CO)_5Br$[b]
1		**1l**	>99, **2l** (83)	>99, **2l** >99[d]
2		**1m**	>99, **2m** (95)	>99, **2m** 71[d]
3		**1n**	>99, **2n** 81	84, **2n** 82[d,f]
4	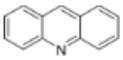	**1o**	>99, **2o** 87	95, **2o** 90[d,f]
5	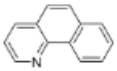	**1p**	85, **2p** 84[d]	90, **2p** 88[d,f]
6	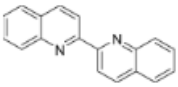	**1q**	95, **2q** (76)[f]	–[e]
7	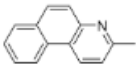	**1r**	>99, **2r** (>99)[g]	>99, **2r** 90[g,f]
8	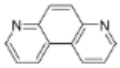	**1s**	>99, **2s** (95)	–[e]
9	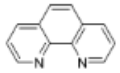	**1t**	89, **2t** 84	–[e]
10	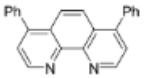	**1u**	64, **2u** (64)[h]	–[e]
11	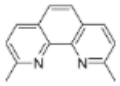	**1v**	28, **2v** (26)[h]	–[e]
12	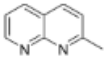	**1w**	>99, **2w** (80)[i]	–[e]
13		**1x**	30, **2x** 15[i,j,h]	–[e]

[a] Standard reaction conditions: 2.5 mol% **Mn-2b**, quinoline **1** (0.5 mmol), KO^{t}Bu (10 mol%), ^{t}amylOH (2 mL), 20 bar of H_2, RT, 16 h. [b] Standard reaction conditions: $Mn(CO)_5Br$ (2 mol%), quinoline **1** (0.5 mmol), THF (2 mL), 15 bar of H_2, 45 °C, 16 h. [c] Conversion of starting material and yield of **2** were calculated by GC using hexadecane as internal standard. Yield of isolated product given in round brackets. [d] 20 bar of H_2 and 80 °C. [e] No conversion of the starting material was detected. [f] 40 bar of H_2 and 80 °C. [g] 20 bar of H_2 and 60 °C. [h] 50 bar of H_2 and 120–150 °C. [i] Combined yield, ratio of isomers 2.5:1, 7-methyl-1,2,3,4-tetrahydro-1,8-naphthyridine is the major isomer. [j] See Reference [23].

Spectroscopic studies on the reactivity of Mn-1b and Mn-2b

Since **Mn-1b** and **Mn-2b** were the most active catalysts (as discussed above), their reactivity was further studied by NMR and IR spectroscopy. As expected, the M-NH moiety of the catalyst precursor can be deprotonated in the presence of a basic additive; the resulting amido complex is proposed to be the catalytically active species, being able to activate H_2 via metal-ligand cooperation.[6,17a,31]

As shown in Scheme 3, NMR spectroscopic studies of the reaction of **Mn-1b** and **Mn-2b** with 1.06 equiv. KO^{t}Bu proved the formation of the corresponding amido complexes **Mn-N-1b** and **Mn-N-2b**.

Both dicarbonyl amido complexes were isolated as sensitive deep red powders and characterized by NMR spectroscopy in benzene-d_6 at 298 K (see Supporting Information). The ^{31}P NMR spectra show a single resonance for both **Mn-N-1b** (δ_P = 124.6 ppm) and **Mn-N-2b** (δ_P = 84.9 ppm), being high frequency shifted with respect to that of the respective starting complexes **Mn-1b** (δ_P = 79.0 ppm in methanol-d_4) and **Mn-2b** (δ_P = 39.5 ppm in methanol-d_4). This indicates that a single isomer is formed.

Importantly, while **Mn-1b** and **Mn-2b** exhibit a set of diastereotopic protons for each methylene group, the ^{1}H NMR spectra of **Mn-N-1b** and **Mn-N-2b** are far simpler and consistent with a more symmetric structure (Figure 2 and Supporting Information). Furthermore, dipolar interactions between the P-^{i}Pr and imidazole fragments are visible in the ^{1}H NOESY spectra of the starting ionic complexes, consistent with the *fac* configuration of the $N^{Im}N^HP$ ligands, while no such coupling is observed for the neutral amido products (see Figure 2 for the representative case of **Mn-N-2b**). All these observations indicate that the deprotonated ancillary ligand coordinates at the Mn(I) center with a *mer* configuration, as depicted in Scheme 3. The above mentioned variations in δ_P are also consistent with a shift from a *trans-C,P* configuration in the starting ionic complexes to a *trans-N^{Im},P* configuration in the neutral products.[32]

The amido complexes were further characterized by IR spectroscopy, each showing the same two CO stretching bands **Mn-N-1b** (ν_{CO} = 1896 cm^{-1}, 1818 cm^{-1}) and **Mn-N-2b** (ν_{CO} = 1896 cm^{-1}, 1818 cm^{-1}), indicating near identical electronic environments for both metal centers. Therefore differences in reactivity are likely caused by other factors. Unfortunately, no crystals suitable for X-ray analysis could be obtained. However, these observed frequencies agree fully with those of several Mn amido complexes, which have been characterized by X-ray structure analysis.[22]

It should be noted here that the ^{31}P NMR signal of **Mn-N-2b** is about 40 ppm shifted to lower frequency with respect to **Mn-**

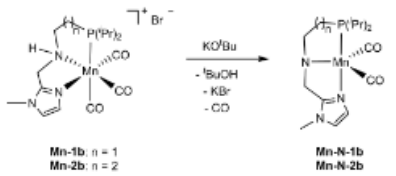

Scheme 3. Reaction of **Mn-1b** and **Mn-2b** with KO^{t}Bu.

Chemistry–A European Journal | Research Article doi.org/10.1002/chem.202202774 | Chemistry Europe European Chemical Societies Publishing

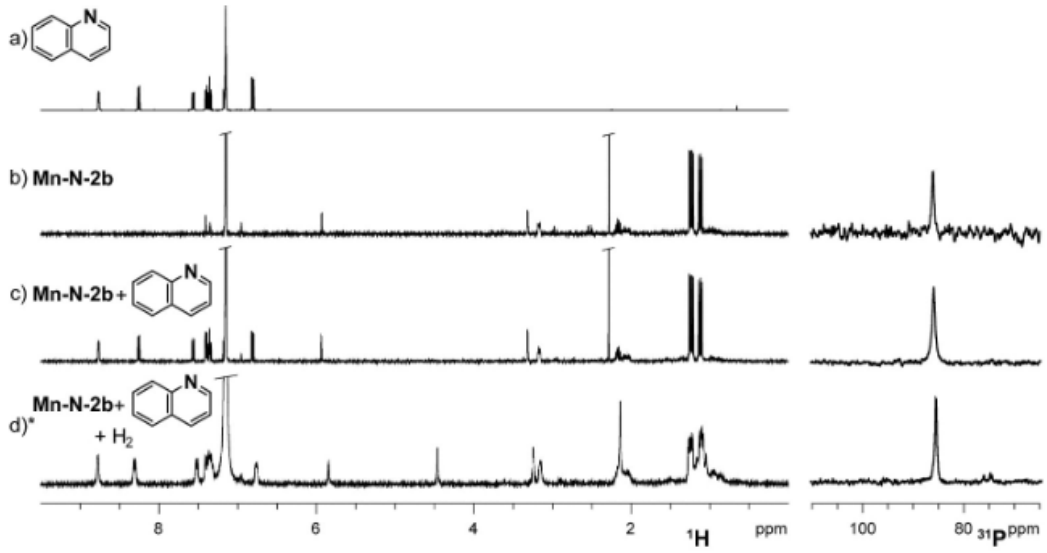

Figure 3. Comparison of ^{1}H and ^{31}P NMR spectra (benzene-d_6, 333 K) of quinoline (a), **Mn-N-2b** (b) and a mixture thereof in the absence (c) and presence (d) of 1 bar of hydrogen (after 24 h). * Recorded at 298 K.

N-1b. That is, the former is appreciably closer to that of the free ligands having similar chemical shifts between 4 and −1 ppm.[26] The same trend is observed also for the starting bromide complexes. This might indicate a looser coordination of the phosphine arm to the manganese center in the **Mn-N-2b** complex, possibly resulting from some geometric constrain induced by the longer propylene vs. ethylene bridge in the ancillary ligand scaffold.

Next, the reactivity of the two amido complexes was explored aiming at probing the potential hemilability of the phosphine arm in **Mn-N-2b**, as a possible origin for its strikingly different activity towards hydrogenation of N-heterocycles with respect to **Mn-N-1b**. Thus, the two complexes were combined with the representative substrate quinoline in benzene-d_6 and monitored by NMR. However, no reaction was observed over 16 h at 333 K. No dipolar interactions are detected between the amido complexes and quinoline by ^{1}H ROESY NMR (Supporting Information). Comparison of ^{1}H and ^{31}P NMR spectra of these mixtures with those of the isolated reagents further confirmed the absence of any detectable chemical interaction (Figure 3 and Supporting Information). In conclusion, no evidence for hemilability of the phosphine arm in **Mn-N-2b** could be obtained. The reaction mixtures were then pressurized with 1 bar of H_2, trying to convert **Mn-N-1b** and **Mn-N-2b** into the corresponding hydride complexes. However, no reaction occurred over 24 h (Figure 3 d) and Supporting Information). Only some line broadening in the ^{1}H NMR spectra was observed, likely due to the formation of minor paramagnetic species. Observation of Mn hydride species was therefore attempted on a preparative scale by reacting **Mn-2b** with KO^{t}Bu in a more polar solvent like THF-d_8, and then pressurizing with 20 bar of hydrogen at 30 °C. Indeed, after 20 h the ^{31}P NMR spectrum of the reaction showed the presence of three largely dominant species in a 2:2:1 integral ratio, resonating at 93.2, 85.5 and 3.1 ppm (Supporting Information).

The latter two peaks can be tentatively ascribed to **Mn-N-2b** and some free $N^{Im}N^{H}P$ ligand or a **Mn-2b** derivative with a decoordinated phosphine arm, due to the potentially hemilabile character of the NNP pincer ligand. Conversely, the former signal is compatible with the formation of a hydride complex, consistent with the observation of a broad doublet at $\delta_H = -9.08$ ppm in the ^{1}H NMR spectrum, which could be assigned to a Mn–H fragment ($J_{PH} = 53$ Hz; Supporting Information), likely of the composition **MnH-NH-2b** (Scheme 5). The broadness of the ^{1}H NMR peaks and the sensitivity of the species, however, hampered detailed characterization and reactivity studies.

Unfortunately, also other attempts to isolate the hydride complexes, for instance by reacting **Mn-1b** and **Mn-2b** with a hydride donor like $NaHBEt_3$, were unsuccessful (see Supporting Information for details).[33] Given the complexity of this catalytic system, the mechanism of catalyst activation and hydrogenation was further analyzed by in situ IR measurements and computational modelling.

First, we performed the in situ IR experiments to monitor the carbonyl spectra during the generation of the amido species **Mn-N-2b** in solution. Starting from **Mn-2b** suspended in THF at room temperature, the titration of an equimolar amount of KO^{t}Bu resulted in a quick and significant change of the spectrum (Scheme 4). By adding one equivalent of base (**Mn-2b** + 1 equiv KO^{t}Bu), the three characteristic CO bands of

Chemistry–A European Journal | Research Article doi.org/10.1002/chem.202202774 | Chemistry Europe European Chemical Societies Publishing

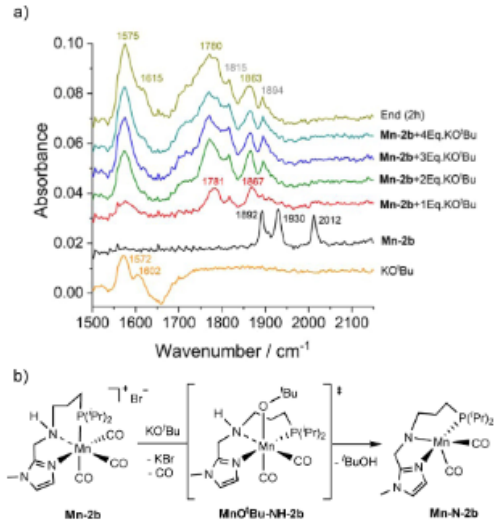

Scheme 4. a) In situ IR measurements monitoring the formation of the amido species **Mn-N-2b**. b) Proposed pathway for the formation of the amido species.

Mn-2b (ν(CO) = 1892, 1930, 2012 cm^{-1}) disappeared, while two new bands appeared (ν(CO) = 1781, 1867 cm^{-1}), indicating the formation of a new intermediate, presumably an O^{t}Bu complex formed by the substitution of one CO ligand by the O^{t}Bu anion.[21] Adding one additional equivalent base (**Mn-2b** + 2 equiv KO^{t}Bu), two other bands (ν(CO) = 1815, 1894 cm^{-1}), belonging to the characteristic peaks of the Mn amido complexes (**Mn-N-2b**), appeared. These four CO bands demonstrate the co-existence of the new intermediate and the Mn amido complex. Adding further base (**Mn-2b** + 3 equiv KO^{t}Bu and **Mn-2b** + 4 equiv. KO^{t}Bu) did not significantly change the shape of the spectra, and the increase of the overall band intensity was probably due to the improved solubility of the intermediates that formed at higher base concentrations.

Next, we computed the energies for the elimination reaction of t-butyl alcohol from the alkoxide complex **MnO^{t}Bu-NH-2b** to form amido complex **Mn-N-2b** (Scheme 5). It is slightly exergonic by −1.0 kcal/mol, indicating a possible equilibrium and co-existence of both complexes, in line with the previous spectroscopic results.

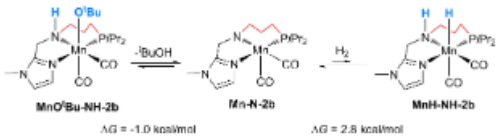

Scheme 5. Computed Gibbs free energy for the transformation between Mn alkoxide, Mn amido and Mn hydrido complexes.

We were also interested to see whether in situ IR spectroscopy is helpful in monitoring the hydride complex formation, to potentially corroborate the previous NMR spectroscopic results. The starting complex **Mn-2b** was therefore treated with the entire amount of four equiv. of KO^{t}Bu in THF. Interestingly, the spectral features differed somewhat from the former stepwise addition, showing a higher ratio of the **Mn-N-2b** species (Supporting Information). After addition of 2.0 MPa of hydrogen rather small changes were observed during a period of 4 h, still showing the Mn amido species as the main species and not allowing for the detection of the proposed hydride species **MnH-NH-2b**. This could be due to potential spectral overlap of the amido and hydrido species as well as the slow formation of the **MnH-NH-2b** species at room temperature over the tested period. Again, the computational data (Scheme 5) supports the spectroscopic results, showing H_2 addition to the amido complex **Mn-N-2b** to be endergonic by 2.8 kcal/mol, indicating once more a possible equilibrium favoring the amido species and explaining the difficulty to observe **MnH-NH-2b** in the previous IR experiment.

Computational Studies

Based on the experimental outcome seen above, density functional theory computations were carried out to gain insight into the catalytic mechanisms of the hydrogenation reaction and to understand the activity difference between **Mn-1b** and **Mn-2b** (Scheme 3). In our computations, we followed the same procedures as reported in literature,[18,19,26,34] especially those reported by Liu et al. for the structure, stability and catalytic activity of **Mn-1b**,[22] and re-calculated some of their results for direct comparison. In these studies, an outer-sphere bifunctional hydrogenation mechanism via a Mn–H transfer step with the formation of an intermediate and a subsequent N–H transfer to the product has been proposed and verified. All these computational details are given in the Supporting Information.

Having the general mechanistic scheme and the reported results for quinoline hydrogenation in hand, here we present only the key results for the stability and catalytic activity for comparison by using the same method as in our previous study of PNP–Mn catalyzed chemoselective semihydrogenation of alkynes.[35] An excellent agreement between theory and experiment has been found, where the reported energies are calculated by using the M06 L[36] functional in combination with the 6-311 + + G(3df,3pd) basis set[37] under the consideration of solvation effect (SMD[38]) of THF as solvent.

First, we computed the stability of the proposed hydrido and active amido catalysts (Figure 4), **MnH-NH-1b** and **Mn-N-1b** as well as **MnH-NH-2b** and **Mn-N-2b**. As shown on Figure 4, both hydrido complexes have nearly the same stability with respect to H_2 elimination (18.3 vs. 18.5 kcal/mol), while the formation of the amido complex **Mn-N-1b** is more exergonic than that of **Mn-N-2b**. Reversibly, the barrier of H_2 addition is 23.6 and 21.1 kcal/mol for **Mn-N-1b** and **Mn-N-2b**, respectively.

Chemistry–A European Journal | Research Article doi.org/10.1002/chem.202202774 | Chemistry Europe European Chemical Societies Publishing

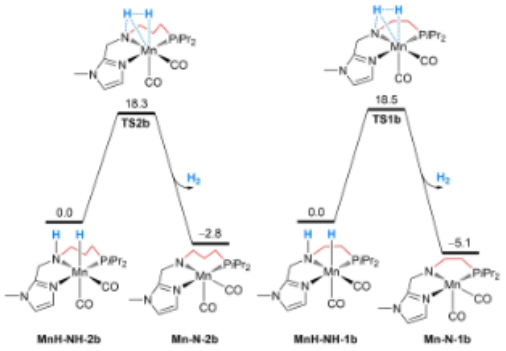

Figure 4. Computed Gibbs free energies (kcal/mol) for the interconversion between the hydrido and amido complexes.

The stability of these complexes might determine the whole reaction conditions.

Next, we computed the catalytic activity of the hydrogenation of quinoline (Figure 5) following the same procedure reported by Liu et al. We also found a stepwise reaction sequence, where the first step is the Mn–H transfer forming an intermediate and the second step is the N–H transfer to the product with a slightly higher barrier. The barrier (15.9 kcal/mol) of Mn–H transfer for **MnH-NH-2b** is lower than that (18.4 kcal/mol) of **MnH-NH-1b** by 2.5 kcal/mol, indicating the higher kinetic activity of **MnH-NH-2b**. A comparison of the computed stability (Figure 4) and the activity (Figure 5) reveals the difference between these two catalysts. For **MnH-NH-2b**, the hydrogenation step has lower barrier than H_2 elimination (15.9 vs. 18.3 kcal/mol), showing that the hydrogenation step is kinetically more favored than H_2 elimination. Therefore, no high H_2 pressure should be needed to maintain the stability of **MnH-NH-2b**. In case of **MnH-NH-1b**, the barrier of the hydrogenation as well as for H_2 elimination step are closer together (18.4 vs. 18.5 kcal/mol), indicating that the reaction needs high H_2 pressure to maintain the stability of **MnH-NH-1b**.

Since H_2 elimination is exergonic for both hydrido complexes (−2.8 and −5.1 kcal/mol), the reverse reaction generating the hydrido complexes is endergonic and the rate-determining step. Therefore, high H_2 pressure is needed to promote the formation of hydrido complexes **MnH-NH-1b** and **MnH-NH-2b** and subsequently the hydrogenation step. In addition, high temperature favors the endergonic H_2 addition, but lowers the solubility of H_2 gas in solution. Thus, high H_2 pressure is required to counterbalance the effect of high temperature. Because of the lower formation barrier of **MnH-NH-2b** compared to **MnH-NH-1b** (21.1 vs. 23.6 kcal/mol), a higher catalytic activity of **MnH-NH-2b** can be expected, especially at low temperature under given H_2 pressure. This relationship has been indeed verified in our experimental studies shown in Table 1. Here, excellent yield can be achieved either at high temperature and high H_2 pressure (100 °C and 40 bar, entry 4) or at room temperature and lower H_2 pressure (20 bar, entry 10). Since the formation of the hydrido complex is the rate-determining step and both hydrido complexes differ only in the length of alkyl bridge, i.e., ethylene (C2) vs. propylene (C3) bridge, we were interested in the effect of both NNP ligand in stabilizing the hydrido and amide complexes as well as in transition state of H_2 addition. Thus, we computed the formal exchange reaction between both NNP ligands, NN–C2–P and NN–C3–P (Figure 6). It shows that not only the hydrido and amido complexes but also the corresponding transition for H_2 addition with the ligand with ethylene bridge are more stable than the corresponding counterparts with propylene bridge by 1.5, 3.7 and 1.2 kcal/mol, respectively. These results indicate a different coordination ability of the same ligand in a different state, i.e., large difference in the amido complexes **Mn-N-2b** and **Mn-N-1b** and small differences in the hydrido complexes **MnH-NH-2b** and **MnH-NH-1b** as well as the corresponding transition states, **TS2b** and **TS1b**. The computed energy difference for the ligand exchange between

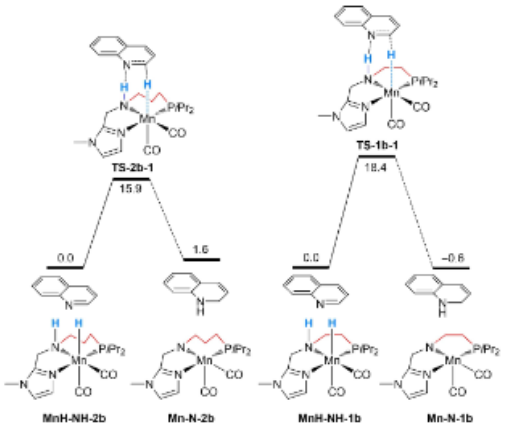

Figure 5. Computed Gibbs free energy barrier (kcal/mol) for the first Mn–H transfer and the reaction free energy of the N=C hydrogenation.

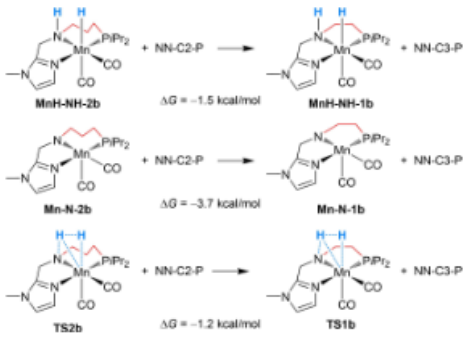

Figure 6. Computed Gibbs free energy barrier (kcal/mol) for ligand exchange.

Chemistry–A European Journal | Research Article doi.org/10.1002/chem.202202774 | Chemistry Europe European Chemical Societies Publishing

the amido complexes and the transition states (−3.7 vs. −1.2 kcal/mol) just reflects the barrier difference for H_2 addition in Figure 6; and this reveals that the enhanced higher kinetic activity of **TS2b** comes from the coordination ability of the ligand in the transition state.

Due to the different bridge lengths, ethylene vs. propylene, we further computed the hemilability of the phosphine ligand, where the $CH_2CH_2P(iPr)_2$ and $CH_2CH_2CH_2P(iPr)_2$ chains become trans-linear. It is found that the decoordination of phosphine ligand is endergonic by 31.7 and 37.9 kcal/mol for **MnH-NH-2b** and **MnH-NH-1b**, respectively. Although the longer bridge has lower coordination energy than the shorter bridge, both energy values are much higher than the barriers of the rate-determining step (Figure 4), i.e., the barriers for the formation of **MnH-NH-2b** and **MnH-NH-1b** (21.1 and 23.6 kcal/mol, respectively). Under the reaction condition, therefore, the coordination of both phosphine ligands are expected to remain intact and stable.

Conclusion

In summary, several imidazolylphosphine pincer ligands and the corresponding Mn complexes were synthesized, fully characterized, and studied by a combination of experimental and theoretical investigations. The complexes were tested in several hydrogenation reactions with good to excellent performance. Especially, the reduction of diverse N-heterocycles can be performed in excellent yields and high selectivity under very mild conditions using catalyst **Mn-2b**. Spectroscopic studies support a classical metal-ligand cooperative mechanism for the activation of the catalyst, revealing amido as well as hydrido species. A third species could also be observed, tentatively assigned as the tert-butoxy species **MnO^{t}Bu-NH-2b**. DFT supported these findings showing the possibility of equilibrium between all three catalyst species in the reaction. It further revealed higher kinetic reactivity as well as lower formation barrier for **MnH-NH-2b** over **MnH-NH-1b** as likely causes for its improved reactivity.

Experimental Section

General procedure for the hydrogenation of N-heteroarenes: In a typical catalytic experiment, a 4 mL glass vial containing a stir bar was sequentially charged with **Mn-2b** (2.0 mol%) and substrate (0.5 mmol) under argon atmosphere (glove box). Afterwards, the reaction vial was capped with a septum cap and removed from the glovebox. Then dry solvent (^{t}amylOH, 2 mL) and base (10.0 mol% KO^{t}Bu, 1 M in THF) were sequentially introduced through the septum. The vial was set in an alloy plate, which was then placed into an argon flushed 300 mL autoclave and the septum cap was pierced with a syringe needle to allow free gas flow. The reactor was closed, attached to a gas line, and the gas line was purged with nitrogen (3×). Afterwards, the autoclave was flushed with hydrogen (3×, about 20 bar) and then pressurized to the desired pressure (20 bar). The reaction was left stirring overnight (16 h) at the desired temperature (25 °C) inside an aluminum block. At the end of the reaction time, the pressure was carefully released, the reactor flushed with argon and opened. The reaction mixture was either analyzed by GC using hexadecane as internal standard or directly purified by flash column chromatography to obtain isolated products.

Acknowledgements

The authors thank the analytical team of LIKAT especially Dr. Wolfgang Baumann and Dr. Marcus Klahn for their excellent support. Furthermore Andrea Vicenzi, Niklas Both and Yixuan Cao are gratefully acknowledged for their experimental assistance. Prof. Johannes G. de Vries, Andrea Dell'Acqua, Claas Schünemann, and Dr. Brian Spiegelberg are thanked for their continued technical support. Open Access funding enabled and organized by Projekt DEAL.

Conflict of Interest

The authors declare no conflict of interest.

Data Availability Statement

The data that support the findings of this study are available in the supplementary material of this article.

Keywords: hydrogenation · nitrogen heterocycles · manganese · pincer ligands · reaction mechanisms

[1] C. Gunanathan, D. Milstein, *Chem. Rev.* **2014**, *114*, 12024–12087.
[2] H. A. Younus, W. Su, N. Ahmad, S. Chen, F. Verpoort, *Adv. Synth. Catal.* **2015**, *357*, 283–330.
[3] a) *The Chemistry of Pincer Compounds* (Eds. D. Morales-Morales, C. M. Jensen), Elsevier, Amsterdam, **2007** ; b) M. Albrecht, M. M. Lindner, *Dalton Trans.* **2011**, *40*, 8733–8744; c) *Organometallic Pincer Chemistry* (Eds. G. van Koten, D. Milstein), Springer, Heidelberg, **2013**.
[4] R. Noyori, M. Yanmakawa, S. Hashiguchi, *J. Org. Chem.* **2001**, *66*, 7931–7944.
[5] a) J. I. van der Vlugt, J. N. H. Reek, *Angew. Chem. Int. Ed.* **2009**, *48*, 8832–8846; *Angew. Chem.* **2009**, *121*, 8990–9004; b) D. Gelman, S. Musa, *ACS Catal.* **2012**, *2*, 2456–2466; c) V. T. Annibale, D. Song, *RSC Adv.* **2013**, *3*, 11432–11449; d) J. R. Khusnutdinova, D. Milstein, *Angew. Chem. Int. Ed.* **2015**, *54*, 12236–12273; *Angew. Chem.* **2015**, *127*, 12406–12445.
[6] C. Gunanathan, D. Milstein, *Acc. Chem. Res.* **2011**, *44*, 588–602.
[7] S. Schneider, J. Meiners, B. Askevolt, *Eur. J. Inorg. Chem.* **2012**, *2012*, 412–429.
[8] E. Peris, R. H. Crabtree, *Chem. Rev.* **2018**, *47*, 1959–1968.
[9] V. Papa, J. R. Cabrero-Antonino, E. Alberico, A. Spannenberg, H. Junge, K. Junge, M. Beller, *Chem. Sci.* **2017**, *8*, 3576–3585.
[10] For selected examples see: a) J. Zhang, G. Leitus, Y. Ben-David, D. Milstein, *J. Am. Chem. Soc.* **2005**, *127*, 10840–10841; b) J. Zhang, G. Leitus, Y. Ben-David, D. Milstein, *Angew. Chem. Int. Ed.* **2006**, *45*, 1113–1115; *Angew. Chem.* **2006**, *118*, 1131–1133; c) C. Gunanathan, Y. Ben-David, D. Milstein, *Science* **2007**, *317*, 790–792; d) E. Balaraman, B. Gnanaprakasam, L. J. W. Shimon, D. Milstein, *J. Am. Chem. Soc.* **2010**, *132*, 16756–16758; e) D. Spasyuk, S. Smith, D. G. Gusev, *Angew. Chem. Int. Ed.* **2012**, *51*, 2772–2775; *Angew. Chem.* **2012**, *124*, 2826–2829; f) D. Spasyuk, C. Vincent, D. G. Gusev, *J. Am. Chem. Soc.* **2015**, *137*, 3743–3746; g) N. A. Espinosa-Jalapa, A. Kumar, G. Leitus, Y. Diskin-Posner, D. Milstein, *J. Am. Chem. Soc.* **2017**, *139*, 11722–11725; h) A. Kumar, T. Janes, N. A. Espinosa-Jalapa, D. Milstein, *Angew. Chem. Int. Ed.* **2018**, *57*, 12076–12080; *Angew. Chem.* **2018**, *130*, 12252–12256; i) V. Zubar, Y. Lebedev, L. M. Azofra, L. Cavallo, O. El-Sepelgy, M. Rueping, *Angew.*

Chemistry–A European Journal | Research Article doi.org/10.1002/chem.202202774 | Chemistry Europe European Chemical Societies Publishing

Chem. Int. Ed. **2018**, *57*, 13439–13443; *Angew. Chem.* **2018**, *130*, 13627–13631; j) U. K. Das, A. Kumar, Y. Ben-David, M. A. Iron, D. Milstein, *J. Am. Chem. Soc.* **2019**, *141*, 12962–12966.
[11] a) P. Braunstein, F. Naud, *Angew. Chem. Int. Ed.* **2001**, *40*, 680–699; *Angew. Chem.* **2001**, *113*, 702–722; b) M. Bassetti, *Eur. J. Inorg. Chem.* **2006**, *2006*, 4473–4482; c) R. Lindner, B. van den Bosch, M. Lutz, J. N. H. Reek, J. I. van der Vlugt, *Organometallics* **2011**, *30*, 499–510.
[12] a) I. Bauer, H.-J. Knölker, *Chem. Rev.* **2015**, *115*, 3170–3387; b) P. Chirik, R. Morris, *Acc. Chem. Res.* **2015**, *48*, 2495; c) G. A. Filonenko, R. van Putten, E. J. M. Hensen, E. A. Pidko, *Chem. Soc. Rev.* **2018**, *47*, 1459–1483; d) F. Kallmeier, R. Kempe, *Angew. Chem. Int. Ed.* **2018**, *57*, 46–60; *Angew. Chem.* **2018**, *130*, 48–63; e) A. Mukherjee, D. Milstein, *ACS Catal.* **2018**, *8*, 11435–11469; f) N. Gorgas, K. Kirchner, *Acc. Chem. Res.* **2018**, *51*, 1558–1569; g) W. Liu, B. Sahoo, K. Junge, M. Beller, *Acc. Chem. Res.* **2018**, *51*, 1858–1869; h) W. Ai, R. Zhong, X. Liu, Q. Liu, *Chem. Rev.* **2019**, *119*, 2876–2953.
[13] a) S. Elangovan, C. Topf, S. Fischer, H. Jiao, A. Spannenberg, W. Baumann, R. Ludwig, K. Junge, M. Beller, *J. Am. Chem. Soc.* **2016**, *138*, 8809–8814; b) F. Kallmeier, T. Irrgang, T. Dietel, R. Kempe, *Angew. Chem. Int. Ed.* **2016**, *55*, 11806–11809; *Angew. Chem.* **2016**, *128*, 11984–11988; c) M. Glatz, B. Stöger, D. Himmelbauer, L. F. Veiros, K. Kirchner, *ACS Catal.* **2018**, *8*, 4009–4016.
[14] F. Freitag, T. Irrgang, R. Kempe, *J. Am. Chem. Soc.* **2019**, *141*, 11677–11685.
[15] Y. Wang, S. Liu, H. Yang, H. Li, Y. Lan, Q. Liu, *Nat. Chem.* **2022**, *14*, 1233–1241.
[16] A. Bruneau-Voisine, D. Wang, T. Roisnel, C. Darcel, J.-B. Sortais, *Catal. Commun.* **2017**, *92*, 1–4.
[17] a) P. Ryabchuk, K. Stier, K. Junge, M. P. Chechinski, M. Beller, *J. Am. Chem. Soc.* **2019**, *141*, 16923–16929; b) A. Kaithal, C. Werle, W. Leitner, *JACS Au* **2021**, *1*, 130–136.
[18] a) V. Zubar, J. Borghs, M. Rueping, *Org. Lett.* **2020**, *22*, 3974–3978; b) C. Liu, M. Wang, Y. Xu, Y. Li, Q. Liu, *Angew. Chem. Int. Ed.* **2022**, *61*, e202202814.
[19] T. Xia, B. Spiegelberg, Z. Wei, H. Jiao, S. Tin, S. Hinze, J. G. de Vries, *Catal. Sci. Technol.* **2019**, *9*, 6327–6334.
[20] a) S. Elangovan, M. Garbe, K. Junge, H. Jiao, A. Spannenberg, M. Beller, *Angew. Chem. Int. Ed.* **2016**, *55*, 15364–15368; *Angew. Chem.* **2016**, *128*, 15590–15594; b) N. A. Espinosa-Jalapa, A. Nerush, L. J. W. Shimon, G. Leitus, L. Avram, Y. Ben-David, D. Milstein, *Chem. Eur. J.* **2017**, *23*, 5934–5938.
[21] V. Zubar, Y. Lebedev, L. M. Azofra, L. Cavallo, O. El-Sepelgy, M. Rueping, *Angew. Chem. Int. Ed.* **2018**, *57*, 13439–13443; *Angew. Chem.* **2018**, *130*, 13627–13631.
[22] a) V. Zubar, J. Sklyaruk, A. Brzozowska, M. Rueping, *Org. Lett.* **2020**, *22*, 5423–5428; b) W. Yang, I. Y. Chernyshov, R. K. A. van Schendel, M. Weber, C. Müller, G. A. Filonenko, E. A. Pidko, *Nat. Commun.* **2021**, *12*, 12; c) A. M. Krieger, V. Sinha, A. V. Kalikadien, E. A. Pidko, *Z. Anorg. Allg. Chem.* **2021**, *647*, 1486–1494; d) W. Yang, T. Y. Kalavalapalli, A. M. Krieger, T. A. Khvorost, I. Y. Chernyshov, M. Weber, E. A. Uslamin, E. A. Pidko, G. A. Filonenko, *J. Am. Chem. Soc.* **2022**, *144*, 8129–8137.
[23] a) Y. Wang, L. Zhu, Z. Shao, G. Li, Y. Lan, Q. Liu, *J. Am. Chem. Soc.* **2019**, *141*, 17337–17349; b) C. Liu, M. Wang, S. Liu, Y. Wang, Y. Peng, Y. Lan, Q. Liu, *Angew. Chem. Int. Ed.* **2021**, *60*, 5108–5113; *Angew. Chem.* **2021**, *133*, 5168–5173.
[24] V. Papa, Y. Cao, A. Spannenberg, K. Junge, M. Beller, *Nat. Catal.* **2020**, *3*, 135–142.
[25] a) K. Junge, B. Wendt, F. A. Westerhaus, A. Spannenberg, H. Jiao, M. Beller, *Chem. Eur. J.* **2012**, *18*, 9011–9018; b) S. Werkmeister, K. Junge, B. Wendt, A. Spannenberg, H. Jiao, C. Bornschein, M. Beller, *Chem. Eur. J.* **2014**, *20*, 4227–4231.
[26] R. Adam, E. Alberico, W. Baumann, H.-J. Drexler, R. Jackstell, H. Junge, M. Beller, *Chem. Eur. J.* **2016**, *22*, 4991–5002.
[27] **Mn-1b** was previously reported (Ref. [9], CCDC 1521775). Deposition Number(s) 2189956 (for **Mn-1a**), 2189957 (for **Mn-1c**), 2189958 (for **Mn-2b**), 2204982 (for **Mn-2a**), 2204983 (for **Mn-2c**), 2204984 (for **Mn-2a-decomp**) contain(s) the supplementary crystallographic data for this paper. These data are provided free of charge by the joint Cambridge Crystallographic Data Centre and Fachinformationszentrum Karlsruhe Access Structures service.
[28] A. Kaithal, M. Hölscher, W. Leitner, *Angew. Chem.* **2018**, *130*, 13637–13641; *Angew. Chem. Int. Ed.* **2018**, *57*, 13449–13453.
[29] Y.-N. Duan, X. Du, Z. Cui, Y. Zeng, Y. Liu, T. Yang, J. Wen, X. Zhang, *J. Am. Chem. Soc.* **2019**, *141*, 20424–20433.
[30] a) W. H. Miller, P. J. Manley, R. D. Cousins, K. F. Erhard, D. A. Heerding, C. Kwon, S. T. Ross, J. M. Samanen, D. T. Takata, I. N. Uzinskas, C. C. K. Yuan, R. C. Haltiwanger, C. J. Gress, M. W. Lark, S.-M. Hwang, I.E. James, D. J. Rieman, R. N. Willette, T.-L. Yue, L. M. Azzarano, K. L. Salyers, B. R. Smith, K. W. Ward, K. O. Johanson, W. F. Huffman, *Bioorg. Med. Chem. Lett.* **2003**, *13*, 1483–1486; b) N. A. Anderson, I. B. Campbell, B. J. Fallon, S. M. Lynn, S. J. F. Macdonald, J. M. Pritchard, P. A. Procopiou, S. L. Sollis, L. R. Thorp, *Org. Biomol. Chem.* **2016**, *14*, 5992–6009; c) P. A. Procopiou, N. A. Anderson, J. Barrett, T. M. Barrett, M. H. J. Crawford, B. J. Fallon, A. P. Hancock, J. Le, S. Lemma, R. P. Marshall, J. Morrell, J. M. Pritchard, J. E. Rowedder, P. Saklatvala, R. J. Slack, S. L. Sollis, C. J. Suckling, L. R. Thorp, G. Vitulli, S. J. F. Macdonald, *J. Med. Chem.* **2018**, *61*, 8417–8443.
[31] a) H. Grützmacher, *Angew. Chem. Int. Ed.* **2008**, *47*, 1814–1818; *Angew. Chem.* **2008**, *120*, 1838–1842; b) T. Ikariya, M. Shibasaki, *Bifunctional Molecular Catalysis (Topic in Organometallic Chemistry)*, Springer, Berlin **2011**; c) J. I. van der Vlugt, *Eur. J. Inorg. Chem.* **2012**, 363–375; d) J. R. Khusnutdinova, D. Milstein, *Angew. Chem. Int. Ed.* **2015**, *54*, 12236–12273; *Angew. Chem.* **2015**, *127*, 12406–12445; e) D. Milstein, *Phil. Trans. R. Soc. A* **2015**, *373*, 20140189.
[32] S. O. Grim, D. A. Wheatland, *Inorg. Chem.* **1969**, *8*, 1716–1719.
[33] a) M. Mastalir, M. Glatz, N. Gorgas, B. Stöger, E. Pittenauer, G. Allmaier, L. F. Veiros, K. Kirchner, *Chem. Eur. J.* **2016**, *22*, 12316–12320; b) S. Elangovan, C. Topf, S. Fischer, H. Jiao, A. Spannenberg, W. Baumann, R. Ludwig, K. Junge, M. Beller, *J. Am. Chem. Soc.* **2016**, *138*, 8809–8814; c) N. A. Espinosa-Jalapa, A. Nerush, L. J. W. Shimon, G. Leitus, L. Avram, Y. Ben-David, D. Milstein, *Chem. Eur. J.* **2017**, *23*, 5934–5938.
[34] a) M. Garbe, K. Junge, S. Walker, Z. Wei, H. Jiao, A. Spannenberg, S. Bachmann, M. Scalone, M. Beller, *Angew. Chem. Int. Ed.* **2017**, *56*, 11237–11241; *Angew. Chem.* **2017**, *129*, 11389–11393; b) Z. Wei, A. de Aguirre, K. Junge, M. Beller, H. Jiao, *Eur. J. Inorg. Chem.* **2018**, 4643–4657; c) Z. Wei, A. de Aguirre, K. Junge, M. Beller, H. Jiao, *Catal. Sci. Technol.* **2018**, *8*, 3649–366.
[35] M. Garbe, S. Budweg, V. Papa, Z. Wei, H. Hornke, S. Bachmann, M. Scalone, A. Spannenberg, H. Jiao, K. Junge, M. Beller, *Catal. Sci. Technol.* **2020**, *10*, 3994–4001.
[36] Y. Zhao, D. G. Truhlar, *J. Chem. Phys.* **2006**, *125*, 194101.
[37] M. J. Frisch, J. A. Pople, J. S. Binkley, *J. Chem. Phys.* **1984**, *80*, 3265–3269.
[38] A. V. Marenich, C. J. Cramer, D. G. Truhlar, *J. Phys. Chem. B* **2009**, *113*, 6378–6396.

Manuscript received: September 6, 2022
Accepted manuscript online: October 4, 2022
Version of record online: November 7, 2022

5.2 Applying Green Chemistry Principles to Iron Catalysis: Mild and Selective Domino Synthesis of Pyrroles from Nitroarenes

J. Fessler, K. Junge, M. Beller, *Chem. Sci.* **2023**, *14*, 11374.

DOI: https://doi.org/10.1039/D3SC02879H

Electronic supporting information is available online.

For this manuscript, I proposed the initial concept of the project and performed all the relevant experiments. This includes initial hit-finding, optimization of the reaction conditions, the preparation of the substrate scope and the isolation/characterization of the products. I wrote the first draft of the paper and the supporting information. After collaborative editing, I finalized the draft and performed the revisions after peer review. My overall contribution to this work accounts for approximately 90%.

Signature of the student (Johannes Fessler)	Signature of the supervisor (Prof. Matthias Beller)

Chemical Science

ROYAL SOCIETY OF CHEMISTRY

EDGE ARTICLE

View Article Online
View Journal

Check for updates

Cite this: DOI: 10.1039/d3sc02879h

All publication charges for this article have been paid for by the Royal Society of Chemistry

Applying green chemistry principles to iron catalysis: mild and selective domino synthesis of pyrroles from nitroarenes†

Johannes Fessler, Kathrin Junge * and Matthias Beller *

Received 6th June 2023
Accepted 2nd August 2023

DOI: 10.1039/d3sc02879h

rsc.li/chemical-science

An efficient and general cascade synthesis of pyrroles from nitroarenes using an acid-tolerant homogeneous iron catalyst is presented. Initial (transfer) hydrogenation using the commercially available iron–Tetraphos catalyst is followed by acid catalysed Paal–Knorr condensation. Both formic acid and molecular hydrogen can be used as green reductants in this process. Particularly, under transfer hydrogenation conditions, the homogeneous catalyst shows remarkable reactivity at low temperatures, high functional group tolerance and excellent chemoselectivity transforming a wide variety of substrates. Compared to classical heterogeneous catalysts, this system presents complementing reactivity, showing none of the typical side reactions such as dehalogenation, debenzylation, arene or olefin hydrogenation. It thereby enhances the chemical toolbox in terms of orthogonal reactivity. The methodology was successfully applied to the late-stage modification of multi-functional drug(-like) molecules as well as to the one-pot synthesis of the bioactive agent **BM-635**.

Introduction

25 years ago Paul Anastas and John Warner formulated the so-called green chemistry principles, in order to lead chemical development and production into a more sustainable future.[1] One of these 12 principles, catalysis, can make processes less energy intensive, faster, more selective and reduce the amount of waste compared to *e.g.* stoichiometric reagents. Within the realm of transition metal catalysis, traditionally emphasis was placed on precious metal catalysts that are in general expensive, toxic, and only present in the Earth's crust in parts per billion (ppb). Iron, however, is the 4th most abundant element in the Earth's crust and the most abundant transition metal.[2] Thus, many iron-based compounds are economical, widely available and generally accepted to have lower toxicity compared to other transition metals.[3] While heterogeneous iron catalysis has been around for over a century, giving us for example the Haber–Bosch process for the indispensable mass-production of ammonia,[4,5] homogeneous iron catalysis has been largely neglected by synthetic chemists and only been on the rise for around the last two decades.[6–9] A field that has flourished incredibly over the last years is the application of iron and its neighboring 3d-metals as catalysts for (transfer) hydrogenations.[10–22] Combining these sustainable reductive transformations with another "green" topic of increasing interest, cascade reactions (also called tandem or domino reactions), can be highly favorable since it reduces synthetic steps, which in turn can lead to further savings in time, labor, resources and generated waste.[23–27] As an example, earth-abundant catalysis has been applied to significantly improve the synthesis of N-heterocycles, which are of importance for many life science applications.[28–40]

Here, pyrroles in particular are interesting targets due to their ubiquitous presence in pharmaceuticals (atorvastatin), agrochemicals (fludioxonil), natural products (porphyrin), dyes (bodipy), materials (polypyrrole) and other fine chemicals.[41–44] Traditionally, pyrroles are prepared though the well-established Hantzsch, Knorr, or Paal–Knorr condensation reactions. Especially, the latter two approaches are still of significant interest to sustainable/process chemists today, due to their great atom-economy, high yields, easily available starting materials and benign side products (water).[45–48] Therefore, *N*-aryl pyrroles are commonly made *via* Paal–Knorr reaction of 1,4-dicarbonyl compounds with anilines, which in turn are typically obtained from the reduction of nitroarenes (Scheme 1). Since nitroarenes are widely available, it is appealing to devise a direct cascade process from nitroarenes to *N*-aryl pyrroles. While there is some precedent for reductive cascade reactions of nitro-compounds for the synthesis of heterocycles, they mostly rely on precious metals such as Rh, Ru, Pt and Pd.[49–52] Recently, a handful of groups have developed nitro reduction cascades using earth-abundant metals such as cobalt and iron.[53–55] In 2017, Zhang *et al.* showed for the first time the cascade synthesis of pyrroles from nitroarenes using a heterogeneous cobalt catalyst and

Leibniz-Institut für Katalyse e.V. (LIKAT), Albert-Einstein-Straße 29a, 18059 Rostock, Germany. E-mail: Kathrin.Junge@catalysis.de; Matthias.Beller@catalysis.de

† Electronic supplementary information (ESI) available: Experimental procedures and characterization data of isolated compounds. See DOI: https://doi.org/10.1039/d3sc02879h

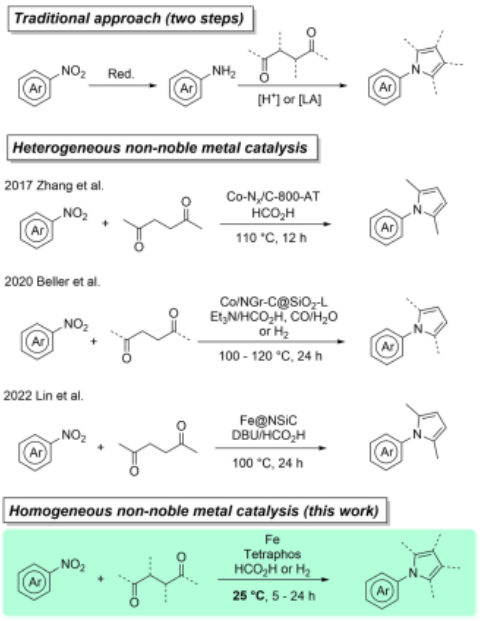

Scheme 1 State of the art in catalytic pyrrole synthesis from nitroarenes using earth-abundant (transfer) hydrogenation catalysts.

formic acid (FA) as a green reductant.[56] This methodology was extended by our group in 2020 to include molecular hydrogen and CO/H_2O mixtures as possible reductants.[57] Highlighting the current scientific interest, very recently the first heterogeneous iron catalyst for this transformation, using reductive base/formic acid mixtures, was reported by Lin *et al.*[58] All the above-mentioned methodologies have in common that they apply heterogeneous catalysts and more importantly they require relatively harsh reaction conditions (100 to 120 °C).

Results and discussion

Inspired by these earlier reports, we wondered if a more active homogeneous iron system could be developed that works under milder conditions and without additives. Furthermore, it should be stable in the presence of water and acidic conditions, which is non-trivial for homogeneous 3d metal catalysts, that tend to be more sensitive than their heavier 4/5d analogs.[6–9] With our previous expertise in iron catalysis, our first candidate of choice was the robust Fe–Tetraphos system.[59–66] Among other interesting transformations such as carbon dioxide hydrogenation or anti-Markovnikov epoxide hydrogenation, this catalytic system is known for the selective reduction of nitro groups, which represents the first step of our cascade, using both hydrogen and formic acid as reductants.[67–70] Considering that formic acid is also a potentially suitable acid catalyst for the second step of the cascade, the Paal–Knorr reaction, its dual role could be particularly desirable. With this idea in mind, we started our investigations, selecting nitrobenzene and hexane-2,5-dione as our benchmark substrates. To our delight, the standard conditions for transfer hydrogenation of nitro arenes (40 °C in EtOH for 2 h) delivered full conversion of nitrobenzene and nearly quantitative yield of the desired phenyl dimethyl pyrrole **3a** (Table 1, entry 1). Compared to the previous methods by the groups of Lin and Beller no additional base was necessary and an excellent chemoselectivity (*i.e.* no reduction of the 1,4-diketone) was observed.[57,58] Further optimization (for highlights see Table 1, full screening see ESI†) revealed that the reaction could also be conducted efficiently at room temperature when slightly extending the reaction time to 5 h (entry 5). In comparison to the previously reported heterogeneous systems, comparable or even improved yields are obtained at a quarter of the temperature and less than half the reaction time, clearly highlighting the potential of this novel catalytic process. Control reactions showed that without ligand, metal, or FA no reactivity was observed (entries 2–4). Aside from their effect on reactivity, solvents also have a large effect on the sustainability of a process, accounting for the majority of generated waste and around 60% of the energy-usage of chemical production processes.[71–76] Accordingly, different solvents were evaluated: alcohols generally showing the most promise, while ethers and

Table 1 Optimization of the reaction conditions[a]

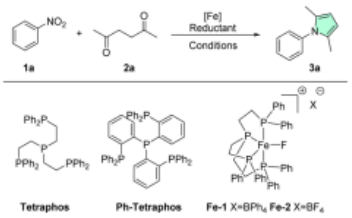

Entry	Metal salt	Ligand	Solvent	Reductant	Yield[b]
1[c]	$Fe(BF_4)_2 \cdot 6H_2O$	Tetraphos	EtOH	HCO_2H	99%
2	$Fe(BF_4)_2 \cdot 6H_2O$	—	EtOH	HCO_2H	0%
3	—	Tetraphos	EtOH	HCO_2H	0%
4	$Fe(BF_4)_2 \cdot 6H_2O$	Tetraphos	EtOH	—	0%
5	$Fe(BF_4)_2 \cdot 6H_2O$	Tetraphos	EtOH	HCO_2H	97%
6	$Fe(OTf)_2$	Tetraphos	EtOH	HCO_2H	99%
7	**Fe-1**, [Fe(Tetraphos)F][BPh_4]		EtOH	HCO_2H	24%
8	**Fe-2**, [Fe(Tetraphos)F][BF_4]		EtOH	HCO_2H	87%
9	$Fe(BF_4)_2 \cdot 6H_2O$	Tetraphos	iPrOH	HCO_2H	89%
10	$Fe(BF_4)_2 \cdot 6H_2O$	Tetraphos	THF	HCO_2H	40%
11	$Fe(BF_4)_2 \cdot 6H_2O$	Tetraphos	Dioxane	HCO_2H	25%
12	$Fe(BF_4)_2 \cdot 6H_2O$	Tetraphos	DMC	HCO_2H	47%
13	$Fe(BF_4)_2 \cdot 6H_2O$	Tetraphos	H_2O	HCO_2H	0%
14[d]	$Fe(BF_4)_2 \cdot 6H_2O$	Tetraphos	THF	H_2	16%
15[d]	$Fe(BF_4)_2 \cdot 6H_2O$	Ph–Tetraphos	THF	H_2	96%
16[e]	$Fe(BF_4)_2 \cdot 6H_2O$	Ph–Tetraphos	THF	H_2	99%

[a] General reaction conditions: 0.5 mmol **1a**, 0.6 mmol **2a**, 0.025 mmol Fe-source, 0.026 mmol ligand, 2.25 mmol FA, 2 mL solvent, 25 °C, 5 h. [b] Determined by GC-FID using *n*-hexadecane as internal standard. [c] 40 °C, 2 h. [d] 0.01 mmol Fe-source, 0.01 mmol ligand, 20 μL TFA, 20 bar, 120 °C, 2 h. [e] 0.01 mmol Fe-source, 0.01 mmol ligand, 20 μL TFA, 20 bar, 100 °C, 6 h.

carbonates gave decreased yields (entries 9–12). Although water was well tolerated in the reactions, indicated by the good reactivity of the iron tetrafluoroborate hexahydrate and the general reactivity of the reaction (generating 4 equiv. H_2O), when water was used as the sole solvent no reactivity was observed (entry 13), possibly due to solubility issues.

In the end, it was decided to proceed with ethanol as the solvent, since it gave the best performance and is considered a relatively green solvent, being biodegradable, low-toxic, and mass-produced from biorenewables.[71–78] Alternative iron sources and molecularly defined catalysts were also tested (entries 6–8). While iron triflate gave equally excellent yields, the commercial **Fe-1**, containing the tetraphenylborate anion, showed significantly reduced yield. On the other hand, the air-stable tetrafluoroborate analog **Fe-2** gave very good yield. However, since the *in situ* prepared catalyst performed the best, it was used for further reactions. Lastly, also hydrogen gas was successfully tested as a reductant for this benchmark reaction (entries 14–16). It is worth noting that to the best of our knowledge, this is the first example of an iron-based catalyst (homogeneous or heterogeneous) directly using molecular hydrogen for this cascade transformation. Substantially increased hydrogenation reactivity was observed when switching from the alkyl bridged Tetraphos ligand used for transfer hydrogenation to the more rigid and less donating phenyl-bridged variant (Ph–Tetraphos). However, more forcing reaction conditions needed to be applied (20 bar, 100–120 °C, trifluoroacetic acid (TFA) additive) as well as a more complex autoclave setup. When applying these harsh hydrogenation conditions in the upcoming substrate scope, the majority of tested examples showed decreased yields. Accordingly, we continued our investigations under the milder transfer hydrogenation conditions.

To test the general applicability of our methodology and the likely improved functional group tolerance, a substrate scope was prepared using our optimized protocol (Schemes 2 and 3). Since pyrroles are commonplace in pharmaceuticals and agrochemicals which are often complex, multifunctionalized molecules, particular focus was placed on a diversity of functional groups prevalent in bioactive molecules. Starting with the unfunctionalized benchmark substrates, phenylpyrrole **3a** was isolated in excellent yield of 91%. Next, to assess the influence of steric factors on the reaction, 2-nitrocumene with a bulky *ortho* isopropyl substituent was tested providing good yields of the corresponding pyrrole **3b**. Nitroarenes bearing the common halide substituents (fluorine **1c**, chlorine **1d**, bromine **1e**, iodine **1f**) were also converted without issues. Reductive dehalogenation, which is a side reaction frequently occurring with precious metal catalysts was never observed in our methodology.[79] Similarly, the trifluoromethyl variant **1g** gave **3g** in good yield, illustrating nicely that electron poor nitroarenes are well suited substrates. Further, remarkable chemoselectivity was observed, when converting 4-nitrostyrene **1h**, showing exclusively nitro reduction and leaving the alkene moiety intact. Additionally, it should be highlighted that polymerization of the starting material **1h** or the styrene product **3h** was also not encountered using such mild conditions. Nitroarenes bearing electron

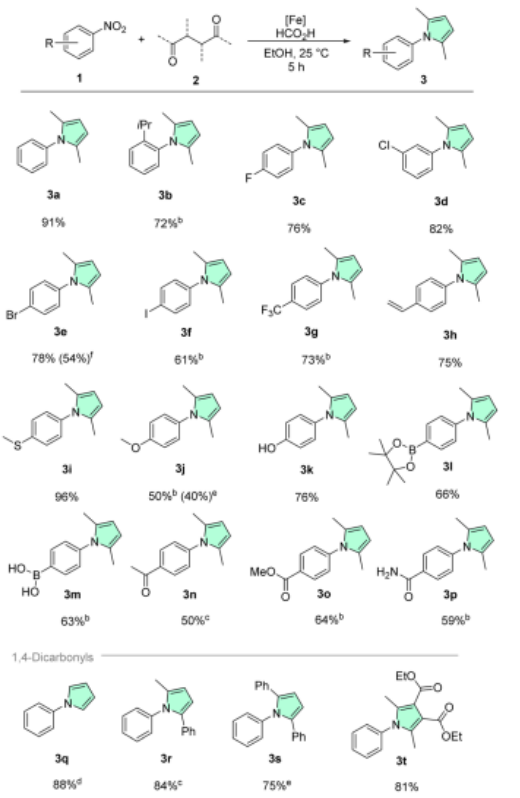

Scheme 2 Scope of nitroarenes and examples of 1,4-dicarbonyl compounds.[a] [a]General reaction conditions: 0.5 mmol 1, 0.6 mmol 2, 0.025 mmol $Fe(BF_4)_2 \cdot 6H_2O$, 0.025 mmol Tetraphos, 2.25 mmol FA, 2 mL EtOH, 25 °C, 5 h. Isolated yields are shown. [b]24 h. [c]40 °C, 24 h. [d]24 h, from 2,5-dimethoxytetrahydrofuran, after 5 h addition of 1.5 mL aq. 50% FA. [e]0.01 mmol $Fe(BF_4)_2 \cdot 6H_2O$, 0.01 mmol Ph–Tetraphos, 20 μL TFA, 1.5 mL THF, 20 bar H_2, 120 °C, 20 h. [f]0.015 mmol $Fe(BF_4)_2 \cdot 6H_2O$, 0.015 mmol Ph–Tetraphos, 20 μL TFA, 1.5 mL THF, 20 bar H_2, 120 °C, 20 h.

donating groups such as ethers (**1j**), thioethers (**1i**) and hydroxy groups (**1k**) were also smoothly converted to the respective pyrroles. Often sulfur containing compounds act as catalyst poisons for transition metal catalysts.[80–82] For instance, 4-nitrothioanisole **1i** specifically was shown to poison Pd/C in hydrogenations.[83] However, when **1i** was tested under our standard reaction conditions, it provided near quantitative isolated yield (96%) of the corresponding pyrrole **3i**. 4-Nitrophenol **1k** on the other hand is quite acidic ($pK_a(H_2O) = 7.15$), and therefore can become a problem in hydrogenations conducted under neutral or basic conditions, but again the desired product was obtained smoothly.[84] Boronic acids and pinacol boronic esters are frequently used building blocks in the fine chemical industry. Noteworthily, boronic acid **1m** and its pinacol boronate **1l** gave the corresponding pyrroles in decent

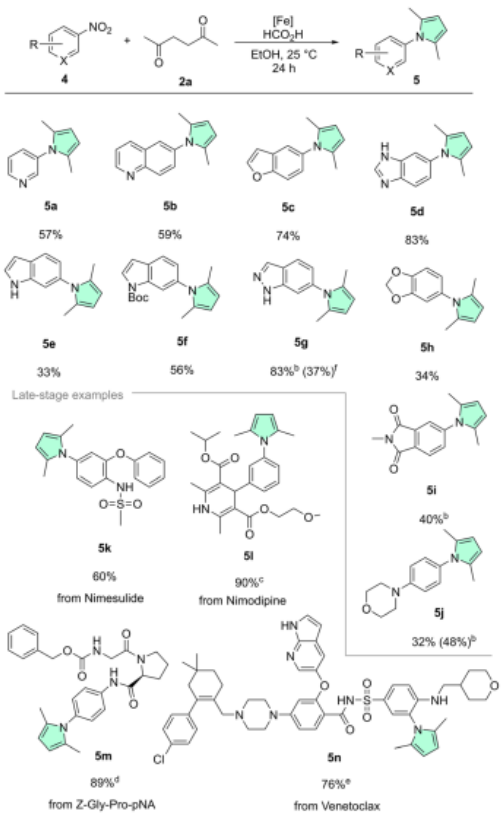

Scheme 3 Scope of heterocyclic nitro compounds and late-stage modifications.[a] [a]General reaction conditions: 0.5 mmol **4**, 0.6 mmol **2a**, 0.025 mmol $Fe(BF_4)_2 \cdot 6H_2O$, 0.026 mmol Tetraphos, 2.25 mmol FA, 2 mL EtOH, 25 °C, 24 h. Isolated yields are shown. [b]40 °C. [c]0.25 mmol scale, 5 h. [d]0.25 mmol scale. [e]0.25 mmol scale, solvent 2 mL (EtOH/toluene, 1 : 1). [f]0.01 mmol $Fe(BF_4)_2 \cdot 6H_2O$, 0.01 mmol Ph–Tetraphos, 20 μL TFA, 1.5 mL THF, 20 bar H_2, 120 °C, 20 h.

yields. Protodeboronation, a common side-reaction of organoboron compounds, was not observed in either case.[85,86] Nitroarenes containing carbonyl groups such as ketone **1n**, ester **1o**, and amide **1p** could also be converted chemoselectively. Primary amides are widely abundant not only in amino acids, vitamins, cofactors *etc.* but also in pharmaceuticals. However, their two protic hydrogens and coordination ability can pose a challenge for transition-metal catalyzed transformations and thus they are oftentimes underrepresented in the substrate scope evaluation of a given synthetic methodology. Remarkably, primary amide **1p** was well tolerated by our catalytic system. Additionally, it should be noted that no pyrrole formation on the amide nitrogen was detected.

Most of the previous reports related to the transformation discussed herein showed little variation in 1,4-dicarbonyl starting materials, we therefore wanted to demonstrate that our protocol also allows to convert different and more challenging diketones efficiently.[56–58] Starting from 2,5-dimethoxy tetrahydrofuran, unsubstituted phenyl pyrrole **3q** was isolated in 88% yield. Phenyl methyl pyrrole **3r** was obtained in very good yield from the corresponding diketone. Even the challenging dibenzoylethane **2s** could be converted with **1a** to form 1,2,5-triphenyl pyrrole **3s** in good yield when using our hydrogenation conditions. Notably, other reported catalysts only showed minimal product formation using this bulky diketone.[57] Finally, also a persubstituted pyrrole **3t** could be synthesized under mild conditions starting from 2,3,4,5-tetrasubstituted diketone **2t**.

Since further heterocycles are often prevalent in bioactive chemicals alongside pyrroles, next we extended the scope to several interesting nitro-containing heterocyclic substrates (Scheme 3, top). Basic nitrogen atoms that could potentially coordinate and thereby poison a catalyst were tolerated very well, as illustrated by 3-nitropyridine **4a**, 6-nitroquinoline **4b**, and 5-nitrobenzimidazole **4d**. Benzofuran derivative **5c** was also isolated in a good yield (74%). Surprisingly, poor conversion and yield were obtained with unprotected nitro indole **4e**. We believe that the highly electron-rich character of the indole system renders the nitro group of **4e** less electrophilic, thus slowing down the reduction. Similar trends were observed for the electron-rich benzodioxole **4h** and the morpholino derivative **4j**. To overcome this limitation, Boc-protection of the indole nitrogen, to remove some electron density from the heteroarene core, was tried. Indeed, this approach led to a significantly improved yield of the N-protected product **5f**. Boc-deprotection was only a minor pathway due to the mild conditions. Another way to tackle the reduced reactivity, in the case of **4j**, was simply to slightly increase the reaction temperature to 40 °C, which was associated with a noticeable improvement of both conversion and product yield. Corroborating our theory of electron density being the culprit, related but less electron-rich indazole **4g** provided very good yield. Finally, imide **4i** was also transformed chemoselectively. Once again, **4i** showed no signs of overreduction.

In addition to examining functional group tolerance individually, it was also important for us to test several multifunctionalized, drug(-like) substrates (Scheme 3, bottom). COX-2 inhibitor Nimesulide, notable for its acidic sulfonamide (pK_a(MeOH) = 6.46) moiety, was transformed to **5k** without problems.[87] The calcium channel blocker Nimodipine gave excellent yield, when converted to **5l** with our protocol. Remarkably, the prolyl endopeptidase probe Z-Gly-Pro-pNA was also converted in high yield, giving pyrrole-substituted dipeptide **5m**. Interestingly, the Cbz-group which would traditionally be cleaved *via* hydrogenolysis using heterogeneous catalysts such as Pd/C was left intact.[88–92] Outstandingly, our methodology was even applicable to the highly-functionalized Bcl-2 inhibitor Venetoclax **4n**, giving 76% yield of the corresponding pyrrole product **5n**, illustrating once more the striking functional group tolerance of our system.

Aside from derivatizing existing drug molecules, it is intriguing to showcase the advantages of this novel methodology for the synthesis of existing bioactive agents. Therefore, we selected **BM-635**, a pyrrole-based antitubercular agent, as

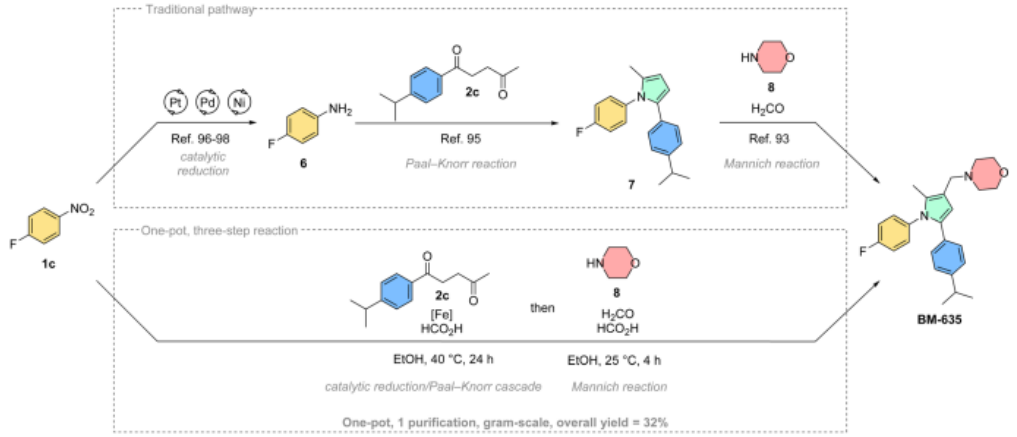

Scheme 4 Synthetic application of the Fe-catalysed domino pyrrole synthesis: traditional route to **BM-635** starting from **1c** (top), scaled-up one-pot, three-step synthesis of **BM-635** (bottom).[93–98]

a synthetic target (Scheme 4).[93,94] This compound is typically synthesized through a stepwise process centered on the Paal–Knorr reaction of 4-fluoroaniline **6** and 1,4-diketone **2c**.[95] **6** is itself traditionally synthesized by reduction of 4-fluoronitrobenzene **1c**.[96–98] Finally, the resulting Paal–Knorr pyrrole **7** is treated with formaldehyde, morpholine (**8**) and acetic acid following a Mannich protocol to give **BM-635** over 3 steps.[95] Initially, we tested our cascade methodology as a replacement for the first two steps (see ESI†). The 1,2,5-substituted pyrrole **7** was isolated with a good yield (73%), and could be further converted to **BM-635** according to the literature method.[93] However, since the final Mannich reaction is run under acidic conditions similar to our methodology, we hypothesized that the cascade reaction could potentially be expanded to include the third step of the sequence. Accordingly, we performed a one-pot, three-step reaction, where formaldehyde and morpholine were added to the reaction mixture after the complete conversion of **1c**. Using this novel multicomponent reaction approach, the practical one-pot synthesis of **BM-635** was achieved in 32% overall yield. This corresponds to a good average yield per step of 68%. The one-pot synthesis was also successfully scaled-up to gram-scale producing 1.27 g of the active ingredient in a single batch. We believe this reduction/Paal–Knorr/Mannich cascade conveniently illustrates the synthetic capabilities of our new method, quickly building up molecular complexity in a one-pot fashion. Furthermore, we consider this transformation a useful tool for combinatorial chemistry and drug discovery to potentially generate novel compound libraries from broadly available building blocks.[99,100]

Conclusions

To summarize, we have developed a cascade synthesis of pyrroles from nitroarenes for the first time using a commercially available homogeneous iron catalyst. This catalyst can be easily prepared *in situ* or used as the molecularly-defined complex. Both formic acid and molecular hydrogen can be used as green reductants in the (transfer) hydrogenation/Paal–Knorr reaction sequence. Particularly, under transfer hydrogenation conditions, the homogeneous catalyst showed remarkable reactivity at low temperatures, exceptional functional group tolerance and excellent chemoselectivity using a wide variety of substrates. This system offers a complementing reactivity to classical heterogeneous catalysts, exhibiting none of the typical side reactions such as dehalogenation, debenzylation, ketone, arene or olefin hydrogenation. The methodology thereby enhances the chemical toolbox in terms of orthogonal reactivity. Finally, the advantages of this novel protocol are highlighted by the successful late-stage modification of multifunctionalized drug(-like) molecules as well as the one-pot synthesis of the bioactive agent **BM-635** on gram-scale. Further investigations concerning a more efficient use of hydrogen gas for this cascade protocol are currently ongoing in our laboratories.

Data availability

The datasets supporting this article have been uploaded as part of the ESI.†

Author contributions

J. F. conceptualized the work, performed the investigations and the writing – original draft. K. J. and M. B. provided resources and supervision. All authors contributed to the final version of the manuscript (writing – review & editing).

Conflicts of interest

There are no conflicts to declare.

Acknowledgements

The authors thank the analytical and technical staff of the Leibniz Institute for Catalysis (LIKAT) for their service. Furthermore, the authors are grateful to Dr Pavel Ryabchuk (now Janssen Pharmaceuticals) for valuable discussions and to Dr Florian Bourriquen (now dsm-firmenich) for assistance during the preparation of the manuscript. Lastly, the State of Mecklenburg–Western Pomerania is acknowledged for generous financial support.

References

1 P. T. Anastas and J. C. Warner, *Green Chemistry: Theory and Practice*, Oxford University Press, New York, 1998.
2 P. A. Frey and G. H. Reed, *ACS Chem. Biol.*, 2012, **7**, 1477–1481.
3 K. S. Egorova and V. P. Ananikov, *Organometallics*, 2017, **36**, 4071–4090.
4 BASF AG, *Ger. Pat.*, DE235421C, 1908.
5 J. W. Erisman, M. A. Sutton, J. Galloway, Z. Klimont and W. Winiwarter, *Nat. Geosci.*, 2008, **1**, 636–639.
6 C. Bolm, J. Legros, J. Le Paih and L. Zani, *Chem. Rev.*, 2004, **104**, 6217–6254.
7 I. Bauer and H.-J. Knölker, *Chem. Rev.*, 2015, **115**, 3170–3387.
8 A. Fürstner, *ACS Cent. Sci.*, 2016, **2**, 778–789.
9 A. Guðmundsson and J.-E. Bäckvall, *Molecules*, 2020, **25**, 1349.
10 S. Gaillard and J.-L. Renaud, *ChemSusChem*, 2008, **1**, 505–509.
11 S. Enthaler, K. Junge and M. Beller, *Angew. Chem., Int. Ed.*, 2008, **47**, 3317–3321.
12 R. H. Morris, *Chem. Soc. Rev.*, 2009, **38**, 2282–2291.
13 G. Bauer and K. A. Kirchner, *Angew. Chem., Int. Ed.*, 2011, **50**, 5798–5800.
14 A. Quintard and J. Rodriguez, *Angew. Chem., Int. Ed.*, 2014, **53**, 4044–4055.
15 R. H. Morris, *Acc. Chem. Res.*, 2015, **48**, 1494–1502.
16 T. Zell and D. Milstein, *Acc. Chem. Res.*, 2015, **48**, 1979–1994.
17 Y.-Y. Li, S.-L. Yu, W.-Y. Shen and J.-X. Gao, *Acc. Chem. Res.*, 2015, **48**, 2587–2598.
18 G. A. Filonenko, R. van Putten, E. J. M. Hensen and E. A. Pidko, *Chem. Soc. Rev.*, 2018, **47**, 1459–1483.
19 T. Zell and R. Langer, *ChemCatChem*, 2018, **10**, 1930–1940.
20 D. Wei and C. Darcel, *Chem. Rev.*, 2019, **119**, 2550–2610.
21 D. Formenti, F. Ferretti, F. K. Scharnagl and M. Beller, *Chem. Rev.*, 2019, **119**, 2611–2680.
22 B. Singh, M. B. Gawande, A. D. Kute, R. S. Varma, P. Fornasiero, P. McNeice, R. V. Jagadeesh, M. Beller and R. Zbořil, *Chem. Rev.*, 2021, **121**, 13620–13697.
23 L. F. Tietze, *Chem. Rev.*, 1996, **96**, 115–136.
24 L. F. Tietze and U. Beifuss, *Angew. Chem., Int. Ed.*, 1993, **32**, 131–163.
25 K. C. Nicolaou, D. J. Edmonds and P. G. Bulger, *Angew. Chem., Int. Ed.*, 2006, **45**, 7134–7186.
26 J. Zhou, *Chem.–Asian J.*, 2010, **5**, 422–434.
27 R. Ardkhean, D. F. J. Caputo, S. M. Morrow, H. Shi, Y. Xiong and E. A. Anderson, *Chem. Soc. Rev.*, 2016, **45**, 1557–1569.
28 E. T. Hennessy and T. A. Betley, *Science*, 2013, **340**, 591–595.
29 M. Mastalir, M. Glatz, E. Pittenauer, G. Allmaier and K. Kirchner, *J. Am. Chem. Soc.*, 2016, **138**, 15543–15546.
30 T. Schwob and R. Kempe, *Angew. Chem., Int. Ed.*, 2016, **55**, 15175–15179.
31 N. Deibl and R. Kempe, *Angew. Chem., Int. Ed.*, 2017, **56**, 1663–1666.
32 R. Sreedevi, S. Saranya, K. R. Rohit and G. Anilkumar, *Adv. Synth. Catal.*, 2019, **361**, 2236–2249.
33 J. C. Borghs, L. M. Azofra, T. Biberger, O. Linnenberg, L. Cavallo, M. Rueping and O. El-Sepelgy, *ChemSusChem*, 2019, **12**, 3083–3088.
34 K. Li, L. Wei, M. Sun, B. Li, M. Liu and C. Li, *Angew. Chem., Int. Ed.*, 2021, **60**, 20204–20209.
35 M. Sohail, M. Bilal, T. Maqbool, N. Rasool, M. Ammar, S. Mahmood, A. Malik, M. Zubair and G. A. Ashraf, *Arabian J. Chem.*, 2022, **15**, 104095.
36 S. Chun, J. Ahn, R. R. Putta, S. B. Lee, D.-C. Oh and S. Hong, *J. Org. Chem.*, 2020, **85**, 15314–15324.
37 R. R. Putta, S. Chun, S. H. Choi, S. B. Lee, D.-C. Oh and S. Hong, *J. Org. Chem.*, 2020, **85**, 15396–15405.
38 R. R. Putta, S. Chun, S. B. Lee, J. Hong, D.-C. Oh and S. Hong, *RSC Adv.*, 2021, **11**, 18225–18230.
39 J. Wu and C. Darcel, *J. Org. Chem.*, 2021, **86**, 1023–1036.
40 S. Das, S. Mallick and S. De Sarkar, *J. Org. Chem.*, 2019, **84**, 12111–12119.
41 P. Daw, S. Chakraborty, J. A. Garg, Y. Ben-David and D. Milstein, *Angew. Chem., Int. Ed.*, 2016, **55**, 14373–14377.
42 T. Yan and K. Barta, *ChemSusChem*, 2016, **9**, 2321–2325.
43 F. Kallmeier, B. Dudziec, T. Irrgang and R. Kempe, *Angew. Chem., Int. Ed.*, 2017, **56**, 7261–7265.
44 B. Emayavaramban, M. Sen and B. Sundararaju, *Org. Lett.*, 2017, **19**, 6–9.
45 C. Paal, *Chem. Ber.*, 1884, **17**, 2756–2767.
46 L. Knorr, *Chem. Ber.*, 1884, **17**, 2863–2870.
47 A. Hantzsch, *Chem. Ber.*, 1890, **23**, 1474–1476.
48 B. Borah, K. D. Dwivedi and L. R. Chowhan, *RSC Adv.*, 2021, **11**, 13585–13601.
49 F. G. Cirujano, A. Leyva-Pérez, A. Corma and F. X. Llabrés i Xamena, *ChemCatChem*, 2013, **5**, 538–549.
50 S. Menuel, E. Bertaut, E. Monflier and F. Hapiot, *Dalton Trans.*, 2015, **44**, 13504–13512.
51 M. A. Fouad, F. Ferretti, D. Formenti, F. Milani and F. Ragaini, *Eur. J. Org. Chem.*, 2021, **2021**, 4876–4894.
52 T. Wagener, M. Pierau, A. Heusler and F. Glorius, *Adv. Synth. Catal.*, 2022, **364**, 3366–3371.
53 C. Bäumler and R. Kempe, *Chem.–Eur. J.*, 2018, **24**, 8989–8993.
54 T. Schwob, M. Ade and R. Kempe, *ChemSusChem*, 2019, **12**, 3013–3017.
55 H. Song, Z. Yang, C.-H. Tung and W. Wang, *ACS Catal.*, 2020, **10**, 276–281.
56 Z. Gong, Y. Lei, P. Zhou and Z. Zhang, *New J. Chem.*, 2017, **41**, 10613–10618.

57 P. Ryabchuk, T. Leischner, C. Kreyenschulte, A. Spannenberg, K. Junge and M. Beller, *Angew. Chem., Int. Ed.*, 2020, **59**, 18679–18685.
58 Y. Lin, F. Wang, E. Ren, F. Zhu, Q. Zhang and G.-P. Lu, *J. Catal.*, 2022, **416**, 39–46.
59 C. Bianchini, M. Peruzzini and F. Zanobini, *J. Organomet. Chem.*, 1988, **354**, C19–C22.
60 C. Bianchini, A. Meli, M. Peruzzini, P. Frediani, C. Bohanna, M. A. Esteruelas and L. A. Oro, *Organometallics*, 1992, **11**, 138–145.
61 C. Federsel, A. Boddien, R. Jackstell, R. Jennerjahn, P. J. Dyson, R. Scopelliti, G. Laurenczy and M. Beller, *Angew. Chem., Int. Ed.*, 2010, **49**, 9777–9780.
62 A. Boddien, D. Mellmann, F. Gärtner, R. Jackstell, H. Junge, P. J. Dyson, G. Laurenczy, R. Ludwig and M. Beller, *Science*, 2011, **333**, 1733–1736.
63 G. Wienhöfer, F. A. Westerhaus, R. V. Jagadeesh, K. Junge, H. Junge and M. Beller, *Chem. Commun.*, 2012, **48**, 4827–4829.
64 G. Wienhöfer, F. A. Westerhaus, K. Junge, R. Ludwig and M. Beller, *Chem.–Eur. J.*, 2013, **19**, 7701–7707.
65 G. Wienhöfer, F. A. Westerhaus, K. Junge and M. Beller, *J. Organomet. Chem.*, 2013, **744**, 156–159.
66 M.-C. Fu, R. Shang, Z. Huang and Y. Fu, *Synlett*, 2014, **25**, 2748–2752.
67 G. Wienhöfer, I. Sorribes, A. Boddien, F. Westerhaus, K. Junge, H. Junge, R. Llusar and M. Beller, *J. Am. Chem. Soc.*, 2011, **133**, 12875–12879.
68 C. Ziebart, C. Federsel, P. Anbarasan, R. Jackstell, W. Baumann, A. Spannenberg and M. Beller, *J. Am. Chem. Soc.*, 2012, **134**, 20701–20704.
69 G. Wienhöfer, M. Baseda-Krüger, C. Ziebart, F. A. Westerhaus, W. Baumann, R. Jackstell, K. Junge and M. Beller, *Chem. Commun.*, 2013, **49**, 9089–9091.
70 W. Liu, W. Li, A. Spannenberg, K. Junge and M. Beller, *Nat. Catal.*, 2019, **2**, 523–528.
71 K. Alfonsi, J. Colberg, P. J. Dunn, T. Fevig, S. Jennings, T. A. Johnson, H. P. Kleine, C. Knight, M. A. Nagy, D. A. Perry and M. Stefaniak, *Green Chem.*, 2008, **10**, 31–36.
72 R. K. Henderson, C. Jiménez-González, D. J. C. Constable, S. R. Alston, G. G. A. Inglis, G. Fisher, J. Sherwood, S. P. Binks and A. D. Curzons, *Green Chem.*, 2011, **13**, 854–862.
73 D. Prat, O. Pardigon, H.-W. Flemming, S. Letestu, V. Ducandas, P. Isnard, E. Guntrum, T. Senac, S. Ruisseau, P. Cruciani and P. Hosek, *Org. Process Res. Dev.*, 2013, **17**, 1517–1525.
74 D. Prat, J. Hayler and A. Wells, *Green Chem.*, 2014, **16**, 4546–4551.
75 L. J. Diorazio, D. R. J. Hose and N. K. Adlington, *Org. Process Res. Dev.*, 2016, **20**, 760–773.
76 C. J. Burrows, J. B. Harper, W. Sander and D. J. Tantillo, *J. Org. Chem.*, 2022, **87**, 1599–1601.
77 D. Jaiswal, A. P. De Souza, S. Larsen, D. S. LeBauer, F. E. Miguez, G. Sparovek, G. Bollero, M. S. Buckeridge and S. P. Long, *Nat. Clim. Change*, 2017, **7**, 788–792.
78 L. M. Rossi, J. M. R. Gallo, L. H. C. Mattoso, M. S. Buckeridge, P. Licence and D. T. Allen, *ACS Sustainable Chem. Eng.*, 2021, **9**, 4293–4295.
79 F. Alonso, I. P. Beletskaya and M. Yus, *Chem. Rev.*, 2002, **102**, 4009–4092.
80 T. Kondo and T.-a. Mitsudo, *Chem. Rev.*, 2000, **100**, 3205–3220.
81 J. K. Dunleavy, *Platinum Met. Rev.*, 2006, **50**, 110.
82 A. Kolpin, G. Jones, S. Jones, W. Zheng, J. Cookson, A. P. E. York, P. J. Collier and S. C. E. Tsang, *ACS Catal.*, 2017, **7**, 592–605.
83 R. Xiong, W. Ren, Z. Wang and M. Zhang, *ChemCatChem*, 2021, **13**, 548–552.
84 G. Kortüm and W. Vogel, *Dissociation Constants of Organic Acids in Aqueous Solution*, Butterworths, London, 1961.
85 H. G. Kuivila and K. V. Nahabedian, *J. Am. Chem. Soc.*, 1961, **83**, 2159–2163.
86 P. A. Cox, A. G. Leach, A. D. Campbell and G. C. Lloyd-Jones, *J. Am. Chem. Soc.*, 2016, **138**, 9145–9157.
87 P. R. B. Fallavena and E. E. S. Schapoval, *Int. J. Pharm.*, 1997, **158**, 109–112.
88 G. S. Vanier, *Synlett*, 2007, **2007**, 0131–0135.
89 P. K. Mandal and J. S. McMurray, *J. Org. Chem.*, 2007, **72**, 6599–6601.
90 F.-X. Felpin and E. Fouquet, *Chem.–Eur. J.*, 2010, **16**, 12440–12445.
91 P. R. Sultane, T. B. Mete and R. G. Bhat, *Tetrahedron Lett.*, 2015, **56**, 2067–2070.
92 S. Lange, D. Formenti, H. Lund, C. Kreyenschulte, G. Agostini, S. Bartling, S. Bachmann, M. Scalone, K. Junge and M. Beller, *ACS Sustainable Chem. Eng.*, 2019, **7**, 17107–17113.
93 G. Poce, R. H. Bates, S. Alfonso, M. Cocozza, G. C. Porretta, L. Ballell, J. Rullas, F. Ortega, A. De Logu, E. Agus, V. La Rosa, M. R. Pasca, E. De Rossi, B. Wae, S. G. Franzblau, F. Manetti, M. Botta and M. Biava, *PLoS One*, 2013, **8**, e56980.
94 G. Poce, S. Consalvi, M. Cocozza, R. Fernandez-Menendez, R. H. Bates, F. O. Muro, D. B. Aguirre, L. Ballell and M. Biava, *Eur. J. Pharm. Sci.*, 2017, **99**, 17–23.
95 M. Biava, G. C. Porretta, G. Poce, A. De Logu, M. Saddi, R. Meleddu, F. Manetti, E. De Rossi and M. Botta, *J. Med. Chem.*, 2008, **51**, 3644–3648.
96 C. Lu, Q. Zhu, X. Zhang, H. Ji, Y. Zhou, H. Wang, Q. Liu, J. Nie, W. Han and X. Li, *ACS Sustainable Chem. Eng.*, 2019, **7**, 8542–8553.
97 X. Deng, B. Qin, R. Liu, X. Qin, W. Dai, G. Wu, N. Guan, D. Ma and L. Li, *J. Am. Chem. Soc.*, 2021, **143**, 20898–20906.
98 L. Huang, F. Tang, F. Hao, H. Zhao, W. Liu, Y. Lv, P. Liu, W. Xiong and H. Luo, *ACS Sustainable Chem. Eng.*, 2022, **10**, 2947–2959.
99 E. M. Gordon, M. A. Gallop and D. V. Patel, *Acc. Chem. Res.*, 1996, **29**, 144–154.
100 Á. Cores, J. Clerigué, E. Orocio-Rodríguez and J. C. Menéndez, *Pharmaceuticals*, 2022, **15**, 1009.

5.3 Cobalt-Catalyzed Reductive Etherification using Phosphine Oxide Promoters under Hydroformylation Conditions

F. G. Delolo[+], J. Fessler[+], H. Neumann, K. Junge, E. N. dos Santos, E. V. Gusevskaya, M. Beller, *Chem. Eur. J.* **2022**, *28*, e202103903.

DOI: https://doi.org/10.1002/chem.202103903

Electronic supporting information is available online.

For this manuscript, I took part in the optimization of the reaction, performed about half of the substrate scope and isolated the corresponding products. I further conducted scale-up reactions, control experiments as well as kinetic experiments. In addition, I cowrote the draft of the paper and the supporting information. I then finalized the draft and performed all the revisions after editing and peer review. Additionally, I conceptualized the cover feature relating to the article and arranged for professional graphic design. My overall contribution to this work accounts for approximately 40%.

[+] Authors contributed equally.

Signature of the student (Johannes Fessler)	Signature of the supervisor (Prof. Matthias Beller)


Chemistry
A European
Journal
Chemistry
Europe
European Chemical
Societies Publishing
Cover Feature:
E. V. Gusevskaya, M. Beller et al.
Cobalt-Catalysed Reductive Etherification Using Phosphine Oxide Promoters
under Hydroformylation Conditions
27Co
BuPO
UFMG
11/2022
WILEY-VCH

Chemistry–A European Journal | Research Article
doi.org/10.1002/chem.202103903
Chemistry Europe
European Chemical Societies Publishing

www.chemeurj.org

Cobalt-Catalysed Reductive Etherification Using Phosphine Oxide Promoters under Hydroformylation Conditions

Fábio G. Delolo+,[a, b] Johannes Fessler+,[b] Helfried Neumann,[b] Kathrin Junge,[b] Eduardo N. dos Santos,[a] Elena V. Gusevskaya,*[a] and Matthias Beller*[b]

Abstract: A phosphine-oxide-promoted, cobalt-catalysed reductive etherification using syngas as a reductant is reported. This novel methodology was successfully used to prepare a broad range of unsymmetrical ethers from various aldehydes and alcohols containing diverse functional groups, and was scaled-up to multigram scale under comparably mild conditions. Mechanistic experiments support an acetalization–hydrogenation sequence.

Introduction

Ethers are an important class of compounds for the bulk and fine chemical industries due to their wide occurrence in solvents, surfactants, liquid fuels, polymers, fragrance ingredients, and pharmaceuticals.[1] Despite the constant development of new methods for their synthesis,[1] there are still many economic, environmental and selectivity issues to be addressed. A particularly problematic subject is the preparation of unsymmetrical ethers. Their preparation via classical Williamson-type synthesis requires strongly basic conditions and leads to stoichiometric salt waste.[2] Alternatively, acid-catalysed methods typically need strongly acidic conditions and high temperatures leading to the formation of undesired side products (e.g., homocoupling, elimination) and poor functional group compatibility. Catalytic reductive etherification of carbonyl compounds with alcohols has therefore been widely investigated as a milder and more selective method for the synthesis of (un)symmetric ethers.[3] However, the use of (over)stoichiometric amounts of reducing agents such as silanes and boranes in these reductive etherifications leads to a low atom economy due to the formation of significant amounts of waste by-products.[2,3]

The use of H_2 as an atom-economical, green, and cheap reducing agent is therefore a desirable alternative. Several heterogeneous systems relying on precious metal catalyst were reported for this transformation over the years.[4] Then in 2015, Yi reported a homogeneous ruthenium-based catalytic system for reductive etherification that uses H_2 as a reducing agent (Scheme 1).[5] More recently, Soós and co-workers have designed an intricate metal-free frustrated Lewis pair (FLP)–catalysed reductive etherification with H_2.[6] The growing emphasis on sustainability in recent years has inspired the replacement of noble metal catalysts with more accessible environmentally benign 3d transition metals.[7]

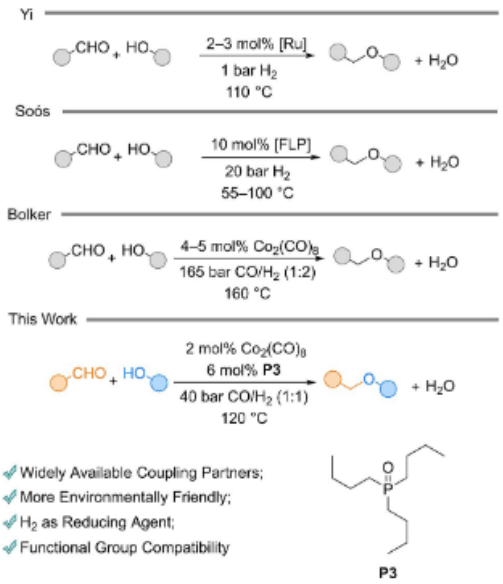

Scheme 1. Overview of the synthesis of ethers by reductive etherification with hydrogen by using homogeneous catalysts.

[a] F. G. Delolo,+ Prof. E. N. dos Santos, Prof. E. V. Gusevskaya
Departamento de Química
Universidade Federal de Minas Gerais
Av. Antônio Carlos 6627, MG 31270-901 Belo Horizonte, (Brazil)
E-mail: elena@ufmg.br

[b] F. G. Delolo,+ J. Fessler,+ Dr. H. Neumann, Dr. K. Junge, Prof. M. Beller
Leibniz-Institut für Katalyse e.V.
Albert-Einstein-Straße 29a, 18059 Rostock (Germany)
E-mail: Matthias.Beller@catalysis.de

[+] These authors contributed equally.

Supporting information for this article is available on the WWW under https://doi.org/10.1002/chem.202103903

Chemistry–A European Journal | Research Article doi.org/10.1002/chem.202103903 | Chemistry Europe European Chemical Societies Publishing

Interestingly, in 1976 Fleming and Bolker showed that the classic industrial hydroformylation catalyst $Co_2(CO)_8$ is able to reduce acetals derived from benzaldehydes to their respective ethers.[8] Unfortunately, this transformation was only used for a handful of substrates and demanded drastic conditions, specifically very high pressure (165 bar CO/H_2), which are difficult to be implemented.[8] Hence, this procedure never gained popularity among synthetic chemists. Recently, we developed a catalytic system for hydroformylation of olefins based on cobalt that operates under mild conditions. Namely, the reaction was made possible by the activation of the classic cobalt precatalyst $Co_2(CO)_8$ with phosphine oxides.[9] We therefore wondered if this promoting effect could also be observed in other cobalt-catalysed reactions. Consequently, herein we report a highly chemoselective formation of unsymmetrical ethers under comparably mild conditions using phosphine oxides as promoters in the cobalt-catalysed reductive etherification under hydroformylation conditions.

Results and Discussion

Our investigations started by screening different phosphine oxides as promoters under the following reaction conditions: benzaldehyde (**1a**; 0.5 mmol), MeOH (1.2 equiv), $Co_2(CO)_8$ (2 mol%), promoter (4 mol%), 40 bar CO/H_2 (1:1), toluene (1 mL), 100 °C, and 24 h (Table 1). First, the reaction was carried out in the absence of promoters obtaining the desired ether **3aa** in only 27% yield. Interestingly, all the phosphine oxide promoters (**P1**–**P13**) tested significantly improved the yield in a range of 36 to 62%. Although the standard triphenylphosphine oxide **P1** showed satisfactory results, it remarkably did not outperform the other promoters as in our previous study on hydroformylation.[9] The bidentate **P13** showed a promising result of **3aa** (54% yield) under the applied conditions. However, promoters containing alkyl chains (**P1**–**P7**) performed better, especially **P3** gave the desired product in 62% yield. Notably, using the non-oxidized equivalent of **P3**, tri(*n*-butyl)phosphine (PBu_3), only 2% of the desired product was detected. Using the simple and widely available **P3** as promoter, the reaction parameters such as amount of alcohol/promoter, temperature, pressure (and partial pressure), and solvent were studied (see the Supporting Information).

Table 1. Cobalt-catalysed reductive etherification of benzaldehyde (**1a**): Evaluation of different phosphine oxides.[a]

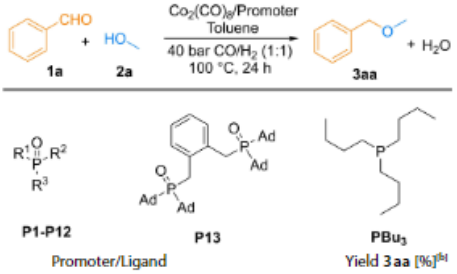

	Promoter/Ligand	Yield **3aa** [%][b]
1	none	27
2	**P1**, $R^1=R^2=R^3=$Ph	51
3	**P2**, $R^1=R^2=R^3=$Me	57
4	**P3**, $R^1=R^2=R^3=n$Bu	**62**
5	**P4** $R^1=R^2=R^3=n$Oct	59
6	**P5**, $R^1=R^2=R^3=$Cy	56
7	**P6**, $R^1=R^2=R^3=$Ad	56
8	**P7**, $R^1=$Bu, $R^2=R^3=$Ad	54
9	**P8**, $R^1=$Hex, $R^2=R^3=$Ad	54
10	**P9**, $R^1=$benzoyl, $R^2=R^3=$Ad	38
11	**P10**, $R^1=$2-naphthoyl, $R^2=R^3=$Ad	36
12	**P11**, $R^1=$2-furoyl, $R^2=R^3=$Ad	47
13	**P12**, $R^1=$2-furoyl, $R^2=R^3=$Cy	47
14	**P13**	54
15	PBu_3	2

[a] Reaction conditions: **1a** (0.5 mmol), **2a** (1.2 equiv), $Co_2(CO)_8$ (2 mol%), promoter (4 mol%), 40 bar CO/H_2 (1:1), toluene (1 mL), 100 °C, and 24 h. [b] Determined by GC analysis using isooctane or hexadecane as an internal standards.

With optimized conditions in hand (aldehyde (0.5 mmol), alcohol (2 equiv), $Co_2(CO)_8$ (2 mol%), **P3** (6 mol%), 40 bar CO/H_2 (1:1), solvent: toluene or neat alcohol (1 mL), 120 °C, and 24 h), the versatility and generality of this methodology was investigated. First, we examined the substrate scope of benzaldehyde analogues, summarized in Scheme 2. Gratifyingly, aldehydes containing electron-donating groups (EDG) or α- and β-naphthalene groups were smoothy converted to their respective ethers in good yields (73–93%). For example, products containing a OMe moiety in the *para* (**3ea**) and *ortho* (**3fa**) positions as well as the cyclic ether (**3ga**) were obtained in 79, 73, and 93% yield, respectively. In addition, substrates containing electron-withdrawing groups (EWG) such as F (**1h**), Cl (**1i**), Br (**1j**) as well as esters (**1l**) and even CF_3 (**1k**) were converted in moderate to good yields. Notably, the boronic ester analogue (**3ma**) was obtained in 89% yield without any problem regarding functional group compatibility. Double reductive etherification of dialdehyde **1n** was also possible with our protocol, giving a diether (**3na**). This process could also be applied to heterocycles that could potentially coordinate and therefore inhibit the catalyst. Furfural is well established as a bio-renewable platform chemical.[10] The etherification of this substrate is considered a green approach for the production of biofuels.[11]

Following our protocol we obtained 72% yield of its respective ether (**3oa**). The reaction with a sulfur-containing analogue also proceeded smoothly to afford the desired product (**3pa**) in 77% yield. Furthermore, a scale-up experiment was conducted with the benchmark-substrate benzaldehyde giving 7.5 g of benzyl methyl ether (**3aa**) at slightly reduced 71% yield after aqueous work-up and fractional distillation. Aliphatic aldehydes such as (**1q**) generally showed reduced reactivity in this protocol, often merely forming acetals that were not converted further.

Next, we turned our attention to evaluating different alcohol coupling partners (Scheme 3). Primary alcohols, ethanol (**2b**) and the Guerbet type alcohol (**2c**) gave 75 and 80% yield, respectively. Alcohols containing further functional groups as well as EWG were also tolerated with good product yields (**3ad** and **3ae**).

Chemistry–A European Journal | Research Article doi.org/10.1002/chem.202103903 | Chemistry Europe European Chemical Societies Publishing

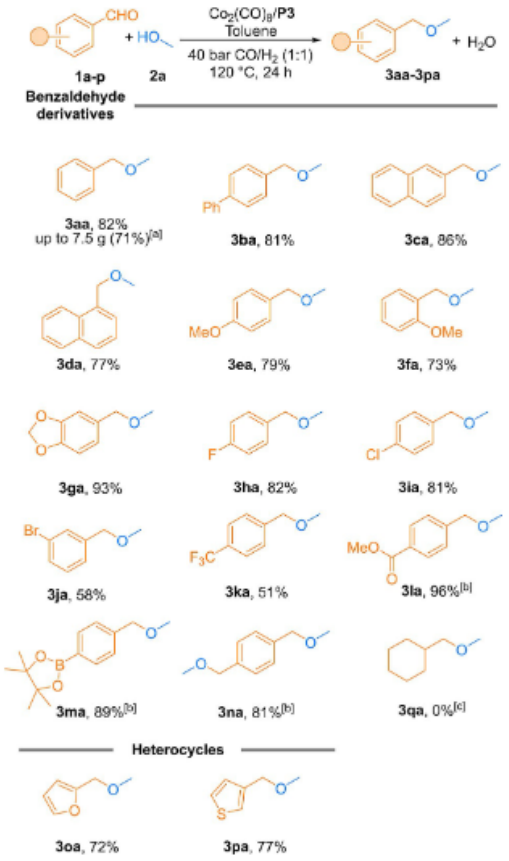

Scheme 2. Cobalt-catalysed reductive etherification: Scope of benzaldehyde analogues. Isolated yields are shown. [a] Multigram scale. [b] Neat MeOH. [c] (Dimethoxymethyl)cyclohexane is the sole isolated product.

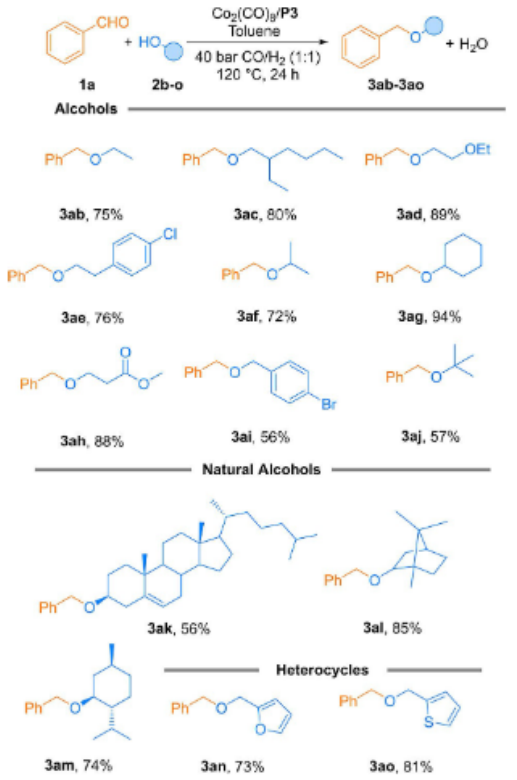

Scheme 3. Cobalt-catalysed reductive etherification: Scope of alcohols. Isolated yields are shown.

This process also showed satisfactory results for secondary and tertiary alcohol coupling partners, which are more challenging to transform in traditional pathways. Indeed, aliphatic (**2f**) as well as cyclic (**2g**) secondary alcohols were converted in 72 and 94% yield, respectively, while even the tertiary alcohol (**2j**) gave a yield of 57%. In addition, this methodology also proved to be efficient for the synthesis of unsymmetric ethers from the terpenic alcohols borneol (**3al**) and isopulegol (**3am**) as well as the steroid cholesterol (**3ak**). Alcohols containing heterocycles were converted to their respective asymmetric ethers in good yield (**3an** and **3ao**), as well.

In order to get a clearer picture of the reaction mechanism as well as the role of CO, we designed some control experiments (Scheme 4). First, the syngas components CO and H_2 were evaluated individually. Neither in the presence of CO nor H_2 alone, was the desired ether product detected. Particularly in the presence of only H_2, the formation of black cobalt nanoparticles from the decomposition of the catalytic precursor

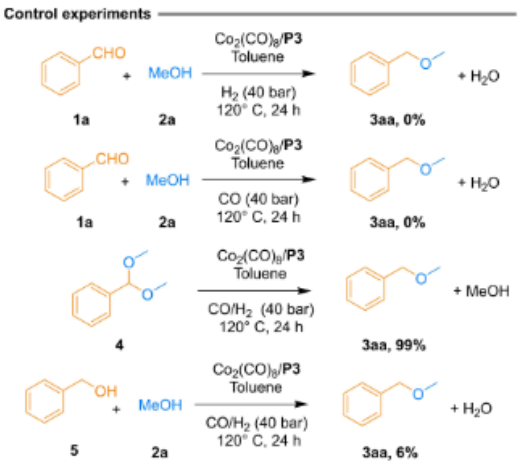

Scheme 4. Control experiments to confirm the general mechanism of the cobalt-catalysed reductive etherification.

Chemistry–A European Journal | Research Article doi.org/10.1002/chem.202103903 | Chemistry Europe European Chemical Societies Publishing

was observed, whereas in the presence of only CO, no reaction took place. These results suggest the important role of syngas (mixture of CO/H_2) for the formation and stabilization of the catalytically active species, where CO aides in the stabilization of hydrido cobalt carbonyl species ($HCo(CO)_4$, $HCo(CO)_3$), while H_2 acts as the reducing agent.[12]

The advantageous effect of the phosphine oxide is explained by its ability to transform dicobalt octacarbonyl or higher cobalt carbonyl clusters into the active monometallic catalyst.[13] In more detail, tri(*n*-butyl)phosphine oxide (**P3**) specifically was shown by Darensbourg et al. to transform cobalt carbonyl by valence disproportionation to the "highly coloured" blue oily $[(Bu_3PO)_4Co][Co(CO)_4]_2$ species.[13b] This species is also observed in our case by solid-state reaction of $Co_2(CO)_8$ and **P3**. The anion of this species $[Co(CO)_4]^-$ represents the monometallic deprotonated form our proposed active catalyst $HCo(CO)_4$. Kinetic studies in our recent work on hydroformylation using a similar system further corroborate this explanation of the phosphine oxide function by revealing a reduction of the catalytic induction period from multiple hours to mere minutes in the presence of phosphine oxides.[9]

Regarding the following reaction steps, Fleming and Bolker proposed (hemi)acetals as intermediates in this process.[8] Indeed, subjecting (dimethoxymethyl)benzene (**4**) to the optimized reductive etherification conditions gave the desired product **3aa** in almost quantitative yield. On the other hand, benzyl alcohol (**5**) afforded only 6% yield of **3aa** under the same conditions showing acid-catalysed etherification of the alcohol as only a minor reaction pathway. These results combined with the detection of acetal traces in the scale-up experiment provide further support for (hemi)acetals as reaction intermediates. Because hydrido cobalt carbonyl complexes are acidic,[14] these species likely catalyse the reversible (hemi)acetalization of aldehydes and alcohols. However, no significant build-up of (hemi)acetal species was observed throughout a kinetic follow-up reaction (Figure S1 in the Supporting Information). This suggests rapid conversion of the intermediates either in a fast direct reduction, or, more likely, via the formation of electrophilic oxocarbenium intermediates, which are then readily reduced by the cobalt catalyst to the respective ethers.[3,4,13] The latter pathway would also explain the high selectivity of this transformation for reductive etherification over the direct aldehyde hydrogenation to form alcohols. As the good hydroformylation catalyst $HCo(CO)_4$ is known to be a poor direct hydrogenation catalyst for aldehydes, highly electrophilic oxocarbenium intermediates would likely be hydrogenated preferentially.

Conclusion

In summary, we have shown that phosphine oxides, especially tri(*n*-butyl)phosphine oxide (**P3**), can be used to promote the cobalt-catalysed synthesis of unsymmetrical ethers from aldehydes and alcohols under comparably mild conditions. This non-noble-metal-catalysed process employs syngas as both a stabilizing agent of the active catalytic species and a reducing agent. It proved to be efficient for a broad range of aromatic aldehydes and alcohol coupling partners (primary, secondary, and tertiary alcohols). In addition, this methodology presented a good functional group tolerance and can be applied to natural alcohols. As this process uses syngas, it could potentially be used in the same industrial facilities employed for olefin hydroformylation.

Experimental Section

General procedure: In a typical catalytic experiment, a 4 mL glass vial containing a stir bar was sequentially charged with $Co_2(CO)_8$ (2.0 mol%), phosphine oxide (6.0 mol%), toluene (1 mL) and substrate (0.5 mmol) under argon (glove box). Afterwards, the reaction vial was capped with a septum cap, removed from the glovebox, and the alcohol (1.0 mmol or 1 mL instead of the toluene solvent) was introduced through the septum. The vial was then set in an alloy plate, which was then placed into an argon flushed 300 mL autoclave and the septum cap was pierced with a syringe needle to allow free gas flow. The reactor was closed, attached to a gas line, and the gas line was purged with nitrogen (2×) and syngas (3×, ~20 bar, 1:1 H_2/CO). The autoclave was then pressurized to 40 bar of syngas and heated to 120 °C for 24 h inside an aluminium block. At the end of the reaction, the autoclave was placed into an ice bath to cool down and stop the reaction. Finally, the pressure was carefully released, the reactor flushed with argon and opened. The reaction mixture was analysed by GC using isooctane or hexadecane as internal standards. Isolated products were obtained by directly submitting the reaction solution to silica gel column chromatography.

Acknowledgements

The authors are grateful for financial support from CNPq, FAPEMIG, INCT-Catálise (Brazil), Coordenacão de Aperfeiçoamento de Pessoal de Nível Superior (CAPES) – Finance Code 001 (88887.364603/2019-00) as well as the State of Mecklenburg–Western Pomerania. The authors thank the analytical staff of the Leibniz Institute for Catalysis, Rostock, especially Sandra Leiminger for their excellent service. Open Access funding enabled and organized by Projekt DEAL.

Conflict of Interest

The authors declare no conflict of interest.

Data Availability Statement

The data that support the findings of this study are available in the supplementary material of this article.

Keywords: base-metal catalysis · cobalt · etherification · hydrogenation · phosphine oxides

Chemistry–A European Journal | Research Article doi.org/10.1002/chem.202103903 | Chemistry Europe European Chemical Societies Publishing

[1] a) T. Tsubogo, F. Okamura, A. Omori, H. Uchiro, *ChemistrySelect* **2021**, *6*, 4224–4228; b) A. R. Rivero, P. Fodran, A. Ondrejková, C.-J. Wallentin, *Org. Lett.* **2020**, *22*, 8436–8440; c) U. Mondal, G. D. Yadav, *J. CO2 Util.* **2019**, *32*, 299–320; d) O. I. Awad, R. Mamat, O. M. Ali, N. A. C. Sidik, T. Yusaf, K. Kadirgama, M. Kettner, *Renewable Sustainable Energy Rev.* **2018**, *82*, 2586–2605; e) G. Rossi, P. F. J. Fuchs, J. Barnoud, L. Monticelli, *J. Phys. Chem. B* **2012**, *116*, 14353–14362; f) H. Hügel, B. Drevermann, A. Lingham, P. Marriott, *Chem. Biodiversity* **2008**, *5*, 1034–1044; g) S. T. Iacono, S. M. Budy, J. Jin, D. W. Smith, *J. Polym. Sci. Part A* **2007**, *45*, 5705–5721.

[2] a) J. Xiang, M. Shang, Y. Kawamata, H. Lundberg, S. H. Reisberg, M. Chen, P. Mykhailiuk, G. Beutner, M. R. Collins, A. Davies, M. D. Bel, G. M. Gallego, J. E. Spangler, J. Starr, S. Yang, D. G. Blackmond, P. S. Baran, *Nature* **2019**, *573*, 398–402; b) M. C. Haibach, C. Guan, D. Y. Wang, B. Li, N. Lease, A. M. Steffens, K. Krogh-Jespersen, A. S. Goldman, *J. Am. Chem. Soc.* **2013**, *135*, 15062–15070; c) E. Fuhrmann, J. Talbiersky, *Org. Process Res. Dev.* **2005**, *9*, 206–211; d) A. W. Williamson, *J. Chem. Soc.* **1852**, *4*, 229–239.

[3] a) J. E. Rorrer, A. T. Bella, F. D. Toste, *ChemSusChem* **2019**, *12*, 2835–2858; b) A. Pelosi, D. Lanari, A. Temperini, M. Curini, O. Rosati, *Adv. Synth. Catal.* **2019**, *361*, 4527–4539; c) A. Prajapati, M. Kumar, R. Thakuria, A. K. Basak, *Tetrahedron Lett.* **2019**, *60*, 150955; d) D. Wu, W. Y. Hernandez, S. Zhang, E. I. Vovk, X. Zhou, Y. Yang, A. Y. Khodakov, V. V. Ordomsky, *ACS Catal.* **2019**, *9*, 2940–2948; e) S. Rahimi, F. Panahi, M. Bahmani, N. Iranpoor, *J. Org. Chem.* **2018**, *83*, 973–979; f) C. Zhao, C. A. Sojdak, W. Myint, D. Seidel, *J. Am. Chem. Soc.* **2017**, *139*, 10224–10227; g) Y. H. Lee, B. Morandi, *Synlett* **2017**, *28*, 2425–2428; h) R. Savela, R. Leino, *Synthesis* **2015**, *47*, 1749–1760; i) N. Sakai, Y. Nonomura, R. Ikeda, T. Konakahara, *Chem. Lett.* **2013**, *42*, 489–491; j) Y.-J. Zhang, W. Dayoub, G.-R. Chen, M. Lemaire, *Tetrahedron* **2012**, *68*, 7400–7407; k) B. A. Gellert, N. Kahlcke, M. Feurer, S. Roth, *Chem. Eur. J.* **2011**, *17*, 12203–12209; l) N. Sakai, K. Nagasawa, R. Ikeda, Y. Nakaike, T. Konakahara, *Tetrahedron Lett.* **2011**, *52*, 3133–3136; m) J. S. Yadav, B. V. Subba Reddy, K. Shiva Shankar, T. Swamy, *Tetrahedron Lett.* **2010**, *51*, 46–48; n) K. Iwanami, H. Seo, Y. Tobita, T. Oriyama, *Synthesis* **2005**, *2*, 183–186; o) S. Chandrasekhar, G. Chandrashekar, B. Nagendra Babu, K. Vijeender, K. Venkatram Reddy, *Tetrahedron Lett.* **2004**, *45*, 5497–5499; p) J. Y. Baek, S. J. Lee, B. H. Han, *J. Korean Chem. Soc.* **2004**, *48*, 220–224; q) W. Makoto, N. Sonoe, M. Kaori, H. Ryoichi, M. Norikazu, *Chem. Lett.* **2002**, *31*, 248–249; r) S. H. Lee, Y. J. Park, C. M. Yoon, *Tetrahedron Lett.* **1999**, *40*, 6049–6050; s) N. Komatsu, J. Ishida, H. Suzuki, *Tetrahedron Lett.* **1997**, *38*, 7219–7222; t) M. Onaka, K. Higuchi, H. Nanami, Y. Izumi, *Bull. Chem. Soc. Jpn.* **1993**, *66*, 2638–2645; u) K. C. Nicolaou, C.-K. Hwang, D. A. Nugiel, *J. Am. Chem. Soc.* **1989**, *111*, 4136–4137; v) M. B. Sassaman, K. D. Kotian, G. K. S. Prakash, G. A. Olah, *J. Org. Chem.* **1987**, *52*, 4314–4319; w) J. M. Aizpurua, B. Lecea, C. Palomo, *Can. J. Chem.* **1986**, *64*, 2342–2347; x) G. A. Olah, T. Yamato, P. S. Iyer, G. K. S. Prakash, *J. Org. Chem.* **1986**, *51*, 2826–2828; y) J. Kato, I. Nobuharu, T. Mukaiyama, *Chem. Lett.* **1985**, *14*, 743–746; z) T. Tsunoda, M. Suzuki, R. Noyori, *Tetrahedron Lett.* **1979**, *20*, 4679–4680; aa) M. P. Doyle, C. T. West, S. J. Donnelly, C. C. McOsker, *J. Organomet. Chem.* **1976**, *117*, 129–140; ab) M. P. Doyle, C. T. West, *J. Org. Chem.* **1975**, *40*, 3835–3838; ac) M. P. Doyle, C. T. West, *J. Org. Chem.* **1975**, *40*, 3829–3834; ad) M. P. Doyle, C. T. West, *J. Org. Chem.* **1975**, *40*, 3821–3829; ae) M. P. Doyle, D. J. DeBruyn, S. J. Donnelly, D. A. Kooistra, A. A. Odubela, C. T. West, S. M. Zonnebelt, *J. Org. Chem.* **1974**, *39*, 2740–2747; af) C. T. West, S. J. Donnelly, D. A. Kooistra, M. P. Doyle, *J. Org. Chem.* **1973**, *38*, 2675–2681; ag) M. P. Doyle, D. J. DeBruyn, D. A. Kooistra, *J. Am. Chem. Soc.* **1972**, *94*, 3659–3661.

[4] a) D. Jadhav, A. M. Grippo, S. Shylesh, A. A. Gokhale, J. Redshaw, A. T. Bell, *ChemSusChem* **2017**, *10*, 2527–2533; b) L. J. Gooßen, C. Linder, *Synlett* **2006**, *20*, 3489–3491; c) Y. Fujii, H. Furugaki, S. Yano, K. Kita, *Chem. Lett.* **2000**, *29*, 926–927; d) V. Bethmont, F. Fache, M. Lemaire, *Tetrahedron Lett.* **1995**, *36*, 4235–4236; e) M. Verzele, M. Acke, M. Anteunis, *J. Chem. Soc.* **1963**, 5598–5600.

[5] a) N. Kalutharage, C. S. Yi, *Org. Lett.* **2015**, *17*, 1778–1781; b) J. Kim, D.-H. Lee, N. Kalutharage, C. S. Yi, *ACS Catal.* **2014**, *4*, 3881–3885.

[6] M. Bakos, Á. Gyömöre, A. Domján, T. Soós, *Angew. Chem. Int. Ed.* **2017**, *56*, 5217–5221; *Angew. Chem.* **2017**, *129*, 5301–5305.

[7] Selected reviews: a) R. M. Bullock, J. G. Chen, L. Gagliardi, P. J. Chirik, O. K. Farha, C. H. Hendon, C. W. Jones, J. A. Keith, J. Klosin, S. D. Minteer, R. H. Morris, A. T. Radosevich, T. B. Rauchfuss, N. A. Strotman, A. Vojvodic, T. R. Ward, J. Y. Yang, Y. Surendranath, *Science* **2020**, *369*, eabc3183; b) L. Piccirilli, D. L. J. Pinheiro, M. Nielsen, *Catalysts* **2020**, *10*, 773; c) L. Alig, M. Fritz, S. Schneider, *Chem. Rev.* **2019**, *119*, 2681–2751; d) W. Ai, R. Zhong, X. Liu, Q. Liu, *Chem. Rev.* **2019**, *119*, 2876–2953; e) T. Irrgang, R. Kempe, *Chem. Rev.* **2019**, *119*, 2524–2549; f) G. A. Filonenko, R. van Putten, E. J. M. Hensen, E. A. Pidko, *Chem. Soc. Rev.* **2018**, *47*, 1459–1483.

[8] B. I. Fleming, H. I. Bolker, *Can. J. Chem.* **1976**, *54*, 685–694.

[9] F. G. Delolo, J. Yang, H. Neumann, E. N. dos Santos, E. V. Gusevskaya, M. Beller, *ACS Sustainable Chem. Eng.* **2021**, *9*, 5148–5154.

[10] a) Y. Luo, Z. Li, X. Li, X. Liu, J. Fan, J. H. Clark, C. Hu, *Catal. Today* **2019**, *319*, 14–24; b) X. Li, P. Jia, T. Wang, *ACS Catal.* **2016**, *6*, 11, 7621–7640.

[11] a) F. Zaccheria, F. Bossola, N. Scotti, C. Evangelisti, V. Dal Santo, N. Ravasio, *Catal. Sci. Technol.* **2020**, *10*, 7502–7511; b) T. A. Natsira, S. Shimazu, *Fuel Process. Technol.* **2020**, *200*, 106308; c) D. R. Chaffey, T. E. Davies, S. H. Taylor, A. E. Graham, *ACS Sustainable Chem. Eng.* **2018**, *6*, 4996–5002; d) R. Mariscal, P. Maireles-Torres, M. Ojeda, I. Sádaba, M. López Granados, *Energy Environ. Sci.* **2016**, *9*, 1144–1189.

[12] D. M. Hood, R. A. Johnson, A. E. Carpenter, J. M. Younker, D. J. Vinyard, G. G. Stanley, *Science* **2020**, *367*, 542–548.

[13] a) F. Hebrard, P. Kalck, *Chem. Rev.* **2009**, *109*, 4272–4282; b) D. Darensbourg, M. Y. Darensbourg, N. Walker, *Inorg. Chem.* **1981**, *20*, 1918–1921; c) D. Darensbourg, N. Walker, M. Y. Darensbourg, *J. Am. Chem. Soc.* **1980**, *102*, 1213–1214.

[14] E. J. Moore, J. M. Sullivan, J. R. Norton, *J. Am. Chem. Soc.* **1986**, *108*, 2257–2263.

Manuscript received: October 29, 2021
Accepted manuscript online: January 12, 2022
Version of record online: February 10, 2022

5.4 Cobalt-Catalyzed Ring Expansion/Ring Opening of Oxetanes using Phosphine Oxides as Promoters under Hydroformylation Conditions

F. G. Delolo[+], J. Fessler[+], H. Neumann, K. Junge, E. N. dos Santos, E. V. Gusevskaya, M. Beller, *Mol. Catal.* **2022**, *530*, 112621.

DOI: https://doi.org/10.1016/j.mcat.2022.112621

Electronic supporting information is available online.

For this manuscript, I took part in the optimization of the reaction, synthesized all the starting materials (oxetanes), performed the substrate scope and isolated the corresponding products. In addition, I cowrote the draft of the paper and prepared the supporting information. Furthermore, I assisted with the editing of the manuscript before and after peer review. My overall contribution to this work accounts for approximately 35%.

[+] Authors contributed equally.

Signature of the student (Johannes Fessler)	Signature of the supervisor (Prof. Matthias Beller)

Molecular Catalysis 530 (2022) 112621

Contents lists available at ScienceDirect

Molecular Catalysis

journal homepage: www.journals.elsevier.com/molecular-catalysis

Cobalt-catalyzed ring expansion/ring opening of oxetanes using phosphine oxides as promoters under hydroformylation conditions

Fábio G. Delolo [a,b,1], Johannes Fessler [b,1], Helfried Neumann [b], Kathrin Junge [b], Eduardo N. dos Santos [a,*], Elena V. Gusevskaya [a,*], Matthias Beller [b,*]

[a] Departamento de Química, Universidade Federal de Minas Gerais, Belo Horizonte, MG 31270-901, Brazil
[b] Leibniz-Institut für Katalyse e.V., Albert-Einstein-Straße 29a, Rostock 18059, Germany

ARTICLE INFO

Keywords:
Carbonylation
Oxo process
Green solvents
γ-lactones
Alcohols
Hydrogenation

ABSTRACT

Phosphine oxides, especially tricyclohexylphosphine oxide (**P7**), promote the cobalt catalyzed carbonylative ring expansion and reductive ring opening reaction of oxetanes under syngas atmosphere. Depending on the substrate structure and the stability of the carbocation intermediate either γ-lactones or primary alcohols are obtained in moderate to excellent yields. Syngas proved to play a crucial role for the catalyst activity and its stability in this process. Green solvents with high sustainability rankings, such as dimethyl carbonate (DMC), can be used in replacement of traditional solvents. The optimized conditions for both procedures were substrate (1 mmol), $Co_2(CO)_8$ (2 mol%), DMC (2 mL), 100 °C, gas phase – CO/H_2 (1:1) 40 atm, 24 h resulting in the yields of 56–94% in the ring expansion, and 65–94% in the ring opening of oxetanes.

1. Introduction

Oxetanes are 4-membered cyclic ethers found in a variety of natural products and modern synthetic drugs. Properties such as being an excellent hydrogen-bond acceptor as well as Lewis base directly affect the pharmacological properties of compounds containing this moiety [1–6]. In organic synthesis, they have been used as versatile synthetic intermediates and precursors to prepare various heterocycles [6–11]. Many reactions employing this class of compounds are based on their ring strain. However, compared to epoxides (oxiranes), oxetanes have been much less explored in organic synthesis [12].

In general, oxetanes can be expanded to γ-lactones, which constitute another important class of compounds. Their key skeleton displays a broad range of biological and odorant properties, which makes them interesting for the fine chemicals industry [13–17]. One of the most attractive and atom-economical methods to synthesize this important moiety is the carbonylative ring expansion of oxetanes.

Nevertheless, only in 1989, Wang et al. described the first example of such processes showing the synergic effect of $Co_2(CO)_8$ and $Ru_3(CO)_{12}$ used in equimolar amounts (10 mol%) to promote this reaction under harsh conditions regarding temperature (165–190 °C), CO pressure (60 atm) and time (48 h) (Scheme 1) [18]. In 2004, Getzler et al. described the synthesis of succinic anhydrides by the carbonylation of β-lactones using a bimetallic cobalt-aluminum catalyst. The key point in their approach was the combination of the acidic activation of the epoxide followed by a nucleophilic attack of the anionic cobalt species $[Co(CO)_4]^-$. However, this report provides only a single example of the carbonylation of oxetanes [19]. In 2019, Jiang and Yoon reported a similar bimetallic cobalt-aluminum carbonylation catalyst based on heterogeneous aluminum phthalocyanines, however just one example of oxetane carbonylation was provided [20]. More recently, Tang et al. and Zheng et al. described a significantly improved protocol for such transformations and showed the important role of 1,2-dimethoxyethane (DME) in the ring expansion of oxetanes under the syngas (CO/H_2) atmosphere. In this reaction, DME acted not only as a solvent but also as a promoter for the cobalt catalyst (Scheme 1) [21,22].

Apart from the carbonylation reactions mentioned above, the ability of oxetanes to undergo a variety of ring opening transformations has led to their use for the synthesis of more complex scaffolds [23]. In this respect, the reductive ring cleavage of oxetanes offers valuable possibilities, but usually requires activation with Lewis or Brønsted acids or elevated temperatures [24]. More specifically, the reductive ring opening of 2,2-disubstituted oxetanes previously involved the use of palladium catalysts and hydrogen as a reducing agent [25–28]. In

* Corresponding authors.
E-mail addresses: nicolau@ufmg.br (E.N. dos Santos), elena@ufmg.br (E.V. Gusevskaya), Matthias.Beller@catalysis.de (M. Beller).
[1] These authors contributed equally to this work.

https://doi.org/10.1016/j.mcat.2022.112621
Received 2 April 2022; Received in revised form 10 August 2022; Accepted 13 August 2022

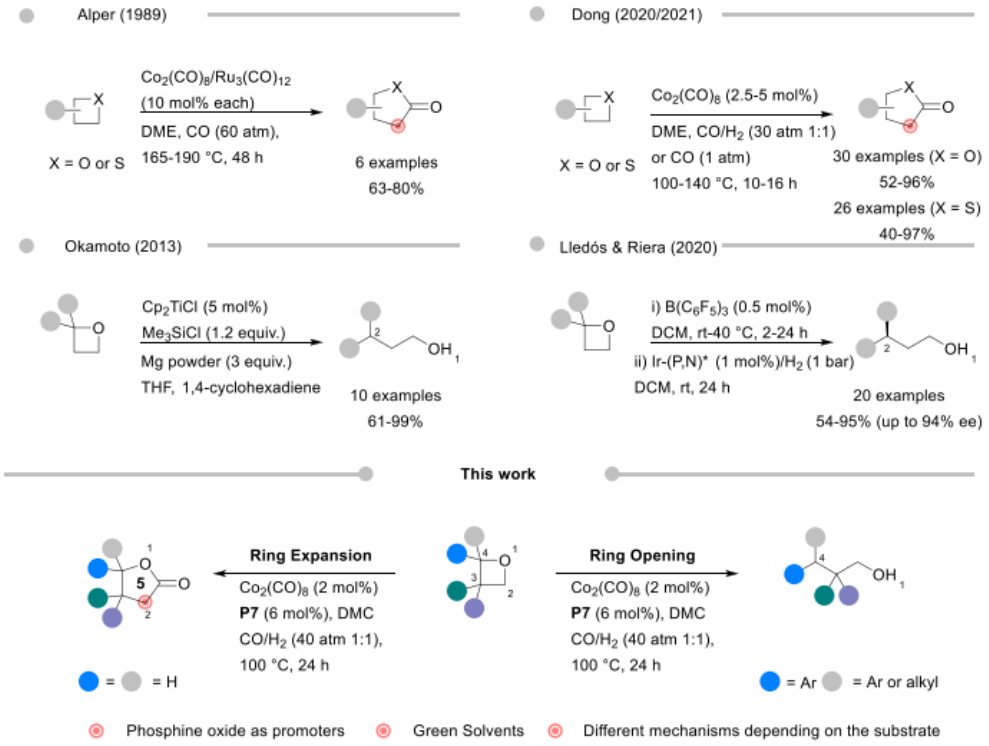

Scheme 1. Overview of the ring expansion and opening of oxetanes.

addition, in 2008, Gansäuer et al. reported the reductive ring opening of oxetanes using the Cp_2TiCl catalyst which operates through a radical mechanism [29]. In 2013, Takekoshi et al. treated a titanatrane complex with trimethylsilyl chloride and magnesium powder in tetrahydrofuran to generate a low-valent titanium species that catalyzed the radical ring opening of oxetanes to produce the corresponding alcohols (Scheme 1) [30]. Recently, Cabré et al. developed a regioselective isomerization of 2,2-disubstituted oxetanes into homoallylic alcohols using tris(pentafluorophenyl)borane ($B(C_6F_5)_3$) as the catalyst under mild conditions. The reaction was combined with a sequential iridium-catalyzed asymmetric hydrogenation to demonstrate a synthetic applicability in the preparation of γ-chiral alcohols (Scheme 1) [31].

Recently, we were able to show that the classic cobalt pre-catalyst $Co_2(CO)_8$ can be successfully applied in combination with phosphine oxides for the hydroformylation of olefins under mild conditions [32] and for the synthesis of non-symmetrical ethers from benzaldehyde derivatives and alcohols also under mild conditions [33]. Based on these works, here we report the carbonylative ring expansion and hydrogenative ring opening of oxetanes catalyzed by a combination of $Co_2(CO)_8$ as catalyst precursor and phosphine oxide as a promoter. The obtained products depend exclusively on the substrate structure. The reactions proceed under mild conditions in a syngas atmosphere and can be performed in green solvents with high rankings in modern solvent sustainability guides [34,35]. Control experiments confirmed the crucial role of both phosphine oxide and syngas in the generation and stabilization of catalytically active cobalt species.

2. Experimental

2.1. General remarks

Air- and moisture-sensitive syntheses were performed under argon atmosphere using standard Schlenk and glovebox techniques. All chemicals were purchased from Aldrich, TCI, Alfa, Fluka, Acros, or Strem and were used without further purification, unless otherwise mentioned. The solvents were collected from an SPS machine and used without any further purification. Anisole, dimethyl carbonate (DMC), and diethyl carbonate (DEC) were purchased in a Sure/Seal™ bottle and used without any further purification.

Thin layer chromatography (TLC) was performed on aluminum backed hand-cut silica plates (5 × 10 cm, pre-coated TLC sheets ALUGRAM® Xtra SIL G/UV_{254}). If necessary, phosphomolybdic acid (20 wt % in 100 mL ethanol) or potassium permanganate (1.5 g of $KMnO_4$, 10 g K_2CO_3, and 1.25 mL 10% NaOH in 200 mL water; a typical lifetime for this stain is approximately 3 months) were used as developing stains. Column chromatography was done using silica (0.035–0.070 mm, silica gel 60, Fluka Chemika). All the products were isolated by silica gel column chromatography using (pentane/ether) or (heptane/ethyl acetate) mixtures as eluents.

NMR spectra were recorded on Bruker AV 300 and 400 spectrometers. Chemicals shifts (δ) are reported in ppm downfield of tetramethylsilane. NMR spectra were treated and interpreted using MestReNova (version 14.0.1-23559). All NMR data, in the manuscript and in the Supporting Information, are expressed as chemical shift in parts per million (ppm) relative to tetramethylsilane (TMS) and attribution was

done according to the residual solvent. The multiplicity of each signal is designed as follow; s (singlet), d (doublet), t (triplet), b (broad), m (multiplet). The residual solvent signals were used as references for ^{1}H and ^{13}C NMR spectra ($CDCl_3$: $\delta H = 7.26$ ppm, $\delta C = 77.12$ ppm; DMSO-d6: $\delta H = 2.50$ ppm, $\delta C = 39.52$ ppm; CD_2Cl_2: $\delta H = 5.32$ ppm, $\delta C = 53.84$ ppm; C_6D_6: $\delta H = 7.16$ ppm, $\delta C = 128.06$ ppm;). Coupling constants (*J*) are quoted in Hz. All measurements were carried out at room temperature unless otherwise stated.

EI (Electron impact) mass spectra were recorded on a MAT 95XP spectrometer (70 eV, Thermo ELECTRON CORPORATION).

2.2. General procedure for the synthesis of oxetanes

The reactions were performed according to a well-established procedure [36–38]. In an oven dried round bottom flask, trimethylsulfoxonium iodide (5.0 equiv.) was weighted and dissolved in *t*-BuOH (7.9 mL/mmol of substrate). *t*-BuOK (5.0 equiv.) was added to the reaction mixture in 4 portions and stirred at 50 °C for 30 min resulting a white suspension. Afterward, a solution of the corresponding ketone (1.0 equiv.) in *t*-BuOH (2.0 mL/mmol of substrate) was added dropwise. The reaction mixture was heated gradually to 70 °C and stirred for 3 days (or until the reaction went to completion after TLC monitoring). Once the reaction was completed, water was added to the reaction mixture and the two resulting layers were separated. The aqueous phase was extracted with hexane (3x). Organic layers were combined, dried over anhydrous $MgSO_4$, and concentrated to dryness under vacuum. The purity of the obtained product was checked by ^{1}H NMR spectroscopy. When using epoxides as substrates only 2.0 equiv. of trimethylsulfoxonium iodide and *t*-BuOK were used (each). The obtained product was used without further purification. For the synthesis of the following compounds, 1 g of ketone was used as starting material in all cases.

2.2.1. 2,2-diphenyloxetane (4)

Pale yellow oil (1,04 g, yield 99%). TLC: $R_f = 0.54$ (5% ethyl acetate/pentane). Stains for developing TLC – phosphomolybdic acid in ethanol 20 wt%. ^{1}H NMR (300 MHz, $CDCl_3$) δ 7.58 – 7.24 (m, 10H), 4.72 (t, J = 7.7 Hz, 2H), 3.27 (t, J = 7.7 Hz, 2H). ^{13}C NMR (75 MHz, $CDCl_3$) δ 146.78, 128.29, 127.04, 124.99, 88.82, 65.41, 36.03. GC/MS: m/z (%) 210 (2), 182 (9), 181 (17), 180 (100), 179 (71), 178 (59), 176 (11), 166 (11), 165 (79), 152 (11), 105 (12), 89 (10), 77 (9). The analytical data for this compound were in excellent agreement with the reported data [39].

2.2.2. 2-methyl-2-phenyloxetane (5)

Pale yellow oil (1.3 g, 88% yield). TLC: R_f = 0.55 (pentane/ethyl acetate = 10/1). Stains for developing TLC: phosphomolybdic acid in ethanol 20 wt%. ^{1}H NMR (300 MHz, $CDCl_3$) δ 7.34 – 7.26 (m, 4H), 7.20 – 7.14 (m, 1H), 4.54 (dt, J = 8.5, 6.8, 1H), 4.44 (ddd, J = 8.7, 7.0, 5.9 Hz, 1H), 2.76 – 2.61 (m, 2H), 1.66 (s, 3H). ^{13}C NMR (75 MHz, $CDCl_3$) δ 148.24, 128.25, 126.69, 123.62, 86.61, 64.54, 35.62, 30.75. GC/MS: m/z (%) 148 (M^+, 31), 147 (9), 133 (26), 130 (8), 120 (23), 119 (11), 118 (100), 117 (96), 115 (52); 105 (95), 103 (54), 91 (31), 78 (42), 77 (40), 51 (14). The analytical data for this compound were in excellent agreement with the reported data [31].

2.3. General procedure for catalytic reactions

In a typical catalytic experiment, the reaction was performed in a 4 mL glass vial containing a stirring bar. The reaction vial was sequentially charged with $Co_2(CO)_8$ (2.0 mol%), phosphine oxide (0–16 mol%), solvent (2 mL) and substrate (1.0 mmol) under argon atmosphere (glove box). Afterward, the reaction vial was capped with a septum, pierced with a syringe needle, and set in the alloy plate, which was then placed into a 300 mL autoclave. The reactor was closed and purged with nitrogen. This was carried out two times before the same procedure was done three times with syngas (about 20 atm). After the last gas release, the autoclave was pressurized with 40 atm syngas (1:1, H_2:CO) and then heated to 80–100 °C for 24 h using an aluminum block. At the end of the reaction, the autoclave was placed into an ice bath to cool down and stop the reaction. Finally, the pressure was released, and the reactor flushed with N_2 and opened. The reaction mixture was analyzed by GC using isooctane as internal standard. The products were isolated by silica gel column chromatography (eluent: *n*-pentane/diethyl ether or *n*-heptane/ethyl acetate) for the identification by NMR and GC/MS.

2.3.1. 4,4-dimethyldihydrofuran-2(3H)-one (1b)

Colorless solid. TLC: $R_f = 0.27$ (pentane/diethyl ether = 2/1). Stains for developing TLC – $KMnO_4$. ^{1}H NMR (400 MHz, $CDCl_3$) δ 3.94 (s, 2H), 2.29 (s, 2H), 1.16 (s, 6H). ^{13}C NMR (101 MHz, $CDCl_3$) δ 177.09, 79.61, 43.09, 36.68, 25.83. GC/MS: m/z (%) 114 (M^+, 17), 99 (2), 86 (2), 70 (25), 69 (3), 56 (100), 55 (38). The analytical data for this compound were in excellent agreement with the reported data [40,41].

2.3.2. 4-ethyl-4-(hydroxymethyl)dihydrofuran-2(3H)-one (2b)

Pale yellow oil. TLC: $R_f = 0.28$ (5% MeOH/DCM). Stains for developing TLC – phosphomolybdic acid stain. ^{1}H NMR (300 MHz, $CDCl_3$) δ 4.13 (dd, J = 75.6, 9.2 Hz, 2H), 3.57 (s, 2H), 2.77 – 2.13 (m, 3H), 1.69 – 1.45 (m, 2H), 0.92 (t, J = 7.5 Hz, 3H). ^{13}C NMR (75 MHz, $CDCl_3$) δ 177.46, 74.68, 65.34, 44.89, 36.27, 27.47, 8.54. GC/MS: m/z (%) 144 (M^+, 1), 126 (1), 114 (43), 113 (12), 112 (10), 102 (74), 96 (26), 86 (13), 85 (11), 84 (43), 83 (16), 72 (10), 71 (36), 69 (35), 68 (41), 67 (31), 57 (100), 55 (29), 53 (11). The analytical data for this compound were in excellent agreement with the reported data [40,41].

2.3.3. 4-methyl-4-(hydroxymethyl)dihydrofuran-2(3H)-one (3b)

Colorless oil. TLC: $R_f = 0.26$ (5% MeOH/DCM). Stains for developing TLC – $KMnO_4$. ^{1}H NMR (300 MHz, $CDCl_3$) δ 4.24 (d, J = 9.0 Hz, 1H), 3.89 (d, J = 9.0 Hz, 1H), 3.44 (s, 3H), 2.55 (d, J = 17.5 Hz, 1H), 2.18 (d, J = 17.5 Hz, 1H), 1.12 (s, 3H). ^{13}C NMR (75 MHz, $CDCl_3$) δ 177.55, 75.98, 67.30, 41.62, 38.29, 21.54. GC/MS: m/z (%) 131 ($M+1^+$, 1), 100 (61), 88 (61), 72 (56), 71 (25), 70 (30), 69 (12), 57 (100), 56 (12), 55 (15). The analytical data for this compound were in excellent agreement with the reported data [42].

2.3.4. 3,3-diphenylpropan-1-ol (4b)

Colorless viscous oil. TLC: R_f = 0.20 (16% EtOAc/Heptane). Stains for developing TLC – $KMnO_4$. ^{1}H NMR (300 MHz, $CDCl_3$) δ 7.28 – 6.95 (m, 10H), 4.02 (t, J = 7.9 Hz, 1H), 3.46 (t, J = 6.5 Hz, 2H), 2.19 (dt, J = 7.9, 6.5 Hz, 2H), 1.81 (s, 1H). ^{13}C NMR (75 MHz, $CDCl_3$) δ 144.59, 128.59, 127.94, 126.34, 61.01, 47.38, 38.26. GC/MS: m/z (%) 212 (M^+, 9), 194 (41), 193 (20), 168 (17), 166 (15), 165 (39), 152 (21). The analytical data for this compound were in excellent agreement with the reported data [43].

2.3.5. 3-phenylbutan-1-ol (5b)

Colorless oil. TLC: Rf = 0.23 (16% EtOAc/Heptane). Stains for developing TLC – $KMnO_4$. ^{1}H NMR (300 MHz, $CDCl_3$) δ 7.30 – 6.94 (m, 5H), 3.60 – 3.27 (m, 2H), 2.79 (h, J = 7.1 Hz, 1H), 1.85 – 1.60 (m, 3H), 1.18 (d, J = 7.0 Hz, 3H). ^{13}C NMR (101 MHz, $CDCl_3$) δ 146.94, 128.52, 127.01, 126.16, 61.08, 40.96, 36.45, 22.45. GC/MS: m/z (%) 150 (M^+, 15), 132 (25), 117 (53), 106 (23), 106 (23), 103 (13), 91 (26), 79 (13), 77 (14). The analytical data for this compound were in excellent agreement with the reported data [44].

NMR spectra of all compounds are presented in the Supporting Information.

3. Results and discussion

At the start of this study, we selected 3,3-dimethyloxetane (**1a**) as a model substrate. The initial test reactions were carried out using the following conditions: $Co_2(CO)_8$ (2 mol%), promoter (4 mol%), gas-phase

Table 1
Evaluation of phosphine oxides (**P1–P7**) and their corresponding phosphines (**L1–L7**) in the carbonylation of 3,3-dimethyloxetane[a].

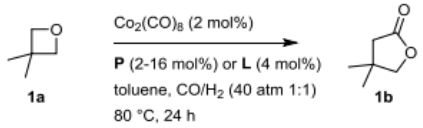

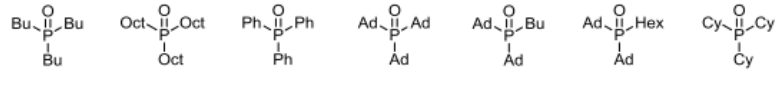

P1 **P2** **P3** **P4** **P5** **P6** **P7**

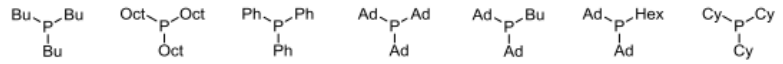

L1, yield 0% **L2**, yield 0% **L3**, yield 0% **L4**, yield 0% **L5**, yield 0% **L6**, yield 0% **L7**, yield 0%

Run	Promoter	[Promoter] (mol%)	Yield (%)[b]
1	none	-	0
2	**P1**	4	68
3	**P2**	4	75
4	**P3**	4	34
5	**P4**	4	35
6	**P5**	4	89
7	**P6**	4	90
8	**P7**	4	94
9[c]	**P7**	2	68
10[d]	**P7**	6	94
11[e]	**P7**	8	95
12[f]	**P7**	16	93

[a] Reaction conditions: **1a** (1 mmol), $Co_2(CO)_8$ (2 mol%), toluene (2 mL), 80 °C, gas phase – CO/H_2 (1:1) 40 atm, 24 h. [b] Determined by GC using isooctane as internal standard.

– CO/H_2 (1:1) 40 atm, 80 °C, 24 h, toluene solution. In the absence of promoters, the substrate remained intact even after 24 h (Table 1, run 1). Next, based on our previous results [32,33], a series of phosphine oxides **P1-P7** was chosen to facilitate the activation of $Co_2(CO)_8$. Indeed, all the phosphine oxides tested did promote the conversion of 3,3-dimethyloxetane to give γ-lactone **1b** as the main product with nearly 100% selectivity. Compound **1b** results from the expansion of the oxetane ring due to the insertion of carbon monoxide into the respective C-O bond. In the presence of aliphatic phosphine oxides **P1** and **P2** the yield of γ-lactone **1b** was 68 and 75%, respectively (Table 1, runs 2 and 3). Then, we tested triphenylphosphine oxide **P3** (Table 1, run 4), which in our previous works showed excellent performance as a promoter for the activation of the cobalt catalyst allowing to perform the hydroformylation reaction under mild conditions [32]. However, the result obtained with **P3** in the oxetane ring expansion reaction was much poorer than with its aliphatic counterparts **P1** and **P2** (37% yield vs. 68 and 75%) (Table 1, run 4). The strong acceleration effect of phosphine oxides in previous hydroformylation studies was explained by favoring the disproportionation reaction of the $Co_2(CO)_8$ pre-catalyst to give active $HCo(CO)_4$ species [32]. This process is also known to be promoted by certain Lewis bases providing larger quantities of the active species [45–47]. At this point, it is worth noting that industrially the activation of $Co_2(CO)_8$ is performed in a synthesis gas atmosphere; however, drastic conditions of temperature and pressure are required [45].

Since aliphatic groups are more electron-donating compared to phenyl groups, the Lewis basicities of **P1** and **P2** are expected to be higher than that of **P3**. For this reason, the reaction of the $Co_2(CO)_8$ disproportionation in the presence of **P1** and **P2** is expected to be more efficient, consequently resulting in a higher yield of the carbonylation product **1b**. Besides the electronic effects of substituents in the phosphine oxides, an important point to be highlighted is the steric properties of the promoters. Considering this factor, we decided to evaluate the effect of tri(1-adamanthyl)phosphine oxide (**P4**) as a promoter in the ring expansion of 3,3-dimethyloxetane. **P4** can benefit from the polarizability inherent to large hydrocarbyl groups exhibiting an electron-donating character that exceeds other alkylphosphines [48,49]. However, this promoter showed poorer results than **P1** and **P2** (Table 1, run 5 vs. runs 2 and 3). The replacement of one adamanthyl group by a butyl (**P5**) or hexyl (**P6**) group led to a significant improvement in the γ-lactone **1b** yield (up to ca. 90%) as compared to the run in the presence of **P4** (35%) (Table 1, runs 6 and 7 vs. run 5). These results are explained by the reduced bulkiness of **P5** and **P6** vs. **P4**. While cone angle determinations for phosphine oxides are rare, the widely available values of their non-oxidized phosphine counterparts may offer a rough estimation of the steric demands of corresponding phosphine oxides. To have a qualitative idea, we can consider the data for the respective phosphines: Ad_3P (**L4**, cone angle 179°) and Ad_2BuP (CataCXium®, **L5**, cone angle 176°) [50] To verify if such cone angles play a role in the promoter performance, we decided to evaluate tricyclohexyl phosphine oxide **P7**, whose unoxidized analog has a cone angle of 170°. This ligand showed the best performance allowing for a 94% yield of **1b** (Table 1, run 8). The results obtained clearly show that the steric and electronic properties of the promoter have a crucial effect in the *in situ* generation of catalytically active species from the $Co_2(CO)_8$ precursor under the

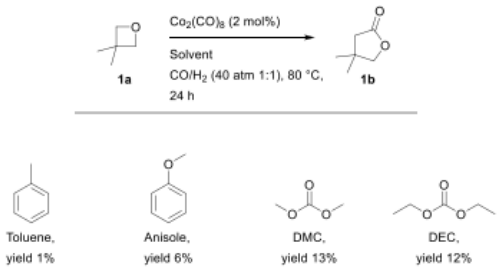

Fig. 1. Evaluation of the ability of solvents to promote the carbonylation of 3,3-dimethyloxetane (**1a**). Reaction conditions: Substrate (1 mmol), $Co_2(CO)_8$ (2 mol%), solvent (2 mL), 80 °C, gas phase – CO/H_2 (1:1) 40 atm, 24 h. The yield of γ-lactone **1b** was determined by GC using isooctane as the internal standard.

Table 2
Evaluation of solvents in the carbonylation of 3,3-dimethyloxetane in the presence of **P7**[a].

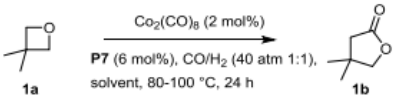

Run	Solvent	Temperature (°C)	Yield (%)[b]
1	Toluene	80	94
2	Anisole	80	89
3	DMC	80	82
4	DEC	80	91
5	THF	80	91
6	Dioxane	80	89
7	DMF	80	0
8	MeCN	80	0
9	MeOH	80	3

[a] Reaction conditions: **1a** (1 mmol), $Co_2(CO)_8$ (2 mol%), **P7** (6 mol%), solvent (2 mL), 80 °C, gas phase – CO/H_2 (1:1) 40 atm, 24 h. [b] Determined by GC using isooctane as internal standard. DMC - dimethyl carbonate; DEC - diethyl carbonate; THF - tetrahydrofuran; DMF - dimethylformamide.

syngas atmosphere.

Notably, the corresponding non-oxidized phosphines (**L1–L7**) showed no positive effect in the activation of the cobalt pre-catalyst with not even trace amounts of the carbonylation product **1b** being detected under the same conditions (Table 1). These results confirm the importance of phosphine oxide Lewis bases in the disproportionation of $Co_2(CO)_8$ [45].

Further optimization of the catalytic system was performed using **P7** as the promoter (Table 1, runs 9–12). In the next step, we determined the amount of promoter required for satisfactory catalytic activity. In the reaction with 2 mol% of **P7**, only 68% yield of the desired product **1b** was achieved (Table 1, run 9). On the other hand, when increasing the promoter amount from 4 to 6, 8, and 16 mol%, the product yield was improved only slightly (Table 1, run 10, 11, and 12 vs. run 8). Based on these results, we selected a promoter concentration of 6 mol% with respect to the substrate for further investigations.

Tang et al. showed a key role of DME to promote the carbonylation of oxetanes with the $Co_2(CO)_8$ pre-catalyst [21]. Since the solvent seems to play an important role in this reaction, we decided to evaluate some representative solvents, including green solvents recommended by modern solvent sustainability guides [34,35]. First, the reactions were performed in toluene, anisole, dimethyl carbonate (DMC), diethyl carbonate (DEC) in the absence of promoter **P7** (Fig. 1). These reactions gave only 1, 6, 13, and 12% yields of the desired product, respectively. On the other hand, the reactions in anisole, DMC, and DEC solutions containing **P7** were nearly as efficient as the reaction in toluene

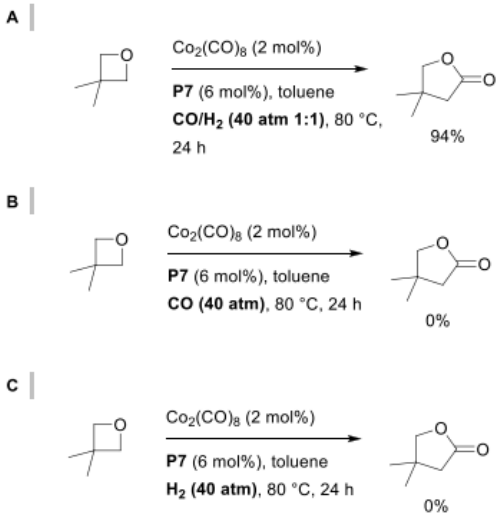

Fig. 2. Control experiments to confirm the role of CO and H_2 in the carbonylation of 3,3-dimethyloxetane.

(Table 2, runs 1–4). Despite moderate scores related to safety and environmental issues, the overall sustainability score of anisole is very high. Furthermore, DMC and DEC are exceptionally well ranked in modern solvent selection guides [34,35], comparable with those of water and ethanol, and the replacement of toluene for these greener alternatives could improve the sustainability of this process [51]. The reactions in THF as well as in dioxane also have shown excellent results; however, both these solvents are considered hazardous (Table 2, runs 5 and 6) [34,35]. Notably, solvents with high dielectric constants and polarity, such as DMF, MeCN, and MeOH, completely inhibited the activity of the cobalt catalyst (Table 2, runs 7, 8, and 9).

Next, other sources of cobalt as well as other metals were evaluated as pre-catalysts for the carbonylation of 3,3-dimethyloxetane; however, none of them promoted the formation of γ-lactone **1b** in detectable amounts (see Scheme S1, Supporting Information). In the reactions with Co(II) and Co(III) acetylacetonates, the substrate remained intact. Other metal complexes commonly used in carbonylations, based on Pd, Ir, and Rh, also did not promote the 3,3-dimethyloxetane conversion. As mentioned in the introduction, Wang et al. described the carbonylative ring expansion of oxetanes catalyzed by a mixture of $Co_2(CO)_8$ and $Ru_3(CO)_{12}$ under harsher conditions of temperature and pressure [18]. Notably, under our standard conditions, the use of these compounds either separately or in combination did not allow for a detectable yield of the desired product. The reactions with $Co_2(CO)_8$ alone or with the $Co_2(CO)_8/Ru_3(CO)_{12}$ combination were successful only in the presence of **P7**. Moreover, carbonyl complexes of other metals, such as Ru, Fe, and Mn, were not active even in the presence of **P7**. Thus, although the tested metals are commonly used as carbonylation catalysts, it seems that only $Co_2(CO)_8$ can undergo the disproportionation reaction under the applied conditions and, consequently, can catalyze the carbonylation of 3, 3-dimethyloxetane.

Next, we turned our attention to the role of syngas as carbonylation source. Several control experiments were designed and performed (Fig. 2). Although the process occurs in a syngas (mixture of CO and H_2) atmosphere, only CO is incorporated into the product molecule, whereas H_2 has no participation in the reaction stoichiometry (Fig. 2A). Remarkably, no reaction was observed in a pure CO atmosphere, i.e., without H_2 (Fig. 2B). Moreover, in the presence of only H_2, the model

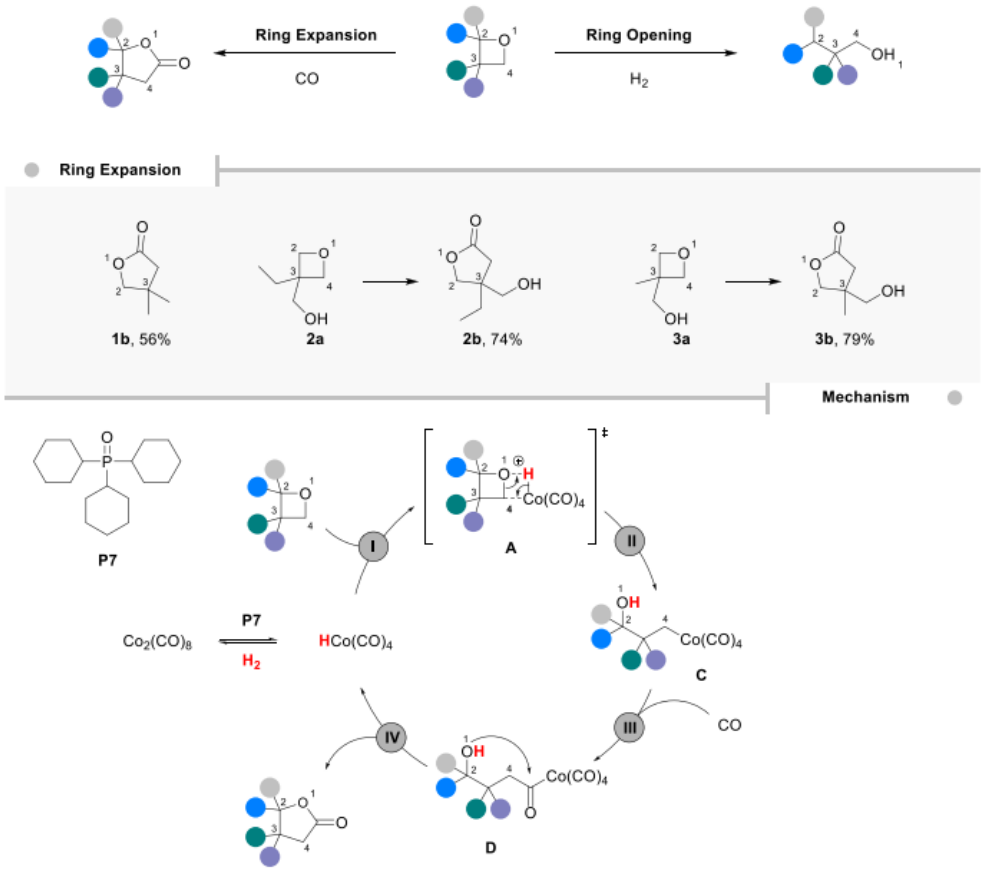

Fig. 3. Substrate scope and proposed mechanism for the cobalt-catalyzed carbonylative ring expansion of oxetanes using phosphine oxide (**P7**) as a promoter. Reaction conditions: Substrate (1 mmol), $Co_2(CO)_8$ (2 mol%), DMC (2 mL), 100 °C, gas phase – CO/H_2 (1:1) 40 atm, 24 h. Isolated yields are shown.

substrate remained intact, with the formation of black cobalt nanoparticles from the decomposition of the catalytic precursor being detected after the run (Fig. 2C). These results suggest that both CO and H_2 are important to generate the active species from the $Co_2(CO)_8$ pre-catalyst. Specifically, CO acts as a ligand for their stabilization, while H_2 provides the acidic properties which are required for the activation of oxetanes. Together, CO and H_2 ensure the formation of catalytically active species from $Co_2(CO)_8$ under mild conditions when phosphine oxides, such as **P7**, are added. The effect of the phosphine oxide in this context can be explained by its ability to convert $Co_2(CO)_8$ or higher cobalt carbonyl clusters into active monometallic species [33,52,53].

To further explore the potential of this catalytic method, we applied the optimized conditions to other substrates (Figs. 3 and 4). Using (3-ethyloxetan-3-yl)methanol (**2a**) as the substrate, the corresponding γ-lactone product **2b** was obtained in 74% yield (Fig. 3). Next, we applied the method to (3-methyloxetan-3-yl)methanol (**3a**). This substrate gave γ-lactone **3b** in 79% yield (Fig. 3).

Surprisingly, the reaction with 2,2-diphenyloxetane (**4a**) resulted in alcohol **4b** in nearly quantitative yield, instead of the corresponding γ-lactone (Fig. 4). Judging from the structure, **4b** is the product of the hydrogenative cleavage of the oxetane ring with the incorporation of two hydrogen atoms in the substrate molecule. Curious about the possibility of modulating the product outcome through the substituents present in the oxetane ring, we decided to evaluate another substrate with similar structural characteristics. Thus, we turned our attention to a 2,2-substituted oxetane containing just one aromatic substituent. A strong tendency to ring opening rather than ring expansion was also exhibited by 2-methyl-2-phenyloxetane (**5a**). The corresponding alcohol **5b** was obtained in a yield of 65% (Fig. 4).

Thus, it became clear that the nature of the substituents in the oxetane ring has a significant impact on the product outcome. The final product of the oxetane transformation under the conditions applied results in either the ring expansion/carbonylation or ring opening/hydrogenation. The proposed mechanisms for both reaction pathways are presented in Figs. 3 and 4. Both reactions depend on the acidic properties of $HCo(CO)_4$ [54], which are important for the oxetane activation. As discussed above, phosphine oxides, in particular **P7**, are supposed to promote the formation of catalytically active $HCo(CO)_4$ species from the

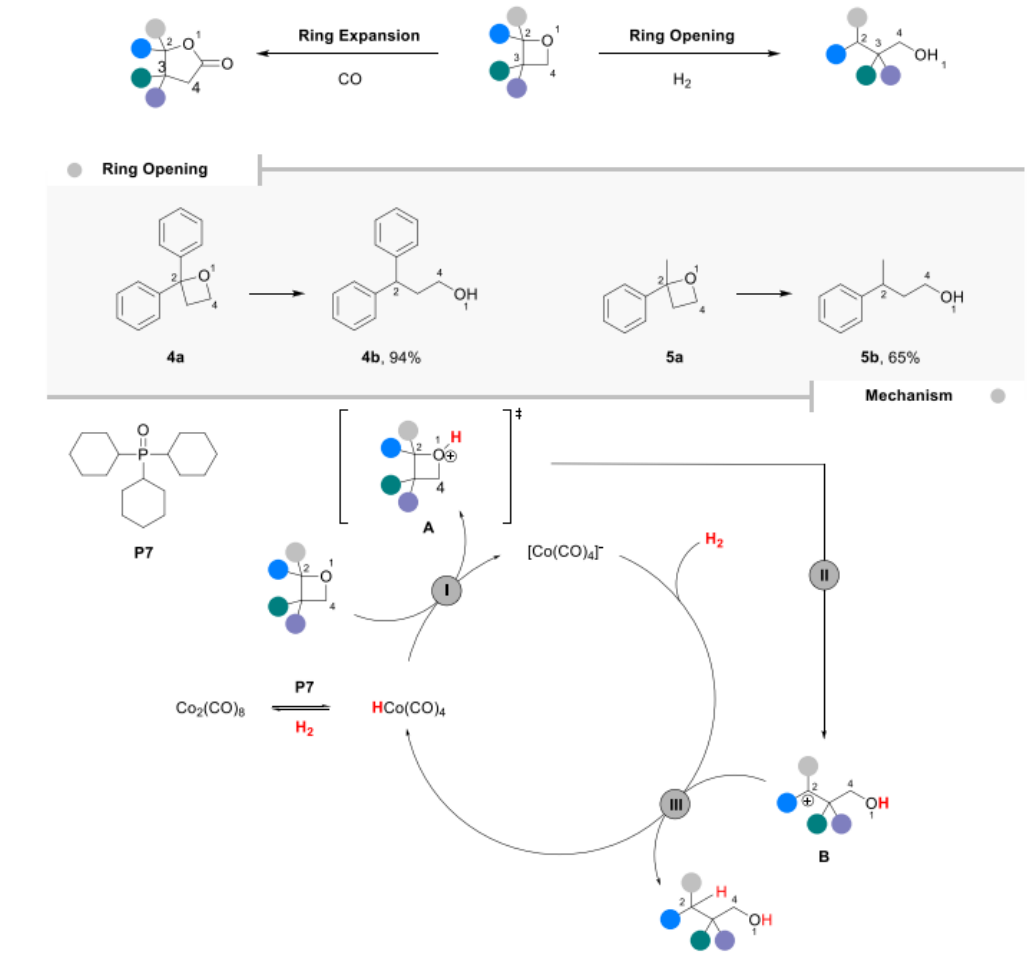

Fig. 4. Substrate scope and proposed mechanism for the cobalt-catalyzed reductive ring opening of oxetanes using phosphine oxide (**P7**) as a promoter. Reaction conditions: Substrate (1 mmol), $Co_2(CO)_8$ (2 mol%), DMC (2 mL), 100 °C, gas phase – CO/H_2 (1:1) 40 atm, 24 h. Isolated yields are shown.

$Co_2(CO)_8$ catalyst precursor under the syngas atmosphere. The further transformation of the protonated substrate (carbocation **A**) formed in step **I** is strongly affected by the nature of substituents in the oxetane ring. In the presence of stabilizing phenyl groups, the ring opening isomerization occurs to give more stable tertiary carbocation **B** (step **II**, Fig. 4), which then reacts with hydride species formed at the reaction of $Co_2(CO)_8$ with H_2 (step **III**, Fig. 4). This reaction pathway leads to the formation of the primary alcohol as the final product with the regeneration of the $HCo(CO)_4$ species.

On the other hand, when carbocation **A**, formed by the acidic activation of the oxetane, is not stable enough, it can undergo a nucleophilic attack by $[Co(CO)_4]^-$ at the less substituted α-carbon resulting in the cobalt alkyl intermediate **C** (step **II**, Fig. 3). Next, a migratory insertion of CO gives cobalt acyl intermediate **D** (step **III**). The intramolecular nucleophilic attack of the hydroxy group on the carbonyl fragment in **D** leads to the formation of the γ-lactone product and catalyst regeneration, thus completing the catalytic cycle (step **IV**). A similar mechanism was proposed by Coates et.al. for the carbonylation of epoxides [55,56].

4. Conclusions

In summary, a novel protocol for the Co-catalyzed carbonylation and hydrogenation of oxetanes is presented. For both catalytic reactions, phosphine oxides were proven to be a low-cost alternative to activate the $Co_2(CO)_8$ pre-catalyst under mild conditions and, consequently, promote efficiently the transformations of oxetanes under syngas atmosphere. Tricyclohexylphosphine oxide **P)** gave the best results as compared to other tested phosphine oxide promoters. The process sustainability was further improved by using several green solvents such as anisole, dimethyl carbonate, and diethyl carbonate. Combined with the use of phosphine oxides, the presence of syngas also helps to generate and stabilize the active catalytic species, in addition to being the carbonylating or reducing agent. The nature of substituents in the oxetane ring was found to be an important factor in this transformation, which

determines the reaction pathway leading to either the carbonylative ring expansion or the reductive ring opening reaction. This study expanded the application of $Co_2(CO)_8$ as a catalyst which operates under mild conditions and can be potentially used in existing industrial hydroformylation plants.

CRediT authorship contribution statement

Fábio G. Delolo: Investigation, Writing – original draft. **Johannes Fessler:** Investigation, Writing – original draft. **Helfried Neumann:** Supervision, Writing – review & editing. **Kathrin Junge:** Supervision, Writing – review & editing. **Eduardo N. dos Santos:** Writing – review & editing. **Elena V. Gusevskaya:** Writing – review & editing. **Matthias Beller:** Supervision, Writing – review & editing.

Declaration of Competing Interest

The authors declare that they have no known competing financial interests or personal relationships that could have appeared to influence the work reported in this paper.

Data Availability

No data was used for the research described in the article.

Acknowledgments

The authors are grateful for the financial support from Coordenação de Aperfeiçoamento de Pessoal de Nível Superior (CAPES) - Finance Code 001 (88887.364603/2019-00), CNPq, INCT-Catálise, FAPEMIG, (Brazil), as well as the State of Mecklenburg-Western Pomerania (Germany). The authors thank the analytical staff of the Leibniz Institute for Catalysis, Rostock, especially Sandra Leiminger for their excellent service.

Supplementary materials

Supplementary material associated with this article can be found, in the online version, at doi:10.1016/j.mcat.2022.112621.

References

[1] E.M. Carreira, T.C. Fessard, Four-membered ring-containing spirocycles: synthetic strategies and opportunities, Chem. Rev. 114 (16) (2014) 8257–8322, https://doi.org/10.1021/cr500127b.
[2] J.A. Burkhard, G. Wuitschik, M. Rogers-Evans, K. Müller, E.M. Carreira, Oxetanes as versatile elements in drug discovery and synthesis, Angew. Chem. Int. Ed. 49 (2010) 9052–9067, https://doi.org/10.1002/anie.200907155.
[3] M. Abe, Recent progress regarding regio-, site-, and stereoselective formation of oxetanes in Paternò-Büchi reactions, J. Chin. Chem. Soc. 55 (2008) 479–486, https://doi.org/10.1002/jccs.200800072.
[4] M. D'Auria, R. Racioppi, Oxetane synthesis through the Paternò-Büchi reaction, Molecules 18 (9) (2013) 11384–11428, https://doi.org/10.3390/molecules180911384.
[5] A. Mahal, Oxetanes as versatile building blocks in the total synthesis of natural products: an overview, Eur. J. Chem. 6 (3) (2015) 357–366, https://doi.org/10.5155/eurjchem.6.3.357-366.1267.
[6] B. Alcaide, P. Almendros, G.W. Gribble, J.A. Joule, Four-membered ring systems, in: Progress in Heterocyclic Chemistry, 23, Elsevier, New York, 2011, pp. 101–125, https://doi.org/10.1016/B978-0-08-096805-6.00004-8. Chapt. 4.
[7] C.A. Malapit, A.R. Howell, Recent applications of oxetanes in the synthesis of heterocyclic compounds, J. Org. Chem. 80 (17) (2015) 8489–8495, https://doi.org/10.1021/acs.joc.5b01255.
[8] T. Zhang, H. Zhuang, L. Tang, Z. Han, W. Guo, H. Huang, J. Sun, Catalytic enantioselective synthesis of 2,3-dihydrobenzo[*b*]oxepines via asymmetric oxetane opening by internal carbon nucleophiles, Org. Lett. 24 (1) (2022) 207–212, https://doi.org/10.1021/acs.orglett.1c03852.
[9] V.A. Bhosale, M. Nigríni, M. Dračínský, I. Císařová, J. Veselý, Enantioselective desymmetrization of 3-substituted oxetanes: an efficient access to chiral 3,4-dihydro-2*H*-1,4-benzoxazines, Org. Lett. 23 (24) (2021) 9376–9381, https://doi.org/10.1021/acs.orglett.1c03419.
[10] T. Kuri, Y. Mizukami, M. Shimogaki, M. Fujita, Oxetane Intermediate during a Direct Aldol Reaction: Stereoselective [5 + 1] Annulation Affording Tetralines, Org. Lett. 22 (19) (2020) 7613–7616, https://doi.org/10.1021/acs.orglett.0c02816.
[11] C. Ni, Y. Zhao, J. Yang, Brønsted acid ionic liquid-catalyzed ring opening of 3,3-disubstituted oxetanes in water: efficient access to furans and benzofurans, ACS Sustain. Chem. Eng. 8 (34) (2020) 12741–12745, https://doi.org/10.1021/acssuschemeng.0c05156.
[12] H. Huang, W. Yang, Z. Chen, Z. Lai, J. Sun, A mild catalytic synthesis of 2-oxazolines *via* oxetane ring-opening: rapid access to a diverse family of natural products, Chem. Sci. 10 (2019) 9586–9590, https://doi.org/10.1039/C9SC03843D.
[13] A. Ghantous, H. Gali-Muhtasib, H. Vuorela, N.A. Saliba, N. Darwiche, What made sesquiterpene lactones reach cancer clinical trials? Drug Discov. Today 15 (2010) 668–678, https://doi.org/10.1016/j.drudis.2010.06.002.
[14] Q. Song, J. Zhao, G. Zhang, F. Peruch, S. Carlotti, Ring-opening (co)polymerization of γ-butyrolactone: a review, Polym. J. 52 (2020) 3–11, https://doi.org/10.1038/s41428-019-0265-5.
[15] L.J. Gooßen, D.M. Ohlmann, M. Dierker, Silver triflate-catalysed synthesis of γ-lactones from fatty acids, Green Chem. 12 (2010) 197–200, https://doi.org/10.1039/B916853B.
[16] L.W. Ye, C. Shua, F. Gagosz, Recent progress towards transition metal-catalyzed synthesis of γ-lactams, Org. Biomol. Chem. 12 (2014) 1833–1845, https://doi.org/10.1039/C3OB42181C.
[17] T. Janecki (Ed.), Natural Lactones and Lactams: Synthesis, Occurrence and Biological Activity, Wiley-VCH, Weinheim, Germany, 2013.
[18] M.D. Wang, S. Calet, H. Alper, Regiospecific carbonylation and ring expansion of thietanes and oxetanes catalyzed by cobalt and/or ruthenium carbonyls, J. Org. Chem. 54 (1) (1989) 20–21, https://doi.org/10.1021/jo00262a010.
[19] Y.D.Y.L. Getzler, V. Kundnani, E.B. Lobkovsky, G.W. Coates, Catalytic carbonylation of β-lactones to succinic anhydrides, J. Am. Chem. Soc. 126 (22) (2004) 6842–6843, https://doi.org/10.1021/ja048946m.
[20] J. Jiang, S. Yoon, An aluminum(III) picket fence phthalocyanine-based heterogeneous catalyst for ring-expansion carbonylation of epoxides, J. Mater. Chem. A. 7 (2019) 6120–6125, https://doi.org/10.1039/C8TA11877A.
[21] Y. Tang, C. Shen, Q. Yao, X. Tian, B. Wang, K. Dong, Efficient synthesis of γ-lactones by cobalt-catalyzed carbonylative ring expansion of oxetanes under syngas atmosphere, ChemCatChem 12 (2020) 5898–5902, https://doi.org/10.1002/cctc.202001294.
[22] J. Zheng, L. Zhang, C. Shen, K. Dong, Dual roles of $Co_2(CO)_8$ enable carbonylative ring expansion of thietane under ambient CO pressure, ChemistrySelect 6 (2021) 13964, https://doi.org/10.1002/slct.202103878.
[23] J.A. Bull, R.A. Croft, O.A. Davis, R. Doran, K.F. Morgan, Oxetanes: recent advances in synthesis, reactivity, and medicinal chemistry, Chem. Rev. 116 (2016) 12150–12233, https://doi.org/10.1021/acs.chemrev.6b00274.
[24] L.G. DeRatt, E.C. Lawson, CY. Wang, S.D. Kuduk, Mild intramolecular ring opening of oxetanes, Org. Lett. 21 (23) (2019) 9642–9645, https://doi.org/10.1021/acs.orglett.9b03810.
[25] E. Kovács, A. Thurner, F. Farkas, F. Faigl, L. Hegedűs, Hydrogenolysis of *N*-protected aminooxetanes over palladium: an efficient method for a one-step ring opening and debenzylation reaction, J. Mol. Catal. A Chem. 339 (2011) 32–36, https://doi.org/10.1016/j.molcata.2011.02.008.
[26] F. Farkas, A. Thurner, E. Kovács, F. Faigl, L. Hegedűs, Hydrogenolysis of *O*-protected hydroxyoxetanes over palladium: an efficient method for a one-step ring opening and detritylation reaction, Catal. Commun. 10 (2009) 635–639, https://doi.org/10.1016/j.catcom.2008.11.007.
[27] T. Bach, H. Bergmann, H. Brummerhop, W. Lewis, K. Harms, The [2+2]-photocycloaddition of aromatic aldehydes and ketones to 3,4-dihydro-2-pyridones: regioselectivity, diastereoselectivity, and reductive ring opening of the product oxetanes, Chem. Eur. J. 7 (2001) 4512–4521, https://doi.org/10.1002/1521-3765(20011015)7:20<4512::AID-CHEM4512>3.0.CO;2-H.
[28] T. Bach, Regioselective ring opening of oxetanes by hydrogenolysis. – A convenient method for the carbohydroxylation of enol ethers, Liebigs Ann. (1995) 1045–1053, https://doi.org/10.1002/jlac.1995199506148.
[29] A. Gansäuer, N. Ndene, T. Lauterbach, J. Justicia, I. Winkler, C. Mück-Lichtenfeld, S. Grimme, Titanocene catalyzed opening of oxetanes, Tetrahedron 64 (2008) 11839–11845, https://doi.org/10.1016/j.tet.2008.08.107.
[30] N. Takekoshi, K. Miyashita, N. Shoji, S. Okamoto, Generation of a low-valent titanium species from titanatrane and its catalytic reactions: radical ring opening of oxetanes, Adv. Synth. Catal. 355 (2013) 2151–2157, https://doi.org/10.1002/adsc.201300368.
[31] A. Cabré, S. Rafael, G. Sciortino, G. Ujaque, X. Verdaguer, A. Lledós, A. Riera, Catalytic regioselective isomerization of 2,2-disubstituted oxetanes to homoallylic alcohols, Angew. Chem. Int. Ed. 59 (2020) 7521–7527, https://doi.org/10.1002/anie.201915772.
[32] F.G. Delolo, J. Yang, H. Neumann, E.N. dos Santos, E.V. Gusevskaya, M. Beller, Cobalt-catalyzed hydroformylation under mild conditions in the presence of phosphine oxides, ACS Sustain. Chem. Eng. 9 (14) (2021) 5148–5154, https://doi.org/10.1021/acssuschemeng.1c00205.
[33] F.G. Delolo, J. Fessler, H. Neumann, K. Junge, E.N. dos Santos, E.V. Gusevskaya, M. Beller, Cobalt-catalysed reductive etherification using phosphine oxide promoters under hydroformylation conditions, Chem. Eur. J. 28 (2022), https://doi.org/10.1002/chem.202103903.
[34] D. Prat, A. Wells, J. Hayler, H. Sneddon, C. Robert McElroy, S. Abou-Shehada, P. J. Dunn, CHEM21 selection guide of classical- and less classical-solvents, Green Chem. 18 (2016) 288–296, https://doi.org/10.1039/C5GC01008J.

[35] C.M. Alder, J.D. Hayler, R.K. Henderson, A.M. Redman, L. Shukla, L.E. Shuster, H. F. Sneddon, Updating and further expanding GSK's solvent sustainability guide, Green Chem. 18 (2016) 3879–3890, https://doi.org/10.1039/C6GC00611F.
[36] A. Cabré, S. Rafael, G. Sciortino, G. Ujaque, X. Verdaguer, A. Lledós, A. Riera, Catalytic regioselective isomerization of 2,2-disubstituted oxetanes to homoallylic alcohols, Angew. Chem. Int. Ed. 59 (2020) 7521–7527, https://doi.org/10.1002/anie.201915772.
[37] E.D. Butova, A.V. Barabash, A.A. Petrova, C.M. Kleiner, P.R. Schreiner, A.A. Fokin, Stereospecific consecutive epoxide ring expansion with dimethylsulfoxonium methylide, J. Org. Chem. 75 (18) (2010) 6229–6235, https://doi.org/10.1021/jo101330p.
[38] K. Okuma, Y. Tanaka, S. Kaji, H. Ohta, Reaction of dimethyloxosulfonium methylide with epoxides. Preparation of oxetanes, J. Org. Chem. 48 (25) (1983) 5133–5134, https://doi.org/10.1021/jo00173a072.
[39] W.B. Han, Y. Wu, Facile perhydrolysis of oxetanes catalyzed by molybdenum species, Org. Lett. 16 (2014) 5706–5709, https://doi.org/10.1021/ol502785u.
[40] J. Richers, M. Heilmann, M. Drees, K. Tiefenbacher, Synthesis of lactones via C–H functionalization of nonactivated C(sp^3)–H bonds, Org. Lett. 18 (2016) 6472–6475, https://doi.org/10.1021/acs.orglett.6b03371.
[41] E. Brenna, F. Distante, F.G. Gatti, G. Gatti, Substituent and catalyst effects on GAC lactonization of γ-hydroxy esters, Catal. Sci. Technol. 7 (2017) 1497–1507, https://doi.org/10.1039/C6CY02177H.
[42] Y. Li, B. Jandeleit, M.A. Gallop, N. Zerangue, P.A. Virsik, W.-N. Fischer, Internally masked neopentyl sulfonyl ester cyclization release prodrugs of acamprosate, compositions thereof, and methods of use, Patent Number US 20090099253A1.
[43] M. Orfanopoulos, I. Smonou, Selective reduction of diaryl or aryl alkyl alcohols in the presence of primary hydroxyl or ester groups by etherated boron trifluoride-triethylsilane system, Synth. Commun. 18 (1988) 833–839, https://doi.org/10.1080/00397918808057852.
[44] J.J. Wu, J.H. Cheng, J. Zhang, L. Shen, X.H. Qian, S. Cao, Non-catalytic conversion of C–F bonds of *gem*-difluoromethylene derivatives to C–H bonds with lithium aluminum hydride under room temperature, Tetrahedron 67 (2011) 285–288, https://doi.org/10.1016/j.tet.2010.11.052.
[45] F. Hebrard, P. Kalck, Cobalt-catalyzed hydroformylation of alkenes: generation and recycling of the carbonyl species, and catalytic cycle, Chem. Rev. 109 (2009) 4272–4282, https://doi.org/10.1021/cr8002533.
[46] I. Wender, H.W. Sternberg, M. Orchin, The chemistry of metal carbonyls. I. New concepts applied to carbonyls of cobalt, J. Am. Chem. Soc. 74 (5) (1952) 1216–1219, https://doi.org/10.1021/ja01125a023.
[47] I. Wender, H.W. Sternberg, M. Orchin, Evidence for cobalt hydrocarbonyl as the hydroformylation catalyst, J. Am. Chem. Soc. 75 (12) (1953) 3041–3042, https://doi.org/10.1021/ja01108a528.
[48] L. Chen, P. Ren, B.P. Carrow, Tri(1-adamantyl)phosphine: expanding the boundary of electron-releasing character available to organophosphorus compounds, J. Am. Chem. Soc. 138 (20) (2016) 6392–6395, https://doi.org/10.1021/jacs.6b03215.
[49] M.M. Rahman, H.Y. Liu, K. Eriks, A. Prock, W.P. Giering, Quantitative analysis of ligand effects. Part 3. Separation of phosphorus(III) ligands into pure .sigma.-donors and .sigma.-donor/.pi.-acceptors. Comparison of basicity and .sigma.-donicity, Organometallics 8 (1) (1989) 1–7, https://doi.org/10.1021/om00103a001.
[50] J. Jover, J. Cirera, Computational assessment on the Tolman cone angles for P-ligands, Dalton Trans. 48 (2019) 15036–15048, https://doi.org/10.1039/C9DT02876E.
[51] F.G. Delolo, E.N. dos Santos, E.V. Gusevskaya, Anisole: a further step to sustainable hydroformylation, Green Chem. 21 (2019) 1091–1098, https://doi.org/10.1039/C8GC03750G.
[52] D. Darensbourg, M.Y. Darensbourg, N. Walker, Studies using tributylphosphine oxide as a carbon monoxide labilizing ligand in the synthesis of metal carbonyl complexes highly enriched in carbon-13 monoxide, Inorg. Chem. 20 (1981) 1918–1921, https://doi.org/10.1021/ic50220a059.
[53] D. Darensbourg, N. Walker, M.Y. Darensbourg, Synthesis of metal carbonyl complexes highly enriched in carbon-13: utilization of the carbon monoxide-labilizing ability of (n-Bu)3P:O, J. Am. Chem. Soc. 102 (1980) 1213–1214, https://doi.org/10.1021/ja00523a075.
[54] E.J. Moore, J.M. Sullivan, J.R. Norton, Kinetic and thermodynamic acidity of hydrido transition-metal complexes. 3. Thermodynamic acidity of common mononuclear carbonyl hydrides, J. Am. Chem. Soc. 108 (1986) 2257–2263, https://doi.org/10.1021/ja00269a022.
[55] Y.D.Y.L. Getzler, V. Mahadevan, E.B. Lobkovsky, G.W. Coates, Synthesis of β-lactones: a highly active and selective catalyst for epoxide carbonylation, J. Am. Chem. Soc. 124 (7) (2002) 1174–1175, https://doi.org/10.1021/ja017434u.
[56] V. Mahadevan, Y.D.Y.L. Getzler, G.W. Coates, [Lewis Acid]$^+$[Co(CO)$_4$]$^-$ complexes: a versatile class of catalysts for carbonylative ring expansion of epoxides and aziridines, Angew. Chem. Int. Ed. 41 (2002) 2781–2784, https://doi.org/10.1002/1521-3773(20020802)41:15<2781. AID-ANIE2781≥3.0.CO;2-S.

6 Appendix

6.1 Curriculum Vitae

Johannes Fessler

Personal Details

Date of Birth	30.01.1992 in Münster, Germany
Nationality	German
Address	Braunschweiger Str. 1, 18057 Rostock, Germany
E-Mail	johannes.fessler@catalysis.de
ORCID	0000-0003-2395-8572

Academic Education & Research Experience

04/2023 – Present	**Postdoctoral Researcher** and **Temporary Research Group Leader** (Maternity Stand-In), Pospech Group, Leibniz-Institut für Katalyse (LIKAT), Rostock, Germany Organic photoredox catalysis
09/2019 – 03/2023	**Doctoral Researcher**, Leibniz-Institut für Katalyse (LIKAT), Rostock, Germany Doctoral Thesis, Group of Prof. Beller, Earth-abundant metal catalyzed hydrogenation reactions
01/2020 - 06/2020	Research Cooperation - Bayer Pharmaceuticals Hydrogenation of pharmaceutical intermediates
11/2018 - 04/2019	**Internship Process Optimization**, Lonza Specialty Ingredients, Lonza AG, Visp, Switzerland
04/2016 - 10/2018	**Master of Science, Chemistry**, LMU Munich, Germany
04/2018 - 09/2018	Visiting Student (Erasmus), Chemistry, University of Oxford, UK Master Thesis, Group of Prof. Davies, Asymmetric synthesis of quinolizidine natural products
09/2016 - 02/2016	Mobility Student (SEMP), Chemistry, ETH Zürich, Switzerland Research Project, Group of Prof. Togni, Electrophilic trifluoromethylation of sulfur nucleophiles

05/2016 - 07/2016	Research Project, Chemistry, LMU Munich, Germany Group of Prof. Trauner, Subgroup Dr. Magauer, Towards the total synthesis of Salimabromide
10/2012 - 03/2016	**Bachelor of Science, Chemistry and Biochemistry**, LMU Munich, Germany
01/2016 - 03/2016	Bachelor Thesis, Group of Prof. Klapötke, LMU Munich, Germany Synthesis and characterization of the new energetic material 5,5'-bis(2,4,6-trinitrophenyl)-2,2'-bi(1,3,4-oxadiazole)
10/2011 - 09/2012	**Bachelor Studies, Mech. Engineering**, University of Hanover, Germany

Further Skills & Achievements

Extracurriculars	2020 Merck Compound Challenge Participant 2021 Merck Compound Challenge Finalist (Top 10 out of over 300 research groups) 2022 Volunteer Long Night of Science (LNDW), Rostock 2023 Merck Compound Challenge Participant (Top 20)
Languages	German (native), English (fluent, spent 2008/2009 school year in US), Spanish (basics), French (basics), Latin (basics)
IT	MS Office (Word, Excel, PowerPoint, Outlook), Endnote, ChemDraw, MestReNova, Scifinder, Reaxys, Synthia, SHELX

6.2 Full Publication List

1. F. G. Delolo[+], J. Fessler[+], H. Neumann, K. Junge, E. N. dos Santos, E. V. Gusevskaya, M. Beller, *Chem. Eur. J.* **2022**, *28*, e202103903.
   "Cobalt-catalyzed reductive etherification using phosphine oxide promoters under hydroformylation conditions"
   Selected for a cover feature.

2. F. G. Delolo[+], J. Fessler[+], H. Neumann, K. Junge, E. N. dos Santos, E. V. Gusevskaya, M. Beller, *Mol. Catal.* **2022**, *530*, 112621.
   "Cobalt-catalyzed ring expansion/ring opening of oxetanes using phosphine oxides as promoters under hydroformylation conditions"

3. V. Papa[+], J. Fessler[+], F. Zaccaria, J. Hervochon, P. Dam, C. Kubis, A. Spannenberg, Z. Wei, H. Jiao, C. Zuccaccia, K. Junge, A. Macchioni, M. Beller, *Chem. Eur. J.* **2023**, *29*, e202202774.
   "Efficient hydrogenation of N-heterocycles catalyzed by NNP-Manganese(I) pincer complexes at ambient temperature"
   Selected as "Very Important Paper".

4. J. Fessler, K. Junge, M. Beller, *Chem. Sci.* **2023**, *14*, 11374.
   "Applying green chemistry principles to iron catalysis: Mild and selective domino synthesis of pyrroles from nitroarenes"
   Selected as "HOT" article.

5. E. Zander, J. Bresien, V. Zhivonitko, J. Fessler, D. Michalik, A. Schulz, *J. Am. Chem. Soc.* **2023**, *145*, 14484.
   "Rational Design of Persistent Phosphorus-Centered Singlet Tetraradicals and Their Use in Small-Molecule Activation"
   Selected for a cover feature.

6. N. F. Both, J. Fessler, A. Vicenzi, K. Andres, A. Spannenberg, K. Junge, M. Beller, *ChemCatChem* **2023**, accepted manuscript.
   "Air-stable manganese NNS pincer complexes enable ketone reduction at room temperature"

   [+] Authors contributed equally.

6.3 Posters & Oral Presentations

1. J. Fessler, C. Schneider, M. Beller, *Life, Light & Matter Graduate Workshop*, Rostock, Germany, January 2020
   Oral Presentation: *"The importance of catalysis for modern society"*

2. J. Fessler, F. G. Delolo, H. Neumann, K. Junge, E. N. dos Santos, E. V. Gusevskaya, M. Beller, *4th International Green Catalysis Symposium*, Rennes, France, April 2022
   Poster Presentation: *"Cobalt carbonyl and phosphine oxide promoters: The reductive etherification of aldehydes under syngas atmosphere"*

3. J. Fessler, V. Papa, F. Zaccaria, J. Hervochon, P. Dam, C. Kubis, A. Spannenberg, Z. Wei, H. Jiao, C. Zuccaccia, K. Junge, A. Macchioni, M. Beller. *56th German Catalysis Meeting*, Weimar, Germany, March 2023
   Poster Presentation: *"Earth-abundant manganese pincer catalysis: Hydrogenation of N-heterocycles at ambient temperature"*

6.4 Selbstständigkeitserklärung

Doktorandinnen/Doktoranden-Erklärung gemäß § 4 Absatz 1 Buchstaben g und h der Promotionsordnung der Mathematisch-Naturwissenschaftlichen Fakultät der Universität Rostock

Name Fessler, Johannes
(Name, Vorname)

Anschrift Braunschweiger Straße 1, 18057 Rostock
(Straße, PLZ, Wohnort)

Ich beabsichtige, eine Dissertation zum Thema

Iron and its neighbors, earth-abundant hydrogenation catalysts the synthesis of heterocycles and ethers

an der Mathematisch-Naturwissenschaftlichen Fakultät der Universität Rostock anzufertigen. Dabei werde ich von Frau/Herrn Prof. Dr. Matthias Beller betreut.

Ich gebe folgende Erklärung ab:

1. Die Gelegenheit zum vorliegenden Promotionsvorhaben ist mir nicht kommerziell vermittelt worden. Insbesondere habe ich keine Organisation eingeschaltet, die gegen Entgelt Betreuerinnen/Betreuer für die Anfertigung von Dissertationen sucht oder die mir obliegenden Pflichten hinsichtlich der Prüfungsleistungen für mich ganz oder teilweise erledigt.
2. Ich versichere hiermit an Eides statt, dass ich die vorliegende Arbeit selbstständig angefertigt und ohne fremde Hilfe verfasst habe. Dazu habe ich keine außer den von mir angegebenen Hilfsmitteln und Quellen verwendet und die den benutzten Werken inhaltlich und wörtlich entnommenen Stellen habe ich als solche kenntlich gemacht.

....., den ....
(Ort) (Unterschrift)